THE UNIVERSITY OF CHICAGO

STAPHYLOCOCCUS AUREUS α-TOXIN DAMAGES THE TISSUE MICROENVIRONMENT DURING SKIN AND SOFT TISSUE INFECTION

A DISSERTATION SUBMITTED TO
THE FACULTY OF THE DIVISION OF THE BIOLOGICAL SCIENCES
AND THE PRITZKER SCHOOL OF MEDICINE
IN CANDIDACY FOR THE DEGREE OF
DOCTOR OF PHILOSOPHY

COMMITTEE ON MICROBIOLOGY

BY

GEORGIA RAFAELLA SAMPEDRO

CHICAGO, ILLINOIS

JUNE 2018

TABLE OF CONTENTS

LIST OF FIGURES

LIST OF TABLES

ACKNOWLEDGEMENTS

This work is dedicated to my parents, Silvana and Gerard Sampedro. May I always be able honor you, serve you, and bring you joy. Los quiero muchisimo.

When my parents returned to university in their early 40s they were the oldest students in their graduating class. Without access to childcare, I regularly attended university with them. I would sit in classes with them when I was allowed- wait in the corridors when I was not- and spent my summers in the university library. I thank them for instilling in me the importance of education.

My mother. I remember during her university, her English was still poor and she would bring her tape recorder to every class. For years, at night she would translate what the professor was saying into Spanish, study the material, and then practice translating the material back into English. She always set her eyes on having the highest class score. As my mother would proudly say- "without knowing English, I got a 4.0 at University!". Mama, thank you for showing me the real meaning of hard-work, dedication, and excellence.

My father. After receiving his four-year degree my father gained an affinity for going to university. Every year since then he has been enrolled in several university courses. He always goes out of his way to pick the most challenging topics- mathematics, accounting, and now computer science. While some of the material looks complex, he always accepts the challenge. I have never met someone who derives so much joy from learning. For him, the harder the topic, the greater the pleasure. Papa, may I always have your courage to learn new hard things.

Joe. Ever since we met you have come to lab with me, moved to St. Louis for me, and helped me put together every figure in this work. I couldn't have dreamed you up. Thank you for your consistency, support, and love. I look forward to our future together.

My Siblings, Carlos (Pipo), José, Gabby, and their families. You are my greatest wealth. The joy, comfort, and counsel you have given me has made me undeniably the most beloved "beba" of all time. I only hope I can take the opportunities given to me to help you and your families as much as you've helped me.

My mentor, Julie. Julie's grandmother has often said to me, "we are so lucky to have Julie". I know exactly how Gram feels. Almost fired from my first job out of college Julie stepped in to teach me how to clone so I could keep my job. When I became her tech she taught me how to think like a scientist and gave me the technical skills I needed to be independent at the bench. In graduate school when I doubted my ability she gave me the confidence to prevail and the encouragement to continue. Julie, I feel so very lucky to have you!

A special thanks to all those who have given me technical and scientific support over the years: My committee members- Dr. Lucia Rothman-Denes, Dr. Sean Crosson, Dr. Dominique Missiakas, Dr. Erin Adams; Light Microscopists- Dr. Christine Labno and Dr. Michael Shih; Wardenburg lab members past and present- Vivian Choi, Aaron Hecht, Bryan Berube, Michael Powers, Russell Becker, and Kelly Tomaszewski.

ABSTRACT

Staphylococcus aureus is a pathobiont that can cause a range of mild to life-threatening infection in otherwise healthy individuals. While *S. aureus* disease has a broad tissue tropism, the most common site for both colonization and infection is in the skin. Nearly half of individuals with a *S. aureus* skin and soft tissue infection (SSTI) suffer from recurrence (Kaplan et al., 2014; Williams et al., 2011; Doung et al., 2010; Chen et al., 2009; Miller et al., 2007, Fritz et al., 2012; Bocchini et al., 2013; Miller et al., 2015). Recurrent infection is a characteristic quality of *S. aureus* SSTIs, however the precise molecular determinants of susceptibility to recurrence have only recently been investigated. Epidemiologic studies focusing on the immunological correlates of natural human immunity against *S. aureus* infection have provided initial insight into the key bacterial factors that thwart the host's production of a protective immune response. Elevated antibody titers against an array of staphylococcal cytotoxins minimize the severity of invasive infection and the recurrence of cutaneous *S. aureus* disease (Adhikari et al., 2012; Fritz et al., 2013). Specifically, serum antibody against one *S. aureus* cytotoxin, α-hemolysin (α-toxin, Hla) correlates with protection against recurrent *S. aureus* skin and soft tissue infection (SSTI) in children (Fritz et al., 2013).

To investigate whether there is a mechanistic link between α-toxin expression and the severity of *S. aureus* reinfection patterns, we developed a mouse model of recurrent *S. aureus* SSTI mouse model. Using an isogenic Hla mutant in this model we observed that Hla expression during primary infection interferes with development of host immunity against recurrent *S. aureus* SSTI. Early neutralization of α-toxin activity either by a dominant-negative toxin mutant or with a small molecule inhibitor against the toxin's cell host receptor, A Disintegrin and

Metalloprotease 10, ADAM10, during primary *S. aureus* SSTI reduces initial and recurrent SSTI abscess severity. Notwithstanding, the mechanism of toxin-mediated cutaneous protection has been perplexing, as toxin injury to keratinocytes and neutrophils have pleiotropic outcomes during *S. aureus* SSTI. Additionally, while the response that mediates durable immunity against *S. aureus* skin infections likely involves neutrophil recruitment by an induced T cell-mediated cytokine, IL-17, the contribution of direct toxin-injury on T cells during *S. aureus* SSTI has remained enigmatic. To evaluate toxin-mediated injury to T cells in cutaneous pathology and pinpoint whether Hla directly impairs the IL-17 induced recruitment of neutrophils by injuring T cells, we excised ADAM10 from peripheral T cells, using Cre-lox technology.

Probing into mechanism, we identified Hla-mediated injury to cutaneous resident innate-like T cells as the cellular gate keeper of *S. aureus* SSTI infection outcomes. α-Toxin kills both neighboring and distant epidermal T cells adjacent to the site of *S. aureus* infection. The total decrease in T cells is commensurate with a dampening of IL-17 production, neutrophil activity, abscess formation, and loss of epidermal integrity that results in large wounds. Identification of γδ T cells as the innate T cell subset impaired by toxin during early *S. aureus* SSTI prompted our investigation into whether injury of γδ T cells would damage epithelial-immune crosstalk. *S. aureus*-infected γδ T cell reporter mice challenged with toxin-deficient *S. aureus* revealed critical spatial clustering of the γδ T cell highly skewed near the abscess border that is diminished in wild-type *S. aureus* infected animals. This evidence advances a model whereby α-toxin mediates injury to the skin microenvironment, simultaneously blocking γδ T cell localization to skin infection sites and dampening the activatory signals secreted by T cell that upregulate keratinocyte proliferation and concentrate neutrophils at the abscess.

In light of our data, we reasoned that Hla intoxication of innate T cells would diminish their wound healing capabilities in a location-dependent manner. Indeed, in a sterile wound healing model, T cells susceptible to the toxin have larger, slower healing wounds than toxin-resistant T cells. Collectively, these findings provide molecular insight into the how α-toxin-mediated injury to cutaneous T cells could have long-term and wide-ranging consequences to skin immunity.

CHAPTER I

INTRODUCTION

Portions of this introduction have been adapted from a manuscript published in The Journal of Infectious Diseases: *Staphylococcus aureus* in the Intensive Care Unit: Are these golden grapes ripe for a new approach? (DOI: 10.1093/infdis/jiw581). The authors of that manuscript are Georgia R. Sampedro and Juliane Bubeck Wardenburg.

The Problem is Skin Deep: *S. aureus* epidemiology and disease-modifying approaches

An excerpt from the 11th Edition (1940) Holt's Diseases of Infancy and Childhood:

> "Once the organisms gain a foothold, they may be very difficult to eradicate; sometimes boil after boil appears and these lesions may continue to develop in crops for months. The scalp, face, and shoulders are favorite sites but any part of the body may be involved; in some instances, the entire body is covered with furuncles."

While these clinical manifestations of *S. aureus* infection were made in a pre-antibiotic era, S. *aureus* is now one of the most common and drug-resistant human pathogens. It is a leading cause of infections in both the healthcare setting and in the community in otherwise healthy individuals. Historic hospital-associated methicillin-resistant *S. aureus* (HA-MRSA) strains as well as community-associated methicillin resistant *S. aureus* (CA-MRSA) strains, genetically distinguishable by their drug-resistance loci, are both causes of infection (Popovich et al., 2008). *S. aureus* is a prominent etiologic agent of many invasive disease manifestations including endocarditis, pneumonia, sepsis, and osteomyelitis (Lowy, 1998). Owning to its invasive disease tropism, *S. aureus* contributes to the death of more than 20,000 individuals in the US alone on an annual basis and presents a significant burden on the healthcare system with an estimated

hospitalization cost of >$25,000 per inpatient and >$140,000 per ICU patient (Naber, 2009; Kyaw et al., 2015). Simultaneously, *S. aureus* is also the very frequent cause of skin and soft tissue infection (SSTI) worldwide and since the emergence of MRSA, the incidence of *S. aureus* SSTI continues to rise (Challagundla et al., 2018; McCaig et al., 2006). Between 2001 and 2009 *S. aureus* SSTI hospitalizations rose 123% and represented the majority share of all *S. aureus* hospitalizations at 51%, with an estimated hospitalization cost of >$19,000 per patient (Suaya et al., 2014). The heterogeneity of *S. aureus* disease, the disease associated cost, and the spread of *S. aureus* from the clinic to the community setting has complicated the treatment and management of infection.

The past two decades have witnessed two waves in the epidemiology of *S. aureus* infections, the first starting with *S. aureus* invasive disease largely limited to the healthcare setting. The second and current wave, starting in the late 1990s, is an epidemic of community-associated SSTIs; precipitated by the USA300 clone and by similar strains that harbor a more aggressive array of virulence factors, an increased doubling time, and resistance to antibiotics (Tong et al., 2015). Perpetuating *S. aureus* SSTI is recurrent infection- a characteristic quality of *S. aureus* cutaneous disease. Human studies have revealed that patients who are colonized or have a primary cutaneous *S. aureus* infection are more likely to develop recurrent cutaneous *S. aureus* infection (Frtiz et al., 2013; Bocchini et al., 2013; Miller et al., 2015; Williams et al., 2011). Intriguingly, and likely related, the skin is not only the most common site of both primary and recurrent *S. aureus* infection but it is also the largest ecological reservoir of *S. aureus* asymptomatic colonization. An estimated 20% of the healthy human population is persistently colonized and 80% of humans are intermittently colonized with *S. aureus* on the upper layers of the cutaneous epithelia (Archer et al., 2013). Previous studies have shown colonization to be a

risk factor for recurrent SSTIs, nosocomial infections, as well as an increased carriage due to immune dysfunction (Archer et al., 2013; Creech et al., 2015). While these studies have been limited in human populations, they have provided compelling evidence that the modus operandi of *S. aureus* is to maintain and transmit itself within the human skin microbiome. If this is the case, a more comprehensive understanding of the strategies staphylococci employ to survive in the skin are required to improve prevention and recovery from infection.

Antibiotic treatment remains the cornerstone of staphylococcal disease management (Lui et al., 2011). In recent years, administration of empiric therapy with *S. aureus*-active antimicrobials has become a standard approach to care of inpatients with presumed *S. aureus* invasive or severe SSTI infection (Lui et al., 2011; Rubinstein et al., 2001). While the use of antibiotics has been shown to have no efficacy on the resolution of uncomplicated *S. aureus* SSTI, abscess drainage and prescription of antibiotics for *S. aureus* SSTI remains the standard of care and one of the most frequent indications for antibiotic use in the ambulatory care setting (Rajendran et al., 2007; Hurley et al., 2013). Of note, inadvertent use of beta-lactam antibiotics to treat TSST-1 or PVL- associated MRSA infections may even contribute to worse outcomes by inducing prolonged toxin production (Stevens et al., 2007). The development of outpatient antimicrobial stewardship interventions hold promise to reduce and optimize the antibiotic use for uncomplicated *S. aureus* SSTIs (Walsh et al., 2017). At this point, long-term and wide-spread implementation of these programs is yet to be realized. Decolonization strategies including intranasal mupirocin treatment and chlorhexidine ‘baths’ are selectively utilized in some populations, however the success of these interventions in clinical studies is variable (Simor, 2011; Huskins, 2007). While recent studies suggest that universal decolonization may be a very cost-effective strategy to prevent MRSA infection (Gidengil et al., 2015; Ziakas et al., 2016),

potentiation of drug resistance in *S. aureus* as well as other pathobionts within the endogenous human microbiota is an inherent risk of this approach. Furthermore, the unintentional modification of the commensal microbiota resulting from decolonization may render patients with severe or protracted underlying illness more susceptible to pathogenic infection through a loss of 'colonization resistance' (Parmer, 2016). The last four epidemic waves of *S. aureus* antibiotic resistance highlight this pathogen's remarkable ability to acquire drug resistance (Chamber et al., 2009). This continual evolution of drug-resistant *S. aureus* strains foreshadows not only the near-future exhaustion of existing antibiotics, but also the transient nature of their efficacy even in a single patient. Novel methods to prevent and treat infection are urgently needed to combat this superbug.

Highly-targeted 'designer' therapies based on molecular knowledge of pathogenesis hold promise to bypass or limit specific concerns associated with antimicrobial therapy. Monoclonal antibody (mAb) prophylaxis and treatment is perhaps the most refined biological technology for targeting pathogens including *S. aureus*. Through knowledge of virulence factor action in disease, a number of mAbs have demonstrated success in preclinical investigations of severe *S. aureus* infection; several of these are now being examined in clinical trials (Cheng et al., 2010; Kim et al., 2010; Kim et al., 2012; Ragle et al., 2009; Hua et al., 2014; Hua et al., 2015; Varshney et al., 2014; Tkaczyk et al., 2016; Anderson et al., 2012; Ebert et al., 2010; Rouha et al., 2015; Skurnik et al., 2010). In addition, pharmacologic agents and monoclonal antibodies that act on host proteins to mitigate the pathophysiological consequences of life-threatening infection have similarly demonstrated promise in preclinical studies of disease (McAdow et al., 2011; Inoshima et al., 2011; Powers et al., 2011; Hinshaw et al., 1992; Alonzo et al., 2013). While anti-infective antibody therapies could reduce the incidence of hospital-acquired

infections and curb the emergence of antimicrobial resistance, these interventions must be applied in a precisely defined clinical setting as the economic cost associated with molecular targeting are unlikely to be cost-effective in population-based low-risk infections such as for *S. aureus* SSTIs. Notwithstanding, the mortality and short and long-term morbidity as a consequence of infection in medical and surgical ICUs - coupled with the cost of advanced care - may provide a unique rationale for implementation of these approaches in patient population suffering from severe *S. aureus* disease.

The state of the field: disease pathogenesis, host susceptibility, and emerging therapies

Considerable advances in the molecular pathogenesis of *S. aureus* infection have been achieved to date. While initial suspicion existed that methicillin-sensitive *S. aureus* was less virulent than MRSA owing to the presence of novel virulence attributes in drug-resistant strains, it is now appreciated that pathogenicity is more closely related to subtle genetic differences between strains that modulate virulence factor expression (DeLeo et al., 2001; Kennedy et al., 2008; Laabei et al. 2014). As such, a discussion the molecular pathogenesis of *S. aureus* disease can be viewed as relevant to MSSA and MRSA variants. Multiple animal models of disease have been utilized to examine the contribution of staphylococcal virulence factors to bacteremia, sepsis, pneumonia, and severe SSTI (Kim et al., 2014). Staphylococcal surface proteins facilitate tissue adherence and immunoevasion (Foster TJ and Höök M, 1998). An array of secreted immunomodulatory proteins and coagulases target soluble host factors present in the blood to collectively alter the inflammatory-coagulation interface that is critical to innate host defense (Ricklin et al., 2008; Rooijakkers et al., 2006; Oikonomopoulou et al., 2012; Foster et al., 2005).

In models of severe tissue injury as observed in sepsis, pneumonia, and dermonecrotic tissue injury, *S. aureus* toxins emerge as important contributors to life-threatening disease states akin to those observed in ICU patients. Collectively, these toxins damage host cell membranes to cause cytolytic injury, alter cellular signaling and function, and facilitate immunoevasion. A comprehensive discussion on the molecular mechanisms of action of these virulence factors is provided in a series of excellent reviews (Oikonomopoulou et al., 2012; Foster et al., 2005; Berube et al., 2013; Vandenesch et al., 2012; Foster et al., 1998; Nizet, 2007; Rooijakkers et al., 2005; Parker et al., 2011). The detailed understanding of molecular pathogenesis at the cellular and tissue level that has emerged from preclinical studies defines 'pathways of injury' within the host that are now amenable to examination as a function of both time post-infection and spatial orientation within the tissue. We propose that such 'temporo-spatial analysis' of disease is needed to fully disease pathogenesis and inform opportunities for therapeutic intervention.

The profile of human antibody responses to *S. aureus* and population-based studies of the carriage state suggest that exposure to this organism is ubiquitous (Holtfreter et al., 2010; Kolata et al., 2011; Dryla et al., 2005; Swierstra et al., 2015; Miller et al., 2009; Mehraj et al., 2016). To date, however, identifying features of the *S. aureus*-susceptible host remain fairly enigmatic. Several known immunodeficiency states including deficiencies of the neutrophil oxidative burst in chronic granulomatous disease, alterations in the STAT3/Th17 signaling pathway, and TLR2 accessory molecules are recognized to increase susceptibility, particularly to *S. aureus* SSTIs (Miller et al., 2011; Rigby et al, 2012; Holland et al., 2007; Israel et al., 2017). However, most individuals with life-threatening staphylococcal infection do not suffer from a definable immunodeficiency. A recent description of human leukocyte antigen (HLA) polymorphisms emerging from a genome-wide association study provides the first population-based insight on

host genetic variation that confers susceptibility to *S. aureus* infection (DeLorenze et al., 2016). The rapid advances in knowledge of virulence factor action in disease now provides the field with a timely opportunity to examine host targeted proteins and signaling pathways for additional polymorphic loci that alter host susceptibility to *S. aureus* infection. Perhaps most notably, the identification of proteinaceous receptors for multiple staphylococcal toxins in the past 5 years affords an opportunity to consider variation in toxin receptor expression and receptor polymorphisms as determinants of host susceptibility. These receptors are particularly attractive to consider given the demonstrated role of toxins in severe disease and the fact that cellular receptors specify both the species and cellular tropism of the bacterial cytotoxins.

On the flip-side of host susceptibility markers, several efforts have commenced in recent years to identify features of the protective host immune response to *S. aureus*. One such approach is definition of the immunological correlates of natural human immunity against *S. aureus* infection. Elevated antibody titers against an array of staphylococcus cytotoxins minimize the severity of invasive infection and the recurrence of cutaneous *S. aureus* disease (Adhikari et al., 2012; Fritz et al., 2013; Wood et al., 2018). Serum antibody to *S. aureus* α-toxin (Hla, α-hemolysin), δ-hemolysin (Hld), PVL, leukotoxin LukAB, staphylococcal enterotoxin C-1 (SEC-1), and PSM family cytotoxins correlate with protection against sepsis in patients with invasive *S. aureus* infections (Adhikari et al., 2012; Thomsen et al., 2014; Wood et al., 2018). Further, anti-Hla antibody levels correlate with protection against recurrent *S. aureus* SSTI in children (Fritz et al., 2013). A second approach has relied on analysis of recurrent *S. aureus* infection to provide insight on both host susceptibility and bacterial genetic factors that modulate the development of immunity to *S. aureus*. Recurrent infection is a characteristic quality of *S. aureus* disease; however, the molecular determinants of recurrent infection have only recently been

investigated. Human studies have revealed that patients who are colonized or have a primary cutaneous *S. aureus* infection are up to 50% more likely to develop recurrent infections (Fritz et al., 2013; Bocchini et al., 2013; Miller et al., 2015; Williams et al., 2011). The majority of *S. aureus* recurrent infections are SSTIs. In contrast, patients with invasive infection demonstrate the lowest overall rate of recurrent infection over 1 year (Fritz et al., 2013). While these studies have been limited in human populations, recent investigation of recurrent *S. aureus* infection in mouse models provides initial insight that *S. aureus* α-toxin and the host T and B cell compartments modulate the development of protective immunity (Sampedro et al., 2014; Montgomery et al., 2014; Montgomery et al., 2015).

Host susceptibility and immunity to *S. aureus* infection are the result of a complex interface between a native human commensal and its host-dependent on multiple variables including the presence or absence of the carriage state, the tissue site, magnitude, and duration of host exposure, and bacterial and host genetic determinants. In the setting of invasive disease, an 'immunostimulation threshold' may be reached that is not achieved in cutaneous disease, leading to the generation of a productive host response that confers resistance to re-infection. Alternatively, in the context of cutaneous infection, *S. aureus* may deliberately subvert the immune response to ensure success as a human commensal. Some evidence from animal modeling systems exists to support the hypothesis that the tissue site of infection is a strong determinant of the nature and efficacy of the host immune response to *S. aureus*. Mice deficient in IL-17 exhibit increased susceptibility to *S. aureus* cutaneous infection relative to wild-type mice, however do not display alterations in the response to systemic infection (Cho et al., 2010; Ishigame et al., 2009). In contrast, IFN-γ receptor deficient mice are hyper-susceptible to intravenous *S. aureus* infection but show no difference in susceptibility to cutaneous infection

when compared to controls (Cho et al., 2010; Brown et al., 2015; Lin et al., 2009). The hypothesis that *S. aureus* immunity relies on the exposure history and tissue context in which exposure occurs may explain the pronounced heterogeneity in anti-staphylococcal antibody levels seen in both children and adults (Dryla et al., 2005). The character and specificity of the native antibody response may mark the colonized state and indicate prior subclinical or clinical infection with *S. aureus* providing fundamental insight that may be utilized as determinants to predict the relative susceptibility of an individual patient to *S. aureus* disease in the hospital setting (Holtfreter et al., 2010; Kolata et al., 2011; Swiestra et al., 2015).

The future prospect: An emerging understanding of α-toxin-mediated manipulation of the immune response

MRSA's status as a global public health threat and the cost associated with designer therapies highlights the unmet clinical need for research driven efforts to develop an anti-*S. aureus* vaccine or a cost-effective prophylactic (WHO, 2014). Novel therapeutic solutions have been challenging as the field lacks pertinent knowledge of the determinants of protective immune response in humans. To date, this precedent has resulted in the failure of all *S. aureus* passive and active immunization candidates to show efficacy in clinical trials (Proctor et al., 2011). Despite lack of success, these clinical trials have been informative. It is now thought that a single antigen vaccine approach will likely not elicit protective immunity and that robust anti-staphylococcal antibody production alone may not confer protection from *S. aureus* disease in humans (Jansen et al., 2013). Vaccine-induced adaptive immunity that includes both T cell and B cell responses will likely be required to generate protective immunity in humans. Additionally, a

Th17 response is likely advantageous as it can both enhance neutrophil function and increase antimicrobial peptide activity on the skin barrier (Proctor et al., 2011; Giersing et al., 2016).

Recently, pharma has been focusing on the inclusion and or specific targeting of *S. aureus* α-toxin in disease-modifying therapies. Currently, two out of the four ongoing clinical trials for active prophylactic vaccines (phase I) and one of two passive prophylactic vaccines (phase IIb) include or solely target Hla, respectively, making Hla the premier virulence target of the staphylococcal field (Wacker et al., 2014; Torre et al., 2015; Yu et al., 2016; Giersing et al., 2016). Certainly, the historical and contemporary success of antitoxin immunization strategies such as for diphtheria, tetanus, pertussis with DTaP and now for *C. difficile* targeting Toxin A and B have shown that toxin-based vaccine strategies are safe, tolerable, and immunogenic (Kretsinger et al., 2006; Wang et al., 2012; Donald et al, 2013).

The unique characteristics of the Hla in human disease and its establishment of specific patterns of adaptive immunity in the human host make α-toxin antagonists a promising therapeutic candidate. Of the *S. aureus* cytotoxins, α-toxin exhibits the broadest range of cellular specificity, contributing to the toxin a broad role in the pathogenesis of *S. aureus* infection- including, but not limited to, sepsis, pneumonia, SSTI, endocarditis, corneal lesions, and neuropathy (Powers et al., 2012; Inoshima et al., 2011; Inoshima et al., 2012; Xiong et al., 2006; Dajcs et al., 2002; Kielian et al., 2001; Blake et al., 2018). While there is no robust animal model for staphylococcal colonization, production of an anti-toxin neutralizing antibody is found to be higher in *S. aureus* colonized individuals suggesting that the toxin is also expressed during colonization (Wu et al., 2017). Owning to its importance in human infection and its role in colonization, it is not surprising that a hallmark of recent epidemic *S. aureus* strains is an increase in Hla production (DeLeo et al., 2010). In animal models of *S. aureus* disease, these

epidemic strains contribute to pathogenesis when compared with toxin deficient hospital isolates from related clones that cluster in the same clonal complex (Montgomery et al., 2008; Bubeck Wardenburg et al., 2008). Furthermore, multiple reports aforementioned have demonstrated that human anti-toxin antibody levels correlate with durable natural immunity against both invasive and cutaneous *S. aureus* infection in adults and children, respectively (Adhikari et al., 2012; Fritz et al., 2013). Collectively, these distinct but congruent lines of evidence make a compelling argument for Hla-mediated injury playing an important role during pathogenesis of *S. aureus* disease in humans.

α-Toxin is a 33.2 kilodalton (kDa) water-soluble polypeptide secreted during late-log and exponential phase of *S. aureus* growth. Expression of the toxin is tightly controlled by at least three global regulatory loci- the accessory gene regulator (*agr*), the staphylococcal accessory gene regulator (*sarA*), and the staphylococcal accessory protein effector (*sae*) (Arvidson et al., 1990; Giraudo et al., 1997; Goerke et al., 2001; Morfeldt et al., 1995; Vandenesch et al., 1991). Once secreted, likely in a lipid-membrane assisted fashion, the toxin oligomerizes into a mushroom-shaped, heptameric pore on host cell membranes upon contact with a membrane anchored cellular sheddase- A Disintegrin and Metalloprotease 10, ADAM10 (Song et al., 1996; Schwiering et al., 2013; Wilke et al., 2010; Popov et al., 2015). The fully assembled 232.4 kDa heptamer has three structural domains: 1) the extracellular cap domain, 2) the C-terminal rim domain, and 3) the N-terminal central stem domain that converts its conformation into a latch enabling the perforating formation of the transmembrane pore (Song et al., 1996; Jayasinghe et al., 2005). A single N-terminal mutation at His_{35} within the monomer to monomer interface blocks the pre-pore to pore transition serving as a genetic tool and vaccination strategy to uncouple Hla binding from toxin mediated- injury (Bubeck Wardenburg and Schneewind, 2008;

Kennedy et al., 2010). The pore's hydrophilic ß barrel interior, 14-46 Å in width and 100 Å in length, is a solvent filled channel. At low toxin concentrations, the channel causes membrane permeabilization via flux of low molecular weight molecules (between 1-4kDa) such as, Ca^{2+}, K^{+}, and ATP -which induce several signaling events in the target cell (Lizak and Yarovinsky, 2011; Rose et al., 2002), at high toxin concentrations, the channel causes cell lysis (Cooper et al., 1964).

The structural and genetic analysis of Hla-ADAM10 interaction are nascent, but emerging evidence of ADAM10's functional characteristics have aided in conceptualizing how Hla may bind to this sheddase. ADAM10 is thought to facilitate binding of the toxin to the cell membrane through the interaction with a specific as yet unidentified ADAM10 surface domain(s). ADAM10 has several structural domains: 1) a prodomain (PD), 2) a metalloproteinase (MP), 3) a disintegrin domain, 4) a cysteine-rich region, 5) a transmembrane domain, and 6) a cytoplasmic tail. ADAM10 precursors are catalytically inactive when the PD is intact and are chaperoned to the cell surface by members of the tetraspanin protein superfamily- thought to regulate ADAM10 subcellular localization, membrane compartmentalization and substrate selectivity (Saint-Pol et al., 2017). Once at the cell surface, the PD is released and the catalytically active enzyme is autoregulated by the MP's intramolecular interface with the disintegrin/cysteine rich domains (Seegar et al. 2017). Analysis of Hla toxicity measured by ATP release as a proxy for Hla binding to ADAM10 genetic domain mutants have shown that truncations to the PD or the MP domain abolish cytotoxicity (von Hoven et al., 2016; Tomaszewski and Berube, unpublished). Notwithstanding, a model whereby the toxin binds to PD extracellularly is perplexing as the PD is thought to be cleaved off surface displayed ADAM10 (Seegar et al. 2017). Intriguingly, both of these studies have uncovered an active site

mutation to MP domain- E384A, rendering ADAM10 catalytically inactive but not altering α-toxin binding to the host cell surface. Both cell culture studies using radio-labeled toxin on cells harboring $ADAM10_{E384A}$ and in mice where the $ADAM10_{E384A}$ mutation has been made specifically to lung epithelial cells phenocopy ADAM10 knockout cell culture lines and ADAM10 knockout, suggesting that ADAM10 activation is the driver of *S. aureus* pathogenesis (Tomaszewski and Berube, unpublished). While Hla binding to ADAM10 is not completely understood, one attractive model is that the α-toxin could displace the MP-disintegrin/cysteine interface activating the protease function of ADAM10 (Bubeck Wardenburg, discussion).

As confirmed by cell culture and animal modeling with $ADAM10_{E384,}$ ADAM10 is not only the binding dock for the toxin but also concomitantly contributes to toxin-mediated damage. Upon toxin binding, although mechanistically enigmatic, ADAM10's function as a ectodomain sheddase becomes activated (Wilke et al., 2010; Inoshima et al., 2011; Inoshima et al., 2012; Powers et al., 2012; Popov et al., 2015). Activation of ADAM10 results in the irreversible proteolytic cleavage of surface substrates that function in cellular signaling cascades that impact development, cell proliferation, inflammation, and epithelial/endothelial barrier integrity, with substrate specificity varying by cell type (Pruessmeyer J et al., 2009). In the skin, Hla-mediated ADAM10 activation results in cleavage of the keratinocyte junctional adhesin, E-cadherin, which disrupts the integrity of the epidermal barrier function and manifests as the formation of a dermonecrotic wound. Subcutaneous infection of transgenic mice harboring a deletion of ADAM10 in keratinocytes restores the integrity of E-cadherin, and mice are resistant to staphylococcal lesion formation (Inoshima et al., 2012). Similar observations from cell-specific genetic ADAM10 knockout animals are made for both *S. aureus* pneumonia and sepsis. α-Toxin injury to the lung epithelium and vascular endothelium also leads to barrier disruption that is

subsequently amplified by inflammation produced from ensuing toxin injury to invading platelets and neutrophils responding to barrier damage (Inoshima et al. 2011; Powers et al., 2015; Sampedro unpublished).

Due to the complex cellular constituency of tissue, the Hla-ADAM10 interaction can appear as synergistic or pleiotropic biological outcomes on an organ level. Each cell type has a unique response to Hla intoxication that will not only be modified by toxin concentration but also by ADAM10 expression levels, ADAM10-mediated cleavage of extracellular substrates, and the contextual signals it receives from neighboring toxin-damaged cells. While investigations using toxin deficient *S. aureus* strains for disease modeling have provided insight into the relative tissue response Hla injury modifies, cell-specific and molecular responses to toxin injury and its impact on the outcome of *S. aureus* infection can only be dissected from the complex tissue milieu by using cell specific ADAM10 knockout mice.

Intriguingly, Hla-mediated injury to host cells may not be limited to the cell surface. Recent investigations have implicated the α-toxin in modulating *S. aureus* induced autophagy. At the organism level and also specifically in endothelial cells, disruption of autophagy gene *Atg16L1* enhances *S. aureus*-mediated lethality in a toxin-dependent manner during systemic infection (Maurer et al., 2015). Importantly, in *Atg16L1*-deficient endothelial cells the increased level of susceptibility correlated with an increase in the surface expression of ADAM10. Maurer and colleagues commented that these data indicated that autophagy dampened the damage of the toxin at the cell surface likely by regulating ADAM10 cell surface expression in the presence of α-toxin- making autophagy a tolerance strategy against *S. aureus*. Differently, in epithelial culture cells, autophagy of *S. aureus*-expressing Hla has been shown to induce cytoplasmic *S. aureus*-induced filaments that both promote *S. aureus* intracellular replication and interfere with

host cellular trafficking (Lopez et al., 2017). Recently, Wang and colleagues have shown that disruption of autophagy genes- *Beclin-1* and *Atg5* in dendritic cell types are protective against invasive *S. aureus* disease suggesting that the role of Hla in autophagy may likely be cell dependent (Wang and Sampedro, unpublished observations). While still incomplete, these studies suggest that autophagy is a double edge sword- it can be a protective mechanism by the host that also is manipulated by α-toxin. Future studies should define the underlying molecular mechanism of Hla-mediated modulation of autophagy and whether ADAM10 activation inside the autophagosome impacts the function of autophagy signaling proteins.

Whether at the cell surface or within the cell, α-toxin-induced cellular injury elicits a robust inflammatory response in the tissue microenvironment. A hallmark response to *S. aureus* infection is the infiltration of neutrophils and monocytes. Numerous studies have now discovered how α-toxin intoxication of these cell types lead to redundant but distinct cellular signaling events that culminate in the production and secretion of inflammatory cytokine, IL-1β. In one pathway, Hla pores on the host cell membrane serve as a conduit for bacterial peptidoglycan cell wall fragments that in turn activate intracellular sensor, NOD2, ultimately leading to the production of immature pro-IL-1β (Hruz et al., 2009). In a second pathway, Hla can activate the NLRP3 inflammasome that results in caspase-1 activation and cleavage of pro-ILβ into its active form (Kebaier et al., 2012). Remarkably, as demonstrated by mice that harbor a specific deletion of *ADAM10* from myeloid lineage cells, *LysM ADAM10*$^{-/-}$, the contribution of Hla-dependent inflammatory release of IL-1β from neutrophils and monocytes to *S. aureus* pathogenesis depends on the specific tissue context. In the murine skin, *LysM ADAM10*$^{-/-}$ mice challenged with *S. aureus* SSTI have exacerbated lesions while *LysM ADAM10*$^{-/-}$ mice challenged with *S. aureus* pneumonia have reduced lethality when compared to controls (Becker et al., 2014).

Collectively, regardless of the tissue, these data suggest that toxin-induced immunostimulation of these cells produces a pro-inflammatory microenvironment. The precise molecular consequences the pro-inflammatory environment has on the local tissue residents is undefined and likely multifactorial; however, it is intriguing to speculate that this excessive inflammatory response is damaging to the host and paramount for potentiating *S. aureus* chance of survival.

Many of the key mechanistic steps of how Hla causes cutaneous immune dysregulation during *S. aureus* SSTI remain elusive. While of interest, the findings from studies investigating the interaction between the Hla and immune cells have led to an incomplete appreciation for the role of the α-toxin in manipulating the immune response in the skin. Using purified α-toxin to stimulate human $CD4^+$ T cells *in vitro* Niebuhr and colleagues found that sublytic concentrations of the toxin induced secretion of IL-17 (Niebuhr et al., 2010). In contrast, *in vivo* studies using a toxin deficient *S. aureus* strain have shown that the level of IL-17 during an *S. aureus* SSTI is significantly increased when compared to controls (Tkaczyk et al., 2013; Sampedro et al., 2014). Additionally confounding, myeloid lineage specific *ADAM10* knockout mice subcutaneously challenged with a *S. aureus* SSTI have increased dermonecrotic lesions while conditional keratinocyte ADAM10 knockout animals, *Ker14 ADAM10*$^{-/-}$, are protected from *S. aureus*-induced wounds (Becker et al., 2014; Inoshima et al., 2012). While many of these observations seem disparate, uncovering the contribution of specific toxin-mediated injury on T cells during *S. aureus* SSTI may resolve and clarify many of these findings as resident T cells have been reported to be the signaling link between injured keratinocyte injury and infiltrating neutrophils. Similarly, these cells are also mediators of the adaptive immune response (Cho et al., 2010; Sampedro et al., 2014; Murphy et al., 2014; Dillen et al., 2018).

Herein, we identify the α-toxin as a key modulator of immunologic imprinting during recurrent *S. aureus* SSTI. We uncover the role of Hla-injury on innate like T cells during primary *S. aureus* SSTI and its impact on wound healing and immune function. Toxin-mediated injury to innate T cells dampens the ability of these cells to orchestrate keratinocyte proliferation and locally confine staphylococci to a neutrophilic abscess. While these observations likely reflect the action of distinct T cell subsets, not parsed in this work, they highlight and substantiate the ability of the α-toxin-T cell interaction to alter the course of staphylococcal infection.

CHAPTER II

CONTRIBUTION OF α-TOXIN TO *STAPHYLOCOCCUS AUREUS* RECURRENT INFECTION

This majority of the work provided for this chapter has been published as a manuscript in The Journal of Infectious Diseases: Targeting *Staphylococcus aureus* α-Toxin as a Novel Approach to Reduce Severity of Recurrent Skin and Soft-Tissue Infections (DOI: 10.1093/infdis/jiu223). The authors of that manuscript are Georgia R. Sampedro, Andrea C. DeDent, Russell E. N. Becker, Bryan J. Berube, Michael J. Gebhardt, Hongyuan Cao, Juliane Bubeck Wardenburg.

Introduction

Staphylococcus aureus is the leading cause of skin and soft tissue infection (SSTI), resulting in more than 10 million outpatient visits, approximately 500,000 hospital admissions per year in the United States and a substantial economic burden (Hersh et al., 2008; David et al., 2010; Lee et al., 2012). Although most SSTIs are successfully managed with surgical drainage and oral antimicrobial therapy, cutaneous infection can potentiate serious invasive disease and is associated with recurrent infection in up to 50% of patients (David et al., 2010). Recurrent infection contributes to increased morbidity and exposes the patient to multiple antimicrobials, promoting drug resistance. Epidemic community-associated methicillin-resistant *S. aureus* strains that have circulated in the United States for more than a decade are adept at causing recurrent infection in healthy adults and children, suggesting that pathogen-associated traits may increase primary SSTI risk and simultaneously blunt the development of protective immunity. To date, however, there has not been a mechanistic link between specific *S. aureus* virulence

factors and potentiation of reinfection, in part owing to a lack of suitable animal model systems of recurrent SSTI.

Host predictors of reinfection susceptibility have been ill-defined, with the exception of immunodeficiency syndromes, including chronic granulomatous disease and hyper-immunoglobulin E syndrome, which are associated with innate immunity defects that predispose to *S. aureus* infection (Miller et al., 2011). On the other hand, *S. aureus* predictors of reinfection susceptibility can be determined by cases of acquired natural immunity against recurrent *S. aureus* skin infection. One such predictor being Hla, as immunity from SSTI reinfection correlates with an increased level of antibody recognizing *S. aureus* α-toxin (Frtiz et al., 2013). Together, these findings suggest a potential role for this toxin in patterning the host response and highlight a specific virulence factor that may be targeted for intervention during primary SSTI.

S. aureus Hla is a small pore-forming cytotoxin expressed by almost all clinical isolates (Berube et al., 2013). Increased Hla expression has been noted in community-associated methicillin-resistant *S. aureus* strain USA300 and in historic clinical isolates associated with epidemic human disease, correlating with increased severity of SSTI and pneumonia (Bubeck Wardenburg et al., 2008; DeLeo et al., 2011). Hla causes dermonecrotic skin injury by interacting with ADAM10, a zinc-dependent metalloprotease that cleaves E-cadherin and destabilizes the epithelial barrier on toxin binding (Wilke et al., 2010; Inoshima et al., 2012). Supporting the role of the Hla-ADAM10 interaction in pathogenesis, primary SSTI is mitigated by immunization strategies targeting Hla as well as a small molecule ADAM10 inhibitor that blocks toxin binding (Inoshima et al., 2012; Kennedy et al., 2012; Tkaczyk et al., 2013). Coupled with human clinical data on the anti-Hla response in protection against recurrent SSTI (Fritz et al., 2013), these observations suggest that identification of a role for Hla in recurrent infection

could accelerate the development of highly targeted interventions. To this end, we developed a tractable mouse model of *S. aureus* recurrent SSTI to examine the molecular contribution of Hla to reinfection.

Results

To investigate the role of Hla in recurrent *S. aureus* SSTI, we used established mouse models of staphylococcal skin infection as a framework to develop a model of recurrent SSTI (Figure 1A). We infected 4-week-old mice with either 1 x 10^7 WT or isogenic variant forms of *S. aureus* USA300 (primary infection). After a 1-week period of recovery following clearance of the primary lesion, mice were subjected to reinfection on the opposite flank with 3-4 x 10^7 staphylococci (secondary infection). We reasoned that the delivery of a low initial dose would allow pathogen modulation of host immune pathways without causing substantial tissue damage observed with higher inocula (Inoshima et al., 2012). In this model, primary SSTI infection with either wild-type (WT) USA300 (Figure 1B) or an isogenic Hla- mutant (Δ*hla*) confirmed the previously observed virulence defect of the Δ*hla* strain (Kennedy et al., 2012).

Reinfection of these mice with WT *S. aureus* demonstrated larger lesions in mice initially infected with WT *S. aureus* than in those initially infected with the Δ*hla* strain (Figure 1B; statistical analysis in Table 1), suggesting that Hla expression during primary infection interferes with the development of host immunity against recurrent infection. *S. aureus* recovery from primary and secondary lesions harvested 1 or 3 days after reinfection did not differ depending on whether the primary infection was caused by WT or Δ*hla S. aureus* (Figure 1C). These findings are consistent with observations that Hla does not substantially modify bacterial load at early time points after infection and that lesion size is not solely determined by bacterial recovery

(Inoshima et al., 2012; Tkaczyk et al., 2013; Becker et al., 2014). Histopathologic analysis of WT- and Δ*hla*-infected primary lesions 3 days after infection revealed abscesses confined to the subcutaneous space without overlying epidermal injury (Figure 1D, left panels). The appearance of lesions harvested after secondary infection was notable for increased epidermal damage and lesion size relative to primary infection, consistent with the increased inoculum (Figure 1D, right panels). These findings, however, were less severe in mice initially infected with Δ*hla* than in those infected with WT *S. aureus* (Figure 1D, right panels). Although a significant inflammatory cell infiltrate is apparent at 3 days after infection in primary lesions, this appears less prominent at the same interval after reinfection. In contrast, the overall histologic appearance of primary and secondary lesions in both conditions appears similar 1 day after infection (Figure 2A), again revealing the earlier onset of epidermal injury in mice that received primary infection with WT versus Δ*hla S. aureus*. Consistent with the findings of Tkaczyk et al (Tkaczyk et al., 2013), who observed that genetic deletion of Hla or immunotherapeutic neutralization of the toxin led to increased host interleukin 1β and 17 responses to skin infection, we observe these cytokine alterations after primary infection in our model system (Figure 2B).

Because Hla pore formation is required for cytotoxicity to epithelial cells and toxin-mediated ADAM10 activation that results in epithelial barrier injury (Wilke et al., 2010; Inoshima et al., 2012; Inoshima et al., 2011), we examined the requirement for toxin activity in susceptibility to recurrent infection. To this end, we used a Δ*hla* mutant USA300 strain complemented with plasmid-encoded WT Hla (Δ*hla*::p*hla*) or an Hla variant containing a single amino acid substitution (Hla_{H35L}, Δ*hla*::phla_{H35L}) that retains ADAM10 binding capability but is unable to form the injurious pore, thereby functioning as a dominant-negative toxin (Wilke et al.,

2010). Complementation leads to approximately 3-fold overexpression of WT Hla or Hla_{H35L} (Figure 5A, inset) (Bubeck Wardenburg et al., 2008).

Primary infection of mice with WT, Δ*hla*, Δ*hla*::p*hla*, or Δ*hla*::phla_{H35L} demonstrated the effect of active Hla on infection severity, because active Hla overexpression by the Δ*hla*::p*hla* strain resulted in severe skin lesions, whereas the Δ*hla*::phla_{H35L} was associated with a minimal lesion similar to the Δ*hla* mutant (Figure 3A; statistical analysis inTable 2). Reinfection of these mice with WT USA300 demonstrated that the most significant degree of protection was afforded by primary infection with the Δ*hla*::phla_{H35L} strain (Figure 3B, followed by the Δ*hla* strain, indicating that the absence of toxin activity during primary infection is beneficial to the host in establishing a protective response to reinfection (statistical analysis in Table 3).

Primary infection with the Δ*hla*::p*hla* strain was significantly less protective than the Δ*hla*::phla_{H35L} strain in spite of the similar level of toxin produced by these strains (Figure 3C). Histopathologic analysis of skin lesions from these two groups of mice revealed larger lesions and increased tissue injury in Δ*hla*::p*hla*-infected mice after reinfection than in those with primary infection caused by Δ*hla*::phla_{H35L} *S. aureus* (Figure 3C). The serum anti-Hla antibody titer after primary infection with Δ*hla*::p*hla* (Figure 4A) and Δ*hla*::phla_{H35L} was significantly elevated relative to Δ*hla* and similar in the two complemented strains (statistical analysis in Table 4). After secondary infection, anti-Hla titers increased in all conditions relative to the corresponding primary infection (Figure 4A). Titers in mice initially infected with Δ*hla*::p*hla* or Δ*hla*::phla_{H35L} were significantly elevated compared with both WT and Δ*hla* primary-infected mice (Figure 4A) but did not differ between mice initially infected with Δ*hla*::p*hla* or Δ*hla*::phla_{H35L}. Examination of serum toxin-neutralizing activity two weeks after reinfection

demonstrated that mice initially infected with Δ*hla*::p*hla* or Δ*hla*::p*hla*$_{H35L}$ (Figure 4B) mount a significant response relative to preinfected animals, whereas those with WT primary infection only demonstrated a trend toward neutralization. The magnitude of this response, however, was indistinguishable between reinfected groups and was significantly weaker than in serum samples harvested from mice passively immunized with a well-characterized, Hla-neutralizing monoclonal antibody (red circles in Figure 4B) (Ragle et al., 2009).

The observation that primary infection with Δ*hla*::p*hla* and Δ*hla*::p*hla*$_{H35L}$ leads to the generation of quantitatively and qualitatively equivalent antibody responses, yet distinct reinfection outcomes, underscores the importance of the active toxin in modulating the host response. Importantly, these data suggest that an anti-toxin antibody response alone is insufficient to optimize protective immunity against recurrent SSTI. We hypothesized that reinfection severity may be reduced by deliberate antagonism of Hla activity, coupled with preservation of antigenic exposure during primary infection to stimulate the development of toxin-neutralizing antibodies. Because SSTI is primarily managed in the outpatient setting, a clinically effective therapeutic intervention must be cost-effective for delivery to a large number of otherwise healthy patients who present with primary SSTI and an indeterminate risk for recurrence. We therefore examined therapeutic delivery of either recombinant, dominant-negative Hla$_{H35L}$ or a small molecule active-site inhibitor of ADAM10 that blocks Hla receptor binding (GI254023X) (Inoshima et al., 2011) to reduce reinfection severity. These novel strategies were predicted to maintain host exposure to Hla while abrogating toxin activity during primary infection. Therapy was delivered as a single intralesional dose 6-8 hours after primary WT *S. aureus* infection (Figure 5A); these treatments blunted primary skin lesions (Figure 5B).

After reinfection, lesion size was substantially reduced in mice treated with either Hla_{H35L} (Figure 6A) or the ADAM10 inhibitor (Figure 6B), compared with the respective control mice.

Because the literature describes disparate susceptibility outcomes for host genetic mutants (IL-17 and IFN-γ deficient mice) infected with *S. aureus* at cutaneous or invasive tissue sites, we hypothesized that tissue context impacts the role of Hla in *S. aureus* recurrence patterns (Cho et al., 2010; Ishigmae et al., 2009; Brown et al., 2015; Lin et al., 2009; Sampedro et al., 2017). In order to address this, we developed a model whereby *S. aureus* cutaneous infection is followed by lethal dose of *S. aureus* pneumonia (Figure 7A). In this model, animals exposed to the toxin subcutaneously during primary *S. aureus* SSTI are less likely to succumb from subsequent *S. aureus* pneumonia (Figure 7B, statistical analysis in Table 5). Further, active Hla overexpression by the Δ*hla*::p*hla* strain correlated with the greatest protection from lethal *S. aureus* disease (Figure 7C). One possible explanation for this phenomenon may be that Hla-mediated injury to the epidermis results in low level *S. aureus* antigen circulation that can potentiate the immune response for invasive infection but not for cutaneous *S. aureus* disease. This finding is interesting in light of human *S. aureus* epidemiologic data that demonstrates that children who develop a primary cutaneous insult are more likely to have repeated cutaneous *S. aureus* SSTIs but children who initially develop an invasive *S. aureus* infection are less likely to develop any type of subsequent recurrent *S. aureus* infection (Fritz et al., 2013). These data suggest the host may develop durable immunity to invasive disease more readily and through a different mechanism than for cutaneous infection. The hypothesis that *S. aureus* immunity relies on the exposure history and tissue context in which exposure occurs may explain the pronounced heterogeneity in anti-staphylococcal antibody levels seen in both children and adults (Dryla et

al., 2005). Future work should provide mechanistic insight into the underlying immunological molecular features that Hla perturbs in specific tissue context during *S. aureus* infection.

Discussion

Together, these results suggest that reinfection abscess severity is a functional integration of two distinct but related processes: (1) the deleterious effects of active Hla on host cells during primary infection and (2) the degree of antigenic exposure to Hla. Although the presence of active Hla impairs host protective responses to reinfection (Figure 1B, 1D, 2B, and 2C), antigenic exposure in the context of toxin overexpression (Figure 4B) or inactive toxin (as with the Hla_{H35L} mutant or in the presence of the ADAM10 inhibitor; Figure 6A, B) seems to promote the generation of a toxin-neutralizing antibody response. Toxin-neutralizing approaches seem to afford the additional benefit of limiting the harmful effects of the active toxin on host immunity. Hla causes direct cytotoxicity to immune cells (Nygaard et al., 2013; Nygaard et al., 2012; Abtin et al., 2014), also demonstrating the ability to modulate immune cell recruitment, inflammasome activation, host cytokine and responses, and bacterial killing (Berube et al., 2013).

To date, the impact of Hla on host immune responses has been investigated only during primary infection, with recent studies underscoring the complex effects of the toxin in the tissue microenvironment. Deletion of Hla or prophylactic passive immunization with an anti-Hla monoclonal antibody augments tissue expression of multiple cytokines and chemokines, correlated with priming of the Th1 and Th17 responses and improved SSTI outcome (Tkaczyk et al., 2013). In contrast, loss of Hla sensitivity by the selective deletion of ADAM10 on myeloid lineage cells leads to exacerbated skin lesions and a dampened host interleukin 1β response to primary infection, indicative of a beneficial effect of toxin immune priming (Becker et al., 2014).

These observations indicate that detailed analysis of cell-type specific immune responses to Hla during primary infection is required to elucidate how the toxin manipulates immunity and predisposes to recurrent infection. Because toxin antagonism does not fully eliminate recurrent infection, our findings clearly indicate that virulence factors other than Hla modulate the host response to reinfection. It will be of interest to define these factors and the molecular mechanisms by which multiple factors act in concert to blunt the development of protective immunity.

CHAPTER III

ANALYSIS OF THE α-TOXIN-ADAM10 INTERACTION ON T CELLS DURING PRIMARY *S. AUREUS* SKIN AND SOFT TISSUE INFECTION (SSTI)

The work provided for this chapter will be submitted for publication. *Staphylococcus aureus* α-toxin targets skin peripheral T cells to impede wound repair. The authors of that manuscript will be Georgia R. Sampedro, Michael Shih, Jakub Kwiecinski and Juliane Bubeck Wardenburg.

Introduction

The epidermis both protects the body from invading pathogens and has the capacity to self-renew and repair epithelial injury as an end to maintain barrier homeostasis. When the epidermis is wounded by a pathogen, resident T cells sense the damage from neighboring injured keratinocytes and can simultaneously trigger the epithelial repair pathway and initiate the cutaneous immune response. Due to their anatomical location and wide-spread spatial distribution across the epithelium where they interdigitate with keratinocytes, epidermal cutaneous resident T cells, namely γδ T cells, are the initial respondents to keratinocyte injury produced during wounding (Hayday 2009; Chodaczek et al., 2012). In the context of infection or chronic wounding, γδ T cells must secrete cytokines like IL-17 and IFN-γ that direct the ensuing immune response to the node of infection and simultaneously release epidermal proliferation factors such as, KGF-1 and KGF-2 to initiate re-epithelialization of the torn tissue (Chien et al., 2013; Jameson et al., 2002; MacLeod et al., 2013). To this end, this makes γδ T cells the nexus between epithelial-immune crosstalk. Studies have demonstrated, in the context of infection, a variety of infectious agents target γδ T cells to cause epithelial damage (Maccario et al., 1993;

Poccia et al., 2009; Knight et al., 2010). To our knowledge, however, the link between the micro-bacterial and cutaneous environment have been limited in scope and do not offer mechanistic insight into how a specific virulence factor can impede γδ T cell function.

S. aureus can infect nearly every tissue space in the human host and for this reason it is a world-wide leading etiologic agent of pneumonia, sepsis, osteomyelitis, and skin and soft tissue infections (SSTI) (Ani et al., 2015; Klevens et al. 2007; Lowy 1998). Notwithstanding, *S. aureus* most commonly causes skin infection (McCaig et al., 2006; Challangundla et al., 2018). While SSTIs are often self-limiting, the skin is the prevailing site of persistent *S. aureus* colonization and *S. aureus* recurrent infections that have the potential to cause non-healing deep tissue infections that can be life-threatening. The success of *S. aureus* as a skin pathobiont relies on its brigade of virulence factors that promote keratinocyte injury, immunoevasion, and nutrient acquisition (Oikonomopoulou et al., 2012; Foster et al., 2005; Berube et al., 2013; Vandenesch et al., 2012; Foster et al., 1998; Nizet, 2007; Rooijakkers et al., 2005; Parker et al., 2011). Due to waning effectiveness of antibiotics against this pathogen and the potentiation of drug resistance, detailed knowledge of the underlying molecular mechanism by which specific virulence factors perturb the complex multi-cellular interactions in the skin is required to inform vaccination strategies and novel host targeted prophylactic therapies.

Observations of the host's immunologic response to *S. aureus* cutaneous infection illuminate the quintessential components of the epithelial- immune response. Keratinocytes and resident cells activate pattern recognition receptors such as, cell surface TLR2 as well as intracellular NOD2 through the detection of *S. aureus* cell wall moieties triggering signaling cascades that produce cytokine, chemokines, and antimicrobial peptides (Fournier B, 2012; Hruz et al., 2009). Likely, through an unknown antigen, injured keratinocytes subsequently activate

resident neighboring T cells to secrete IL-17 and along with secreted signals from perivascular macrophages these cells induce neutrophil-attracting chemokines and granulopoiesis factors including keratinocyte chemoattractant (KC/CXCL1), macrophage inflammatory protein-2 (MIP-2/CXCL8), and granulocyte monocyte colony stimulating factor (GM-CSF) that promote neutrophil recruitment and abscess formation to contain *S. aureus* (Cho et al., 2010; Dillen et al., 2018; Cua and Tato, 2010; Witherden et al., 2010; McLoughlin et al., 2006; Abtin et al., 2014). Subsequently, at the site of infection, activated neutrophils produce myeloid peroxidase (MPO) and hypohalous acids to carry out their antimicrobial function in addition to secreting IL-1β to mobilize additional neutrophils from the bone marrow (Cho et al., 2012).

One of the earliest events during *S. aureus* skin infection is the breach of the epidermal barrier and destruction of the local skin tissue microenvironment by *S. aureus* cytotoxins that is distinguishable by necrotic wounds overlying the infection nidus (Kennedy et al., 2010; Inoshima et al., 2012; Berube et al., 2014; Wang et al., 2007; Malachowa et al., 2012). Of particular interest, α-toxin activity in the skin modulates most of the events that comprise a productive epithelial-immune response. The dual-nature of Hla intoxication triggers immune cell activation but also damages host cells both by lytic pore formation and ADAM10 activity. On keratinocytes and innate cells, α-toxin-pores are a conduit for *S. aureus* cell wall moieties to activate intracellular pattern recognition receptor, NOD2. Also, α-toxin injury to neutrophils and monocytes stimulates NLRP3-inflammasome signaling that ultimately, enhances neutrophil production of IL-1β (Craven et al., 2009; Kebaier et al., 2012; Becker et al., 2014). Concurrently, Hla-mediated ADAM10 activation on keratinocytes potentiates injury via cleavage to both E-cadherin that links the epidermal meshwork and CXCL1 that serves as a neutrophil chemotactic gradient (Inoshima et al., 2012; Norrby-Teglund, oral presentation). Additionally, perivascular

macrophages intoxicated by Hla also have altered neutrophil homing signals preventing neutrophil extravasation into the injured skin (Abtin et al., 2014).

We identified Hla as a key *S. aureus* determinant in primary and recurrent cutaneous disease models (Sampedro et al., 2014). Probing into mechanism, we found two inflammatory cytokines, IL-17 and IL-1β, were upregulated in toxin-deficient *S. aureus* infected skin homogenates when compared to controls (Sampedro et al., 2014; Tkaczyk et al., 2013). Conversely, purified α-toxin *in vitro* has been shown to stimulate human $CD4^+$ T cells to secrete IL-17 (Niebuhr et al., 20120). Furthermore, *Ker14 ADAM10*$^{-/-}$ mice challenged with *S. aureus* SSTI are resistant to lesion formation whereas *LysM ADAM10*$^{-/-}$ mice have larger necrotic lesions when compared to controls (Inoshima et al., 2012; Becker et al., 2014). The toxin's perturbation of this pathway seems to exemplify the dual-nature of α-toxin injury and cellular activation.

To resolve the role of the toxin in immune-cutaneous pathology and assess whether Hla mediated injury directly impairs cutaneous T cells *in vivo*, we excised ADAM10 from peripheral T cells, using Cre-lox technology. To this end, the current study exposes how a single *S. aureus* virulence factor, Hla, can mediate injury to cutaneous resident T cells to concomitantly impede immune response and barrier renewal during a *S. aureus* SSTI.

Results

Generation of T cell-specific ADAM10 knockout mice

To examine the contribution of the Hla-ADAM10 complex on peripheral T cells during *S. aureus* SSTI, we generated peripheral T cell ADAM10 knockout mice, *dLck*$^{+/-}$ *ADAM10*$^{+/+}$. Deletion of *ADAM10* during early stages of thymocyte development impairs TCR function and

generates a block in T-cell development (Manilay et al., 2005). To circumvent this problem, *ADAM10* deletion was activated under the T-cell specific distal src-family protein tyrosine kinase promoter (*dLck*) that is upregulated only in mature lymphocytes (Zhang et al., 2005). Mice harboring floxed alleles of *ADAM10* exon 3 (*ADAM10*$^{loxP/loxP}$) were crossed to mice expressing a Cre recombinase under control of this distal *Lck* promoter (Figure 8A). Throughout this work, *dLck*$^{+/-}$ *ADAM10*$^{-/-}$ and *dLck*$^{+/-}$ *ADAM10*$^{+/+}$ (control) mice were then bred to a double fluorescent reporter mouse line whereby Cre-mediated excision turns *dLck*$^{+/-}$ cells green (GFP^{+}) and Cre negative cells remain red (Tdtomato, RFP^{+}) (*Rosa*$^{+}$ *dLck*$^{+/-}$ *ADAM10*$^{+/+}$ *or Rosa*$^{+/-}$ *dLck*$^{+/-}$ *ADAM10*$^{-/-}$ mice) (Muzumdar et al., 2007) or a single fluorescent reporter mouse line by which Cre-mediated excision turns *dLck*$^{+}$ cells red (RFP^{+}) (*Ai9*$^{+/-}$ *dLck*$^{+/-}$ *ADAM10*$^{-/-}$) (Madisen et al., 2010). Loss of *ADAM10* exon 3 by the cre-excision of the floxed genomic region was documented in primary GFP^{+} and RFP^{+} splenic lymphocytes harvested from control and *Rosa*$^{+/-}$ *dLck*$^{+/-}$ *ADAM10*$^{-/-}$ mice (Figure 8B, lane 3). Consistent with the initial report describing the use of *dLck* promoter as a driver of Cre expression we find that recombination in *dLck*$^{+/-}$*ADAM10*$^{-/-}$ mice does not alter splenic T cell counts on subpopulations of CD3^{+}, CD4^{+}, and CD8^{+} T cells (Figure 8G). In the cutaneous epithelium, microscopic analysis of GFP^{+} *dLck*$^{+}$ T cells confirms the morphological pattern and distribution of T cells in naïve skin to be equivalent between groups (Figure 8C, D, F). And while lymphocytes are numerically equivalent amongst groups, *in vitro* functional analysis of toxin mediated injury to splenic derived *dLck*$^{+/-}$ *ADAM10*$^{-/-}$ primary T cells demonstrate that ADAM10 knockout T cells are resistant to lysis when exposed to a concentration gradient of Hla that is able to elicit lysis of wild-type cells as measured by LDH release (Figure 8E).

Contribution and dynamics of α-toxin injured cutaneous T cells during *S. aureus* SSTI

To test whether *dLck*$^{+/-}$ *ADAM10*$^{-/-}$ mice are susceptible to the toxin *in vivo* we subcutaneously infected the backskins of 4-6-week-old mice with 2-3 x 10^7 staphylococci. Over the 10-day monitoring period when compared to controls, *dLck*$^{+/-}$ *ADAM10*$^{-/-}$ mice demonstrate faster healing wounds (Figure 9B). Representative examples of backskin wounds on these mice on day 5 post *S, aureus* infection are shown in Figure 9A. Colony forming unit enumeration from homogenized *dLck*$^{+/-}$ *ADAM10*$^{-/-}$ and control *S. aureus*-infected backskin following challenge have equivalent loads of *S. aureus* between groups with an overall decrease in bacterial load overtime indicative of bacterial clearance (Figure 9C). These findings are consistent with prior observations that α-toxin does not substantially modify the bacterial load at early time points after infection and that lesion size is not solely determined by bacterial recovery (Inoshima et al., 2012; Tkaczyk et al., 2013; Becker et al., 2014; Sampedro et al., 2014).

The delay in backskin wound closure in *dLck*$^{+/-}$ *ADAM10*$^{+/+}$ animals agreed with ear wounded area and thickness recordings from epicutaneous *S. aureus* challenge with in ear pinnae of mice. Representative examples of and lesion recordings from day 2 *S. aureus* infected ears of control and *dLck*$^{+/-}$ *ADAM10*$^{-/-}$ animals demonstrate that in this model α-toxin protected T cells also have diminished wounding (Figure 9D and E). In this infection model, control mice also reveal the development of larger purulent lesions at the infection site with broader areas of epidermal crusting and increased inflammation that are significantly diminished in *dLck*$^{+/-}$ *ADAM10*$^{-/-}$ mice (Figure 9F).

Spanning from *S. aureus* infection onset to later time points, macroscopic histopathologic analysis of backskin from *dLck*$^{+/-}$ *ADAM10*$^{-/-}$ and control mice from day 2 and 7 post *S. aureus* infection reveal alterations in disease pathology. *dLck*$^{+/-}$ *ADAM10*$^{-/-}$ infected backskins have a

singular, defined abscess that are confined to the subcutaneous space with a minor eschar (scab) overlying the abscess. In contrast, *dLck*$^{+/-}$ *ADAM10*$^{+/+}$ *S. aureus* wounds often form multiple, smaller discontinuous abscesses and display large areas of overlying wound beds that often span almost the entirety of the collected skin specimen (Figure 10A and B, main images, black arrows demarcate wound bed).

Underlying with the striking differences in wound bed sizes between groups, analysis of the epidermis reveals that *dLck*$^{+/-}$ *ADAM10*$^{-/-}$ animals have an overall preservation of epidermal architecture, epidermal proliferation, and epidermal T cells. Higher magnification at the unwounded edges of the tissue sample in hematoxylin and eosin and Ki67^{+} serially stained sections from *S. aureus* infected backskins demonstrate that the epidermis even at distant sites from the infection nidus are more preserved overtime in *dLck*$^{+/-}$ *ADAM10*$^{-/-}$ animals when cpmaored to control (Figure 10A and B, boxed images). Furthermore, a comparison of epidermal thickness between day 2 and day 7 *S. aureus* infected backskin samples reveals that *dLck*$^{+/-}$ *ADAM10*$^{-/-}$ animals have increased epidermal thickness overtime while control epidermal thickness is stagnant (Figure 11C). Immunostaining with anti-CD3^{+} antibody exposed an increased number of CD3^{+} T cells sustained adjacent to the wounded edge of *dLck*$^{+/-}$ *ADAM10*$^{-/-}$ suggesting that the number of toxin resistant T cells were contributing to the regulation of epidermal homeostasis post wounding (Figure 11A, B). Additionally, corresponding with quantification of CD3^{+} T cell counts from Figure 11A, macroscopic analysis of max projected fluorescent tile scans counterstained with Dapi from backsinks of control and *Ai9*$^{+}$ *dLck*$^{+/-}$ *ADAM10*$^{-/-}$ mice harvested 2 days after *S.aureus* infection also show an increased level of *Ai9*$^{+}$ *dLck*$^{+}$ epidermal T cell adjacent to *S. aureus* wound bed (Figure 12A, C).

Due to the striking difference in the backskin between *dLck*$^{+/-}$ *ADAM10*$^{-/-}$ and control animals as early as day 2 we assayed the functional capacity of keratinocytes to proliferate and migrate to the wound bed in response to *S. aureus* injury. To this end, we infected backskins of *Ai9*$^{+}$ *dLck*$^{+/-}$ *ADAM10*$^{-/-}$ and control animals and at the day 2 interval pulsed the mice with 5-ethynyl-20-deoxyuridine (EdU) for 4 hours before harvesting and analyzing their skins. Immunstaining for EdU incorporation, as quantified in tissue sections, also demonstrates there are more EdU labeled keratinocytes adjacent to the wound bed in *Ai9*$^{+}$ *dLck*$^{+/-}$ *ADAM10*$^{-/-}$ than in controls (Figure 12B, D) indicating that accelerated keratinocyte proliferation contributes to faster wound healing in *dLck*$^{+/-}$ *ADAM10*$^{-/-}$ mice. These results are consistent with the functional capacity of epidermal T cells to stimulate re-epithelialization of wounded skin (Havran and Jameson, 2010). Tissue specimen also demonstrate more EdU labeled cells in the hair follicles of *dLck*$^{+/-}$ *ADAM10*$^{-/-}$ animals when compared with controls; although, more testing with a larger sample size is required to know if this phenomenon is reproducible. Nevertheless, this is an exciting possibility as recently, it has been reported that IL-1 and IL-17 producing epidermal T cells stimulate keratinocyte proliferation during wounding by mobilizing stem cells within the bulge of the hair follicle (Lee et al., 2017).

To further characterize the spatial relationship between *S. aureus* and cutaneous *dLck*$^{+}$ T cells we infected *Rosa*$^{+/-}$ *dLck*$^{+/-}$ *ADAM10*$^{-/-}$ and control mouse ears with yellow fluorescent expressing protein, YFP^{+} *S. aureus*. As early as 24-hr post infection, maximum intensity projections of whole-mounted ear challenged with YFP^{+} *S. aureus* reveal that mutant mice have more T cells adjacent to the *S. aureus* origin. In contrast, control mice show a dramatic decrease in the number T cells near the infection nidus, suggesting that direct Hla intoxication of T cells changes the skin's immune potential by killing resident T cells in early hours of skin infection

(Figure 13A-D). Irrespective of body site or infection method, together, these studies expose Hla-specific injury to resident T cells to cause perturbations to T cell number that is accompanied by a loss of epidermal barrier integrity during *S. aureus* SSTI.

α-Toxin injury to cutaneous T cells alters the level of IL-17 and neutrophil activity in the tissue microenvironment

During *S. aureus* SSTI, resident lymphocytes detect keratinocyte injury and upregulate IL-17. Increases in the level of Il-17 in the tissue microenviornment induces the expression of neutrophil-attracting chemokines from keratinocytes that recruit circulating neutrophils to the site of infection. In temporal waves, recruited neutrophils encapsulates the staphylococci, termed the staphylococcus abscess (Cheng et al., 2011). Previously, we reported that Hla-mediated injury to keratinocytes during an *S. aureus* SSTI manifests as the necrotic epidermis above the abscess (Inoshima et al., 2012). We reason that Hla-mediated injury to keratinocytes is a prerequisite for lymphocyte cutaneous release of IL-17. Indeed, when we tested IL-17 levels in *S. aureus* infected skin homogenates by ELISA from *Ker14 ADAM10*$^{-/-}$, the level of IL-17 in the tissue was minimal when compared to controls (Figure 14A). Thus, while toxin injury to keratinocytes may activate T cells, simultaneously, Hla intoxication of resident T cells may decrease the overall lymphocyte function in the skin microenvironment. Correspondingly, when compared with controls, significantly higher levels of IL-17 are found in *S. aureus*-infected skin homogenates from animals with T cells that are resistant to α-toxin (Figure 14B). To determine whether the lower levels of IL-17 in *dLck*$^{+/-}$ *ADAM10*$^{+/+}$ mice were associated with a reduction in neutrophil recruitment into the skin, we assessed the level and location of myeloid peroxidase activity (MPO), a proxy of neutrophil activity during *S. aureus* infection. *Ex vivo* biochemical

analysis for MPO in *S. aureus* infected backskins were higher in *dLck*$^{+/-}$ *ADAM10*$^{-/-}$ animals when compared with controls (Figure 14C). Further, *dLck*$^{+/-}$ *ADAM10*$^{-/-}$ *S. aureus*-infected backskin but not control sections from day 2 and day 7 post infection reveal MPO is localized to the staphylococcus abscess in a temporal ring-manner that both contain the *S. aureus* infection and focus immune infiltrate (Figure 14D). Lastly, restoring IL-17 function to control mice by intralesional addition of recombinant IL-17 (rIL-17) during early hours of *S. aureus* infection increases wound healing rates to the level of *dLck*$^{+/-}$ *ADAM10*$^{-/-}$ animals and protects them from secondary *S. aureus* SSTI (Figure 23A-D). These results provide compelling evidence that if resident T cells are resistant or protected from toxin-mediated injury, containment of *S. aureus* by the IL-17-neutrophil axis can accelerate primary wound repair and improve immunocompetence to subsequent *S. aureus* SSTI.

γδ T cells are a main Hla-intoxicated T cell subset during *S. aureus* SSTI

T cells expressing the Vδ1^{+} γδ T cell receptor are abundant and preferentially localize in epithelial tissue such as the skin, intestine, uterus, and tongue (Witherden and Havran, 2011). In mice, γδ T cell represent over 90% of the epidermal T cells (Sulcova et al., 2015). Following a stress signal such as keratinocyte wounding, γδ T cells can become activated and promote epidermal stem cell proliferation by secreting, FGF7 (Jameson and Havran, 2007). Furthermore, γδ T cells can also recruit other immune cells such as macrophages and neutrophils by secreting IL-17 (Jameson et al., 2002; Pantelyushin et al., 2012; Cho et al., 2010). Due to the striking site-specific reduction of epidermal T cells, the decrease in keratinocyte proliferation, and reduction of IL-17 and neutrophil activity in wild-type animals, we postulated that the subset of *dLck*$^{+}$ T cells being targeted by the toxin are γδ T cells.

To visualize the percentage of GFP^{+} *dLck*$^{+}$ T cells that were γδ T cells in epidermal sheets from naïve, PBS treated (mock), and *S. aureus* infected *dLck*$^{+/-}$ *ADAM10*$^{-/-}$, and *dLck*$^{+/-}$ *ADAM10*$^{+/+}$ animals were subjected to γδ TCR immunostaining. Subsequently, 3D surface reconstructions of both GFP^{+} *dLck*$^{+}$ T cells and γδ TCR immunostaining in these experimental groups were rendered and analyzed using an Imaris surface-to-surface co-localization algorithm. In every group, detection of co-localization between *dLck*$^{+}$ T cells and the γδ TCR antibody, was equal to or higher than 70%, exposing most *dLck*$^{+}$ T cells to be bona fide dendritic epidermal γδ T cells (DETCs) (Figure 15A, B). DETC quantification revealed that DETC numbers were equivalent in naïve and PBS-injured groups confirming that our *S. aureus* delivery modality alone did not cause *dLck*$^{+}$ T cell aberrations. When compared with *S. aureus* infected *dLck*$^{+/-}$ *ADAM10*$^{-/-}$ samples, epicutaneous *S. aureus* challenge in wild-type animals lead to >4-fold reduction in DETCs proximal to the *S. aureus* wound edge (Figure 15C). Additionally, *S. aureus* infected *dLck*$^{+/-}$ *ADAM10*$^{-/-}$ epidermal sheets also contained more DETCs than in naïve and mock infected groups reminiscent of the γδ T cell phenotype of clustering around wound edges (Figure 15A, bottom right panel) (Jameson et al., 2002). In sterile injury studies, DETCs are not only known to cluster but also to change from a dendritic to a rounded morphology as they enter an activated state around a wound edge (Chodaczek et al., 2012; Jameson et al., 2002). We therefore examined DETC morphology changes in *dLck*$^{+/-}$ *ADAM10*$^{-/-}$ and controls. Intriguingly, DETCs in both groups near the *S. aureus* nidus were more rounded and displayed fewer dendrites than in naïve or mock conditions indicating that the activation status may not differ between *dLck*$^{+/-}$ *ADAM10*$^{-/-}$ and *dLck*$^{+/-}$ *ADAM10*$^{+/+}$ animals. Instead, it is plausible that toxin susceptibility in control animals may result in cell death that in totality reduces the amount of activated γδ T cells that can respond to *S. aureus* insult (Figure 15D).

To measure Hla-mediated cytotoxicity, primary DETCs from *dLck*$^{+/-}$ *ADAM10*$^{-/-}$ and controls were challenged *ex vivo* with increasing concentrations of the toxin and measured for lactate dehydrogenase release and ATP release. When compared to controls, *dLck*$^{+/-}$ *ADAM10*$^{-/-}$ γδ T cells remain resistant to toxin-mediated cell death supporting the likely scenario that *dLck*$^{+/-}$ *ADAM10*$^{-/-}$ γδ T cells near the *S. aureus* wound site survive while control T cells die in an Hla-dependent manner (Figure 16A, B).

TCRδ$^{-/-}$ mice harbor a pfk-neomycin cassette disrupting the TCRδ constant gene segment, Cδ, preventing the expression of a TCRδ chain and resulting in the complete loss of γδ T cells (Itohara et al., 1993). These mice still express T cells in the epidermis but they are T cells bearing the αβ TCR (Itohara et al., 1993). During *S. aureus* SSTI, TCRδ$^{-/-}$ mice have been reported to have lower IL-17 levels, decreased neutrophil activity, less bacterial clearance, and larger, slower healing wounds than both WT animals and TCRβ$^{-/-}$ animals, suggesting that αβ T cells cannot recapitulate the functional role of γδ T cells in *S. aureus* disease pathogenesis (Cho et al., 2010). In order to confirm if γδ T cells are the subset of Hla-intoxicated T cells that account for the improved wound healing rates in *dLck*$^{+/-}$ *ADAM10*$^{-/-}$ mice, TCRδ$^{-/-}$ mice were crossed with *dLck*$^{+/-}$ *ADAM10*$^{-/-}$ to generate TCRδ$^{-/-}$ *dLck*$^{+/-}$ *ADAM10*$^{-/-}$ mice. Epidermal sheets from TCRδ$^{+/-}$ *dLck*$^{+/-}$ *ADAM10*$^{-/-}$ and TCRδ$^{-/-}$ *dLck*$^{+/-}$ *ADAM10*$^{-/-}$ animals were immunostained with anti-TCRδ confirming that TCRδ$^{-/-}$ *dLck*$^{+/-}$ *ADAM10*$^{-/-}$ mice are γδ T cells deficient (Figure 17A). Although further testing and controls are needed, TCRδ$^{-/-}$ *dLck*$^{+/-}$ *ADAM10*$^{+/+}$ and TCRδ$^{-/-}$ *dLck*$^{+/-}$ *ADAM10*$^{-/-}$ subcutaneously infected with 3 x 10^7 *S. aureus* were both highly susceptible to infection demonstrating that γδ T cells are likely a target of early α-toxin-mediated injury in the skin (Figure 17B).

α-Toxin alters the spatial arrangement of γδ T cell around the abscess and wound edge

C57BL/6 mice infected with Δ*hla S. aureus* SSTI have increased levels of γδ T cells secreting IL-17, improved secretion of neutrophil chemoattractant such as- KC, MIP-2, G-CSF, more neutrophil infiltrate, and smaller wounds when compared with animals infected with WT *S. aureus* (Tkaczyk et al., 2013; Sampedro et al., 2014). Thus, we wanted to examine whether the spatial distribution of γδ T cells is also altered by the presence of Hla in the skin tissue microenvironment. To this end, we examined the anatomical location of γδ T cells in the backskins of either WT or Δ*hla*-infected animals, utilizing a γδ T cell reporter mouse, Tcrd-H2BEGFP$^{+/+}$, in which γδ T cells can be visualized by GFP fluorescence independently of TCR surface expression (Prinz et al., 2006). Assuredly, when we compare the number of epidermal γδ T cells from Tcrd-H2BEGFP$^{+/+}$ mice infected with Δ*hla* versus mice infected with WT *S. aureus* there is a dramatic increase in the number of γδ T cells proximal to the wound bed in Δ*hla*-infected micE (Figure 18B, C, and E); similar to but with a higher intensity than the increase of epidermal γδ T cells seen in both ear and backskin samples of *dLck*$^{+/-}$ *ADAM10*$^{-/-}$ when compared to controls. Further, we observe that dermal γδ T cells spatially cluster to surround the neutrophilic abscess (Figure 18A and B). The number of γδ T cells in Δ*hla* infected backskin sections is not only higher than in backskins infected with WT *S. aureus* but also higher than in naïve samples suggesting that the dermal γδ T cells visible in the Δ*hla* infected samples may be infiltrating γδ T cells (Figure 18D and E). Using an Imaris distance transformation, we calculated the proximity of γδ T cells to the abscess to be closer than that of γδ T cells in backskins infected with WT *S. aureus* (Figure 18C). In contrast to this finding, we do not observe dermal γδ T cells in *Ai9*$^{+/-}$ *dLck*$^{+/-}$ *ADAM10*$^{-/-}$ to display this spatial distribution surrounding the *S. aureus* abscess. Presumably, in *Ai9*$^{+/-}$ *dLck*$^{+/-}$ *ADAM10*$^{-/-}$ animals the direct intoxication of T cells does not eliminate the possibility that there is toxin-mediated damage to other cell-types in the tissue

micro-environment that may be required to signal to the γδ T cells to aggregate around the abscess. It is attractive to hypothesize that the clustering of γδ T cells near the abscess and wound bed provides a spatial signal that in conjunction with their chemical activatory signal can form a spatial-chemical gradient that correctly orients both keratinocyte proliferation and neutrophils infiltrate to the nidus of infection.

Discussion

In our study, we demonstrate that Hla-mediated injury to cutaneous T cells slows *S. aureus* wound healing. Underlying this disease pathology, we trace how both components of the epithelial wound repair cascade and the immune response are linked to the initial Hla-mediated injury of epidermal T cells. Hla-mediated intoxication to resident T cells causes an overall decrease in T cell number adjacent to the *S. aureus* wound site following both subcutaneous and epicutaneous challenge that is accompanied by a delay in re-epithelialization. Simultaneously, immune function is dampened as measured by lower levels of IL-17, a decrease in neutrophil activity, and larger *S. aureus*-induced wounds.

Due to the toxin-induced perturbation of keratinocyte proliferation and the dampening of IL-17 levels in the *S. aureus* infected tissue of control animals we reasoned that the $dLck^{+}$ T cells we were investigating are γδ T cells. Staining of GFP^{+} $dLck^{+}$ T cells with an anti- γδ TCR antibody confirmed their overlap and paralleled the deficit of $dLck^{+}$ T cells near the *S. aureus* nidus we had previously been examining. Additionally, both control and $TCR\delta^{-/-}$ $dLck^{+/-}$ $ADAM10^{-/-}$ mice are highly susceptible to *S.aureus* SSTI, displaying uncontrolled infection spreading over the entiretiy of backskin. In the future, *S. aureus*-infected skin homogenates from $TCR\delta^{-/-}$ $dLck^{+/-}$ $ADAM10^{-/-}$ and controls will be examined for difference IL-17 and neutrophil

activity. We hypothesize that these underlying biological correlates critical to the wound healing cascade will support the findings of the phenotypic wound healing rates.

Interestingly, backskin infections of Tcrd-H2BEGFP$^{+/+}$ mice with WT or *Δhla* S. *aureus* reveal that the presence of the toxin impairs γδ T cell clustering around the abscess and the wound bed. It is intriguing to speculate that γδ T cells likely serve as a beacon for keratinocyte proliferation and neutrophil infiltrate that subsequently close the wound and contain *S. aureus*. Future studies will aim at determining whether the spatial distribution of γδ T cells is associated with their secretory activity. Additionally, the underlying signal presumably destroyed by toxin activity that results in γδ T cells homing to the abscess remains enigmatic; however, assessing the spatial distribution of γδ T cells in *Ker14*$^{-/-}$ *ADAM10*$^{-/-}$ and *LysM ADAM10*$^{-/-}$ animals will be insightful.

In conclusion, our findings provide evidence that upon *S. aureus* challenge cutaneous T cells are required to upregulate the immune response and direct re-epithelialization to close the wound and rebalance the skin homeostatic environment in the host's favor (Figure 19, model). To our knowledge, we are the first to attribute a mechanistic link between the action of a single bacterial virulence factor to cutaneous T cells damage and subsequently delineate its impact on both epithelial barrier repair and immune imprinting. Further, our discovery that γδ T cells encase the *S. aureus* abscess in the absence of the toxin add an exciting and missing detail to the model of *S. aureus* abscess formation. In light of these data, it is clear that γδ T cells are responding to and communicating with other cellular constituents of the epidermis to orchestrate *S. aureus* containment and restoration of the skin barrier following injury. It will be interesting to probe deeper into their interactions and functions both at the wounded and *S. aureus* abscess edge.

CHAPTER IV

ANALYSIS OF THE IMPACT OF α-TOXIN INTOXICATION DURING STERILE WOUND HEALING AND RECURRENT *S. AUREUS* SSTI

Sections of the work provided for this chapter will be submitted for publication. *Staphylococcus aureus* α-toxin targets skin peripheral T cells to impede wound repair. The authors of that manuscript will be Georgia R. Sampedro, Michael Shih, Jakub Kwiecinski and Juliane Bubeck Wardenburg.

Introduction

S. aureus is the most common cause of skin infections word-wide (McCaig et al., 2006; Challangundla et al., 2018). The current wave in the epidemiology of *S. aureus* infections, starting in the late 1990s, is an epidemic of community-associated skin and associated soft tissue infections (SSTIs); precipitated by the USA300 clone and by similar strains that harbor a more aggressive array of virulence factors, an increased doubling time, and resistance to antibiotics (Tong et al., 2015). Notwithstanding, both hospital and community acquired methicillin-resistant *S. aureus*, HA-MRSA and CA-MRSA, respectively, cause *S. aureus* SSTIs. In the skin, *S. aureus* is routinely associated with the ability to infect both acute and chronic wounds but also with the ability to cause susceptibility to recurrent *S. aureus* SSTIs (Demling and Waterhouse, 2007; Serra et al., 2015; Dunyach-Remy et al., 2016; Gardner et al., 2004; Fritz et al. 2013; Creech et al., 2015). While acute/chronic wounds and recurrent *S. aureus* infection are biologically different processes, the predominant presence of *S. aureus* suggests that the underlying pathophysiology induced by *S. aureus* may alter the skin's microenvironment to favor prolonged association with staphylococci.

The increasing reservoir of *S. aureus* both in the community and hospital settings has led staphylococci to be widespread and readily able to contaminate both acute and chronic wounds (Moranet al., 2006; Drews et al., 2006). There are principally two types of acute wounds- 1) traumatic wounds (penetrating deep cuts, common in combat related injuries), and 2) surgical site (SI) wounds. While traumatic wounds have not been as readily documented, epidemiological surveys on surgical wounds document an *S. aureus* incidence rate of 20-82%, the range in incidence rate chiefly reflective of the surgical site and procedure (Giacometti et al., 2000; Saadatian-Elahi et al., 2008).

Unlike acute wounds, chronic wounds are not as defined by their etiology as they are by the substantial time the wounds take to heal. Wounds in this category typically take four weeks to more than three months to heal (Werdin et al., 2009; Mekkes et al., 2003; Cazander et al., 2013). Nomenclature is far from agreed upon, however, the Wound Healing Society classifies chronic wounds into four major categories: pressure ulcers, diabetic ulcers, venous ulcers, and arterial insufficiency ulcers (Krisner et al., 2006; Jarbink et al., 2016). The most comprehensive epidemiological studies on the effect of *S. aureus* in chronic wounds are in the diabetic ulcer population. While ulcers are often polymicrobial, several reports indicate that the incidence of *S. aureus* growth in diabetic ulcer to be up to 50% where the presence of *S. aureus* makes them more likely to be infected (Roghman et al., 2001; Dang et al., 2003; Lipsky et al., 2004).

Laboratory animal models used to investigate *S. aureus* role in wounding have shown that many of the known host and pathogen modulators of *S. aureus* SSTI biology are also present and contribute to the pathogenesis in *S. aureus* wound models. In a thermal wound model, at the level of mRNA, inflammatory cytokine- IL-1 β, antimicrobial peptide-human β defensin, and pattern recognition receptor, TLR2 are all upregulated within the *S. aureus* colonized wound

(Haisma et al., 2013). In a surgical wound model, *S. aureus*-infected wounds have higher levels of neutrophil chemoattractant KC/CXCL1, MIP-2/CXCL8 and subsequent neutrophil infiltrate both of which are not present in control sterile wounds (McLoughlin et al., 2006). In *S. aureus*-infected wound model, both in non-diabetic and diabetic mice, wound healing was accelerated with the application of a neutralizing α-toxin antibody (Ortines et al., 2018). Together, these studies suggest that the key signatures of *S. aureus*-infected skin biology may transverse the modality and situational context of how staphylococci were introduced to the skin.

Even after successful antimicrobial therapy is applied, *S. aureus* recurrent SSTI over one year are as high as 70% (Kaplan et al., 2014; Williams et al., 2011; Doung et al., 2010; Chen et al., 2009; Miller et al., 2007, Fritz et al., 2012; Bocchini et al., 2013; Miller et al., 2015). The risk factors governing recurrent infections are multifactorial and recent studies have pinpointed variables on the level of the environment, host, and pathogen that can contribute to the susceptibility to *S. aureus* recurrence.

Household fomites have been demonstrated to be an environmental risk factor in recurrent *S. aureus* SSTIs. A longitudinal study examining environmental risk factors found that patients with a *S. aureus* SSTI were more likely to suffer from a recurrence if household fomites are MRSA contaminated (Miller et al., 2015). A detailed examination of household environmental surfaces exhibited the highest prevalence of *S. aureus* to be isolated from bathtub/shower at 71% and the bathroom hand towel to be 68% (Morelli et al., 2015). Consequently, environmental surfaces may provide a reservoir for re-inoculation of *S. aureus* although it is unclear whether the surface is an active mediator of infection or if *S. aureus* recurrent patient is contaminating fomite surfaces.

γδ T cells have been implicated as a central cellular modulator of immunity in S. *aureus* recurrent infections. In a model of recurrent *S. aureus* peritonitis, $V\gamma4^+$ δ T cells expand and produce IL-17 during a subsequent *S. aureus* re-challenge. Further, adoptive transfer of *S. aureus*-primed γδ T cells confer protection against *S. aureus* peritonitis in naïve mice (Murphy et al., 2014). Notwithstanding, a peritoneal infection model may not be able to approximate primary or recurrent *S. aureus* skin biology as immune T cell residents including, γδ T cells are known to have specialized functions intrinsic to their anatomical location. Recently, in a *S. aureus* skin recurrent model, Dillen and colleagues have demonstrated that IL-1 $\beta^{-/-}$ mice are protected from secondary *S. aureus* skin challenge by TNF-α and IFN-γ secreting Vγ5and Vγ6 γδ T cells from the draining lymph nodes that are activated in a TLR2/MyD88 dependent manner (Dillen et al., 2018). While these findings are intriguing, developmental and wound healing studies have highlighted the contribution IL-1 β signaling has on the expansion of IL-17 secreting γδ T cells both at the periphery and in the dermis (Muschaweckh et al., 2017; Nielsen et al., 2014). Accordingly, the results of Dillen and colleagues seem confounding as the use of IL-1 $\beta^{-/-}$ mice may profoundly alter the population of peripheral γδ T cells that expand into stable IL-17 producers upon stimulation from IL-1 β and IL-23 signals distinctively produced during skin inflammation.

Both data from human epidemiology studies and laboratory animal modeling have demonstrated that α-toxin mediated injury contributes to recurrent *S. aureus* SSTIs. Chapter I gives a complete overview of these findings. Briefly, the key pieces of data demonstrating a role for α-toxin in recurrent *S. aureus* infection are: 1) anti-α-toxin antibody titers correlate with protection against recurrent *S. aureus* SSTI in children (Fritz et al., 2013) and 2) in an animal

model of recurrent *S. aureus* SSTI α-toxin activity increases the severity of recurrent *S. aureus* SSTI (Sampedro et al., 2014).

Together, these studies demonstrate that many of the key pathogen and host signatures of infection are present regardless of skin infection context-primary *S. aureus* infection, *S. aureus*-infected wounds, and recurrent *S. aureus* infection. Accordingly, the presence of *S. aureus* in wounds and recurrent SSTIs suggests that the signaling networks that underlie the host-pathogen interaction in the skin are likely manipulated in similar ways to produce a microenvironment that favors staphylococci. In light of this, we reasoned that interrogating specific α-toxin injured cell populations, using host genetics, would yield greater molecular insight into how α-toxin-mediated injury to the microenvironment modulates the biology of *S. aureus* wounding and recurrent infection.

Results

α-Toxin modulates sterile wound healing by targeting cutaneous T cells

Upon sterile wounding, epithelial tissue must rapidly regenerate in the face of damage to maintain barrier homeostasis. Keratinocytes, stem cells, and γδ T cells communicate in a spatiotemporal manner to coordinate re-epithelization of the wound bed (Keyes et al., 2016). The role of γδ T cells in clustering and generating activatory signals such as, IL-17 and FGF-7, upon recognizing a yet unknown stress antigen that emerges in response to keratinocyte injury has been previously documented in the response to full thickness wounding (Jameson et al., 2002; Witherden et al., 2010). Further, TCR$\delta^{-/-}$ animals and animals specifically lacking V$\gamma5^{+}\delta1^{+}$ T cells (DETCs) display a delay in re-epithelization to full-thickness wounds highlighting the

functional role of γδ T cells in wound healing (Jameson et al., 2002; Barbee et al., 2011; Lewis et al., 2006; Keyes et al., 2016; Lee et al., 2017).

Because α-toxin specifically injures γδ T cells in the context *S. aureus* skin infection, we hypothesized that Hla intoxication to γδ T cells *in vivo* would diminish their wound healing capabilities during subsequent sterile wounding. In order to test this hypothesis, we first rendered keratinocytes resistant to toxin by conditionally excising *ADMA10* to ensure that toxin-mediated damage to keratinocytes would not be a confounding variable. To do so, we topically applied tamoxifen to a 6 cm^2 area of the epidermis in *Ker14*$^{+/-}$ *dLck*$^{+/-}$*ADAM10*$^{-/-}$ and *Ker14*$^{+/-}$ *dLck*$^{-/-}$ *ADAM10*$^{-/-}$ animals as previously reported for *Ker14*$^{-/-}$ *ADAM10*$^{-/-}$ mice (Inoshima et al, 2012). Subsequently, subcutaneous challenge with purified α-toxin was localized to the tamoxifen-treated area and then subjected to full-thickness wounds on the animals' backs elicited with a 6mm punch biopsy tool (Figure 20A). As shown in images from a representative experiment, *Ker14*$^{+/-}$ *dLck*$^{+/-}$*ADAM10*$^{-/-}$ mice consistently closed their wounds faster than their genetic controls (Figure 20B). When quantified, the biggest differences in wound area were consistently between d3 and d5 post wounding, where the rate of wounded area was always smaller in *Ker14*$^{+/-}$*dLck*$^{+/-}$*ADAM10*$^{-/-}$ mice when compared with controls (Figure 20C). Additionally, the serum anti-Hla antibody titer after sterile wounding were not significantly elevated from naïve mice in either *Ker14*$^{+/-}$ *dLck*$^{+/-}$*ADAM10*$^{-/-}$ mice (Figure 20D), indicating that the accelerated wound healing rates came solely from innate T cells capacity to heal wounds and was not attributable to the humoral immune response. Remarkably, these studies confirm prior suspicion, never tested, that direct-toxin mediated injury in the skin not only damages keratinocytes but debilitates T cells from performing their role in wound healing. In light of this data, it is

intriguing to wonder whether toxin-mediated injury to T cells in the context of *S. aureus* colonization prior to sterile wounding or to *S. aureus* SSTI could impair the subsequent outcome.

α-Toxin impacts recurrent infection in *dLck ADAM10*$^{-/-}$ and *LysM ADAM10*$^{-/-}$

Aside from the IL-17 producing γδ T cells reported to have a role in *S. aureus* recurrent infection, Montgomery and colleagues have also reported that $CD4^+$ T cell depletion prior to secondary challenge abrogated protection against *S. aureus* SSTI. Additionally, they observe that an intact humoral response is also a critical independent mechanism of protection against *S. aureus* recurrence (Murphy et al., 2014; Montgomery et al., 2014; Dillen et al., 2018). Together, these data are compatible and illustrate the complex nature of recurrent *S. aureus* SSTI where protection is afforded by both humoral and innate/adaptive cellular immunity. In light of α-toxin mediated injury to innate T cells during primary *S. aureus* SSTI, we wanted to investigate whether direct Hla injury to T cells would impact the outcome and the underlying biology of *S. aureus* recurrent infection.

Using a recurrent infection model, we infected 4-week-old *dLck*$^{+/-}$ *ADAM10*$^{-/-}$ with 1 x10^7 WT *S. aureus*. After a 1-week period of recovery following clearance of the primary lesion, mice were subjected to reinfection on the opposite flank with 3-4 x 10^7 staphylococci. Reinfection of *dLck*$^{+/-}$ *ADAM10*$^{-/-}$ animals demonstrate smaller lesions than in control (Figure 21A). Macroscopic histopathologic analysis of secondary lesions on day 2 revealed that abscesses of *dLck*$^{+/-}$ *ADAM10*$^{-/-}$ mice were more confined to the subcutaneous space and that the overlying epidermal wound was smaller when compared with genetic controls (Figure 21B). Further, *S. aureus* SSTI *dLck*$^{+/-}$ *ADAM10*$^{-/-}$ animals displayed regular epidermal architecture adjacent to the wound site that corresponded with an overall increase in epidermal thickness that

was not displayed in the controls (Figure 21C and E). Epidermal T cells counts were also higher in *dLck*$^{+/-}$ *ADAM10*$^{-/-}$ animals and this preservation was accompanied by higher levels of IL-17 and MPO activity from *S. aureus* infected tissue homogenates (Figure 21D, F, G, and H). MPO staining of serially sectioned *S. aureus*-infected samples also display MPO-activity to be confined to the abscess whereas, anti-MPO staining in control animals was diffuse and did not co-localize with the abscess (Figure 21I). Collectively, the analysis of the underlying biology of *dLck*$^{+/-}$*ADAM10*$^{-/-}$ animals was relatively similar to the attributes of *dLck*$^{+/-}$ *ADAM10*$^{-/-}$ animals infected with a primary *S. aureus* SSTI. In part, the similarities between the underlying biology of *S. aureus* primary and secondary infection in *dLck*$^{+/-}$ *ADAM10*$^{-/-}$ animals is likely due to the dominant genetic phenotype of cutaneous innate toxin-protected γδ T cells.

In the context of recurrent *S. aureus* infection, if a tissue resident or primary infiltrating cell rendered resistant to the toxin by genetic excision of *ADAM10* exhibited a comparable phenotype to primary *S. aureus* infection one would not be able to readily distinguish the impact of toxin-mediated injury between primary and secondary *S. aureus* infection on this cell population. If this is true, the anticipated pathology of a secondary *S. aureus* infection in animals genetically modified to be resistant to the toxin should be similar to that of primary *S. aureus* infection. To test this possibility, we examined *LysM ADAM10*$^{-/-}$ animals in the recurrent *S. aureus* SSTI model. In this case, *LysM ADAM10*$^{-/-}$ also had comparable wound healing rates to that displayed in primary *S. aureus* SSTI, having larger lesions than the genetic controls (Figure 22A, B). In order to segregate the impact of primary toxin injury on the modification of cells in the secondary environment excision of ADAM10 would have to be conditional and local. *Ker14 ADAM10*$^{-/-}$ mice in which ADAM10 excision is both conditional and local afford an exciting opportunity to address whether toxin-injury to a primary cell type impacts the pathophysiology

of recurrent *S. aureus* infection. Recently, it has been demonstrated that both epithelial stem cells and innate cells have a prolonged memory to acute inflammation that enables them to accelerate wound healing in the context of secondary challenge (Naik et al., 2017; Netea et al., 2016). It is intriguing to suspect other epidermal residents such as keratinocytes and γδ T cells also possess this type of "memory". This memory is referred to as "trained immunity" and it is orchestrated by epigenetic reprogramming that allows a heightened response to a secondary infection from barrier cells and innate immune cells that can be exerted both to the same pathogen and to a different one. Future studies should assess whether other epidermal residents such as, keratinocytes exposed to toxin-injury also have trained memory and whether the impact of this memory is local and/or far-reaching.

Application of rIL-17 mitigates recurrent *S. aureus* SSTI

Previously, it was demonstrated that the administration of intralasional rIL-17 during early hours of primary *S. aureus* infection restores an effective immune response against *S. aureus* in γδ T cell deficient animals (Cho et al., 2010). We reasoned that because $dLck^{+/-}$ $ADAM10^{+/+}$ mice have impaired IL-17 levels and decreased amounts of epidermal γδ T cells, that restoring the level of IL-17 during primary *S. aureus* infection would favorably impact wound healing rates. In order to test this, $dLck^{+/-}$ $ADAM10^{-/-}$ and control mice were administered an intralesional 1μg dose of rIL-17 4-6 hours after primary *S. aureus* infection. Wound healing rates in rIL-17 treated $dLck^{+/-}$ $ADAM10^{+/+}$ animals where accelerated when compared to vehicle controls and comparable to the wound healing rates of $dLck^{+/-}$ $ADAM10^{-/-}$ animals. Administration of rIL-17 to $dLck^{+/-}$ $ADAM10^{-/-}$ did not reduce their lesion size any further when compared to vehicle-treated $dLck^{+/-}$ $ADAM10^{-/-}$ animals suggesting that the endogenous level of IL-17 in $dLck^{+/-}$ $ADAM10^{-/-}$ was enough to afford protection against *S. aureus* infection (Figure

23A, B, and C). After a 1-week long period of recovery following clearance of the primary lesion, mice were subjected to reinfection on the opposite flank with 3-4 x 10^7 staphylococci. Intriguingly, secondary wound healing rates in *dLck*$^{+/-}$ *ADAM10*$^{+/+}$ that were treated with rIL-17 during primary infection was accelerated when compared to vehicle control treated *dLck*$^{+/-}$ *ADAM10*$^{+/+}$ mice to a level comparable to that of *dLck*$^{+/-}$ *ADAM10*$^{-/-}$ animals (**Figure 23**D, E, and F). While the underlying affected T cell population(s) during *S. aureus* recurrent SSTI remains enigmatic, this study illustrates that α toxin-mediated impairment to the T cell(s) that contributes to recurrent *S. aureus* SSTI can be functionally restored with addition of IL-17. The results of secondary *S. aureus* protection in wild-type infected animals treated with rIL-17 were reminiscent of the level of protection afforded by the therapeutic delivery of toxin antagonist, Hla_{H35L} and the ADAM10 inhibitor (Figure 6A, and B). It is intriguing to speculate that the subset of T cells injured by the toxin during primary *S. aureus* skin infection and potentially responding to secondary infection is a subpopulation of IL-17 secreting T cells, likely in the T_H17 family.

Discussion

While the underlying molecular mechanism is not fully delineated, collectively, these experiments demonstrate that α-toxin-mediated injury to T cells impacts both sterile wounding and recurrent *S. aureus* infection outcomes. Using purified toxin to injure T cells but not keratinocytes in *Ker14*$^{+/+}$ *dLck*$^{-/-}$ *ADAM10*$^{-/-}$ mice, we demonstrate that Hla-mediated injury of resident innate T cells diminishes the functional wound healing capabilities of innate T cells in a location-dependent manner during full-thickness sterile wounding. Future studies should examine whether the skin microenvironment in which Hla- mediated intoxication of these T cells

occurs has any “trained-memory” and whether it is attributable to the γδ T cell population and/or occurs in other epidermal constituents.

Using either *dLck*$^{+/-}$ *ADAM10*$^{-/-}$ and *LysM*$^{+}$ *ADAM10*$^{-/-}$ animals in a *S. aureus* recurrent SSTI infection model we observe that the biology of primary infection in toxin protected T cells and neutrophils, respectively, remains a dominant phenotype not easily segregated from their function during recurrent *S. aureus* infection. Notwithstanding, *dLck*$^{+/-}$ *ADAM10*$^{+/+}$ animals displayed diminished wounds comparable to *dLck*$^{+/-}$ *ADAM10*$^{-/-}$ animals when they were administered intralesional rIL-17 during primary infection and the protection endured through secondary *S. aureus* challenge. This study suggests that the specific T cell population damaged by the toxin during primary infection that also protects against secondary *S. aureus* infection is a subpopulation of T_H17 T cells. While peripheral IL-17 secreting γδ T cells have been implicated in *S. aureus* recurrent SSTIs, an additional candidate maybe IL-17 secreting FOXP3^{+} CD4^{+} T cells. Recently, Bjorkander and colleagues have demonstrated that *in vitro* stimulation of CD4^{+} T cells with *S. aureus* cell-free supernatants expands the percentage of FOXP3^{+} cells among the CD4^{+} T cell population that can induce pro-inflammatory cytokines such as, IL-17 and IFN-γ (Bjorkander et al., 2016). Additionally, in a mouse model of psoriasiform dermatitis IL-23-induced inflammation, also an inflammatory upregulated during *S . aureus* SSTI, increased the accumulation of FOX3P^{+} T cells in the skin (Kannan et al., 2017). In this scenario, one could envision that cutaneous regulatory T cells most likely, an IL-17 secreting FOXP3^{+} CD4^{+} T cell could potentially suppress IL-17 secreting γδ T cell by adopting their transcriptional program and thereby dampening the amount of inflammation in the skin as the wound heals. Subsequently, these cells expanded in the skin could also contribute to immune response during secondary *S. aureus* SSTI.

Until recently, the approach to anti-*Staphylococcus aureus* vaccines have been focused on neutralizing/opsonizing antibodies. Due to their failure in clinical trials, however, there is now a trend in including components of cellular immunity into vaccine design (Lacey et al., 2016). Further, preclinical vaccine designs that target cellular immunity demonstrate enhanced antigen-specific T cell responses that confer protection against *S. aureus* invasive disease (Misstear et al., 2014; Spellberg et al., 2008). While a T-cell based immunity that elicit an IL-17 response seems particularly important in the context of *S. aureus* recurrent infection, our studies indicate that this response is damaged by the α-toxin creating an impediment to successful T cell activation and signaling both during wounding and recurrent *S. aureus* SSTIs.

CHAPTER V

CONCLUSION

Skin barrier surfaces are repeatedly damaged by opportunistic pathogens throughout an individual's lifetime. Herein, we show that damage to the epithelium is not restricted to barrier cells but also can impact the function of immune cells that protect the barrier in the context of bacterial infection. *S. aureus* α-toxin mediated injury to the tissue microenvironment has been characteristically recognized to be a potent source of tissue destruction and to cause of a hyper-inflammatory response in the tissue microenvironment (Inoshima et al., 2011; Inoshima et al., 2012; Powers et al., 2012; Frank et al., 2012). Nevertheless, the studies described here and by others in our laboratory, warrant a broader understanding for α-toxin-mediated cellular injury in both modulating the immune response and altering the tissue repair pathways that simultaneously orchestrate a confinement of *S. aureus* and a restoration of barrier function (Becker et al., 2014; Powers et al., 2015). Establishing a model for *S. aureus* recurrent infections, we identify α-toxin as the bacterial determinant of *S. aureus* reinfection outcomes. Utilizing this knowledge, we administered toxin antagonists to the wound site and demonstrate that targeting the α-toxin is a promising therapeutic strategy for primary and recurrent *S. aureus* SSTIs. Using complementary host genetics, we further go on to characterize toxin-mediated injury on innate T cells as resulting in delays to *S. aureus*-induced wound healing. Probing into mechanism, we demonstrate that the intoxication of γδ T cell correlates with a decline in keratinocyte proliferation, decrease in IL-17, and a dampening of neutrophil activity. Additionally, we label T cells with a genetically fluorescently and demonstrate how T cell spatial distribution around the

wound is impacted during *S. aureus* infection on a macroscopic scale. Further, in a full-thickness wound model we show that exogenous addition of α-toxin prior to wounding can intoxicate T cells and diminish the skin's ability to re-epithelialize.

While the activity of α-toxin-mediated injury in the tissue microenvironment is complex and not completely understood, by uncovering the link between toxin-mediated injury to the skin microenvironment as an important mediator of both *S. aureus*-wound healing and recurrent infection our work opens the door to designing: 1) improved *S. aureus* patient risk assessments important for patient diagnosis and prognosis and 2) a novel substrate selective ADAM10 inhibitor on the physiological integration of toxin antagonism required for a productive immune response during primary and secondary *S. aureus* SSTIs.

Development of an integrated understanding of molecular pathogenesis and epidemiology to guide intervention for severe *S. aureus* infections

Epidemiological surveys on the prevalence of *S. aureus* in the clinic and community setting suggest that traditional *S. aureus* risk factors such as colonization, immune deficiency/suppression, and demographic information may be too narrow or limited to accurately predict individual risk for the development of *S. aureus* infection. Accordingly, the unique factors that capture specific details of the molecular battle between the host and the pathogen from both clinical observations and experimental animal disease models may increase the accuracy of patient risk assessments. In light of this, we propose a conceptual model of risk for *S. aureus* disease based on molecular features of pathogenesis and epidemiology, or molecular pathological epidemiology (MPE) (Ogino et al., 2012). MPE examines the intersection of

exposures, cellular and molecular signatures of disease, host genetic variation, and disease evolution and progression – essential variables that modulate disease outcome. This integrative approach recognizes disease heterogeneity to be the result of these variables, the so-named 'unique disease principal' (Ogino et al., 2016; Ogino et al., 2012; Ogino et al., 2015). While this theory suggests that the precise molecular complexities of disease vary between individuals, fundamental principles of molecular pathophysiology that underlie disease can be defined and utilized to guide therapy. The application of MPE has been most prominent in the oncology field, where knowledge of molecular disease pathogenesis has been successfully applied to advance the development of personalized medicine and inform the implementation of clinical therapeutics (Ogino et al., 2016; Ogino et al., 2012; Nishi et al., 2016).

The common and potentially devastating occurrence of *S. aureus* infection, existing knowledge of epidemiology, rapid advances in knowledge of molecular pathogenesis, and advent of targeted therapeutics in clinical trials position this organism as an ideal candidate to usher in MPE-based approaches to life-threatening *S. aureus.* Given the clinical mandate to reduce hospital-associated MRSA infection (Antibiotic Resistance Threats in the United States, 2013), we propose a multi-faceted MPE-based approach to facilitate risk-stratification and strategic modification of disease, predicated on the following: 1) defining *S. aureus* exposure, which in this case is two-fold –a) colonized vs. non-colonized state and b) clinical history of *S. aureus* infection. 2) Analyzing cellular and molecular signatures of disease, focused on disease-specific virulence factors whose molecular mechanism of action in pathogenesis is understood and essential for pathogenesis. The current state of knowledge derived from preclinical cellular and animal modeling studies can be leveraged to define host biomarkers of tissue injury in specific disease states. 3) Investigation of the human serologic response to essential virulence factors in

appropriate patient populations. We propose that this be approached by the definition of response thresholds that differentiate susceptible vs. non-susceptible individuals. While such studies to date have been limited to examination of Hla responses in highly refined patient populations with *S. aureus* infection (Adhikari et al., 2012; Fritz et al., 2013), these hold promise that very specific predictive correlates of protection or risk can indeed be successfully identified. 4) Definition of a limited host genomic susceptibility panel that can enable rapid, patient-focused analysis for genetic polymorphisms that are associated with risk states. Currently, HLA polymorphisms (DeLorenze et al., 2016), toxin receptor polymorphisms (DuMont et al., 2014; Cui et al., 2015), and variants that govern host immunity (Skevaki et al., 2015; Kerschen et al., 2015) may be considered leading candidates for further investigation. This overall approach would render it feasible to conduct patient-specific analysis (capturing the 'unique disease principle') predicated on a deep understanding of molecular pathogenesis. A patient would therefore have a multi-dimensional risk stratification that can be utilized to provide clinical decisional support and guide the delivery of novel biological therapies including monoclonal antibodies.

We depict a conceptual model of an MPE-based *S. aureus* risk matrix that illustrates the key features of exposure, disease severity, and the host response (Figure 24). This depiction captures a patient's severity of *S. aureus* infection and the probability that exposure to the pathogen will either elicit host immunity to infection or predispose to disease. The lower left quadrant illustrates a low-risk health state observed in a host with genetic 'resistance' characterized by a favorable T cell response to *S. aureus* and a protective antibody response against key virulence factors. The upper quadrants depict more severe forms of invasive *S. aureus* infections; a setting in which the host is unable to effectively combat infection. Cutaneous *S. aureus* infection as depicted in the lower right quadrant, while often minor in

clinical presentation, may adversely modulate host immunity and predispose to both a colonized state and subsequent infection especially following surgery or device implantation. Both applied therapies and natural host variation including genetic polymorphisms or protective antibody responses can modulate an individual patient's risk. Defining this risk as the intersection of molecular pathogenesis and clinical epidemiology will establish a paradigm for molecular classification of severe *S. aureus* disease in the hospital setting, laying the groundwork for risk stratification and the cost-effective utilization of 'designer' therapies in the specific patients for whom these can be most beneficial. This approach addresses a longstanding problem in care of the *S. aureus*-infected patient with life-threatening infection –heterogeneity of clinical course and disease outcome in patients that initially present with similar clinical findings –attributable to a single infectious agent. Importantly, the implementation of a MPE-based strategy may enable a refinement of clinical trials for conduct in the hospital setting wherein studies of infection caused by individual pathogens are limited by sample size and complicated by unique patient exposure history profiles and the need for multi-institutional collaboration to support patient accruals.

Substrate selective inhibition of ADAM10: The future of *S. aureus* novel therapeutics

This work highlights the ability of both host and bacterial components- α-toxin antagonism and addition of IL-17- to have an enduring impact on ameliorating *S. aureus* skin disease. Anti-Hla monoclonal antibodies have been the sole focus of anti-α-toxin-based therapeutics and as such, are currently being tested in clinical trials. While anti-α-toxin antibodies have promising efficacy, and are appropriate for a critically-ill *S. aureus*-infected

patient, the cost of these therapies are cost-prohibitive for the application of population-based routine *S. aureus* skin disease (Sampedro and Bubeck Wardenburg, 2017). Not only is *S. aureus* skin disease the most prominent type of staphylococcal infection, likely sustaining the circulating reservoir of staphylococci, but the skin microenvironment may participate in patterning immunity to more lethal, invasive *S. aureus* disease. Illuminating other strategies that particularly target α-toxin-mediated pathology in the context of the skin infection will be highly impactful for broadening therapeutic avenues for *S. aureus* SSTIs. Studies from our laboratory suggest that disruption of the interaction of Hla-ADAM10 or blunting the downstream pathological consequences of α-toxin-mediated injury may serve as additional novel targets for therapeutic design. The discovery and utility of the ADAM10 inhibitor as a therapeutic agent in separate distinct pathological processes has led to its development and testing in pre-clinical trials. Recent advances the development of a novel ADAM10 inhibitor offers insight into whether it will be a suitable therapy for use in *S. aureus* SSTIs.

The wide variety of pathological states that metalloproteinases are associated with including- neurodegenerative disease and several malignancies- has justified the chemical efforts to develop synthetic compounds able to block their activity (Vandenbroucke and Libert et al., 2014). Early metalloproteinase agonists, metzincin inhibitors, are short linear peptides that interfere with the active site of proteases. While these inhibitors are potent and broad-spectrum they have poor oral bio-availability, can be toxic- in part due to their lack selectivity, and have lacked efficacy in advanced clinical trials (Cathcart and Cao; 2015). The identification of ADAM17 (TACE) as the receptor for TNF- α led to the development of a more selective active site inhibitor, INCB7839, that blocks the activity of both ADAM10 and ADAM17 (Murumkar et al., 2013). But moreover, INCB7839 provided proof of concept for inhibitors that selectively

target specific zinc metalloproteinases by binding to the catalytic Zn^{2+} ion through a chelating hydroxamate group. Subsequently, using a hydroxamate inhibitor screen, the selective inhibitor for ADAM10, GI254023X, was found (Ludwig et al., 2005). While GI254023X is potent, as with many other hydroxamates, it is metabolically unstable and also has off-target toxicity because of its zinc-chelating moiety. Notwithstanding, in the context of *S. aureus* disease, GI254023X has been shown as a potent inhibitor of α-toxin mediated disease pathology in *S. aureus* sepsis, pneumonia, and recurrent *S. aureus* SSTIs in animal models of disease (Powers et al., 2012; Inoshima et al., 2011; Sampedro et al., 2014). However, aside from its limited bioavailability and off-target toxicity, more advanced testing of GI254023X in the setting of clinical trials seems high-risk especially in the context of skin application. It is speculated that the complete block of ADAM10 -especially in a wound setting- may damage the biological role ADAM10 has in repair and maintenance of barrier function. Illustrating ADAM10's physiologic role in barrer homeostasis, epidermal deletion of *ADAM10* in the adult mouse, leads to precocious epidermal differentiation and hyperproliferation that is directly linked to defective Notch processing and signaling (Weber et al., 2011).

The discovery and development of exosite inhibitors provides an exciting new type of ADAM10 inhibitor that is highly amenable for use in pathological settings including *S. aureus* disease. Exosite inhibitors are a class of molecules that act via a non-zinc binding mechanism and target secondary substrate binding sites, also known as exosites (Bannawarth et al., 2012; Gooljarsingh et al., 2008). Exosite inhibitors have the potential advantage of not only increasing selectivity to a single metalloproteinase but they also inhibit cleavage of specific proteinase substrates (Minond et al., 2012; Kothapalli et al., 2016). Having substrate-level selective inhibition of ADAM10 would dramatically change the level of risk the inhibitor would have to

ADAM10's role in barrier repair and maintenance while maintaining its ability to curb its pathogenic activity during infection and malignancies. Excitingly, an ADAM10 exosite inhibitor, CID 3117694, with selective inhibition of ADAM10 glycosylated substrates has been discovered (Madoux et al., 2016). CID 3117694 selectively inhibits hydrolysis and ultimate cleavage of exosite-binding glycosylated substrate-CXCL16 but not shedding of non-glycosylated substrate-syndecan-4. Further, to test CID 3117694 impact on wound repair, in a sterile wound closure assay, CID 3117694, significantly improved wound closure rates but did not impact wound repair to the the extent of GI254023X, suggesting a subtler impact on ADAM10's role in barrier repair and homeostasis (Madoux et al., 2016). Surely identification and development of other exosite ADAM10 inhibitors will also be made easier with the recent ectodomain crystallization of ADAM10 (Seegar et al., 2017). CID 3117694 is a first-in-class inhibitor of ADAM10 making it applicable for FDA's fast track designation to expedite its review and approval. On the recent backdrop of epidemiologic data that demonstrates ADAM10 overexpression is a mechanism of resistance in Trastuzumab-treated $HER2^+$ breast cancer, it seems likely that the development and use of a novel ADAM10 exosite inhibitor will only be a matter of time for this indication (Feldinger et al., 2014; Friedman et al., 2009).

While ADAM10 exosite site inhibitors are surely the future of the chemical manipulation of ADAM10, there may also be a relevant biological way of modifying ADAM10 substrate selectivity. Recently, it has been demonstrated that a cell regulates ADAM10's substrate selectivity by ADAM10's differential association with various tetraspanin superfamily proteins (Tspan) (Saint-Pol et al., 2017). For example, ADAM10 association with Tspan5, Tspan10, and Tspan14 but not Tspan15 promote ADAM10-dependent Notch shedding (Dornier et al., 2012; Zhou et al., 2014). While the mechanism of ADAM10 regulation is still under investigation, it is

speculated that the Tspan-ADAM10 association allows ADAM10 to adopt distinct ectodomain conformations exposing discrete substrate binding domains (Matthews et al., 2017). Because cell-surface tetraspanins have been minimally studied and do not interact with soluble ligands or counter-receptors on opposing cells no drug targeting of tratraspanins has been initiated (Hemler et al., 2008). Tetraspanins have already been implicated in a number of pathological processes that may be of relevance to *S. aureus* disease biology including-wound healing, platelet aggregation, and pathological angiogenesis (Cowin et al., 2006; Lau et al., 2004; Takeda et al, 2007). As more reagents are developed for this superfamily it is likely that they could have a potential role in modulating the substrate cleavage produced by α-toxin-ADAM10 mediated activation during *S. aureus* infection.

Collectively, these data suggest either by development of ADAM10 exosite inhibitors or via the manipulation of the tetraspanin association with ADAM10, in the foreseeable future reagents that allow a refinement of ADAM10-mediated cleavage of specific substrates will be available. Staphylococcal biologists should begin to identify what substrates produced by α-toxin-mediated activation of ADAM10 can ameliorate staphylococcal disease without readily interfering with ADAM10's physiological role in barrier repair and homeostasis. In light of our work, immune specific substrates may be attractive candidates. One such ADAM10 substrate target may be, JAM-L. JAM-L is the co-activating receptor on epidermal γδ T cells (Witherden et al., 2010; Verdino et al., 2010). Co-stimulation of JAM-L by CAR-A on neighboring keratinocytes is required for γδ T cells to become fully activated. Only once activated, do γδ T cells secrete IL-17 and FGF-7 to attract neutrophil infiltrate and stimulate keratinocyte proliferation, respectively (Nielsen et al., 2017). Exploring novel immune specific Hla-mediated ADAM10 cleavage substrates such as, JAM-L provide scientists with a unique and exciting

avenue of future research. Aside from substrate identification, it will also be important to understand how ADAM10 substrates can be classified into distinct groups based on their chemical moieties or their ADAM10-substrate reaction mechanism.

In an era where the scientific community has become increasingly aware of the harms of antibiotics disrupting the host-microbe commensal niche we need to be equally thoughtful about the long-term and off-target consequences of the using antagonists or agonists that perturb a protein or molecules physiologic function. Substrate selective inhibition and manipulation of ADAM10 ushers in the future and a new standard for studying the biology of α-toxin-ADAM10 mediated activation. Assuredly, ADAM10 exosite inhibitor utility in *S. aureus* disease biology, especially in the context of the skin, offers a promising application.

CHAPTER VI

EXPERIMENTAL METHODS

Mouse breeding and strains. All animal work was performed in accord with protocols approved by the Institutional Animal Care and Use Committee at the University of Chicago or at the University of Washington in St. Louis.

Experiments using C57Bl/6 wild-type mice were bought from Taconic and γδ TCR GFP knockin mice- Tcrd-H2BEGFP ($Trdc^{tm1Mal+}$) were purchased from Jackson Laboratories and bred in house to homozygosity (Prinz et al., 2006).

Generation of peripheral T cell knockout mice and fluorescent cre reporter lines. $dLck^{cre}$ transgenic C57Bl/6 mice (Jackson Laboratories) were bred to $ADAM10^{loxp/loxp}$ transgenic C57Bl/6 mice (Jackson Laboratories) to generate $dLck^{cre}$ $ADAM10^{loxp/loxp}$ mice ($dLck^{+/-}$ $ADAM10^{-/-}$). Simultaneously, double fluorescent cre reporter mice Rosa $^{mT/mG+/+}$ (Jackson Laboratories) were bred to $ADAM10^{loxp/loxp}$ transgenic C57Bl/6 mice to generate $Rosa^{mT/mG+/-}$ $ADAM10^{loxp/loxp}$ ($Rosa^{+/-}$ $ADAM10^{-/-}$) mice that were subsequently bred to controls or $dLck^{+/-}$ $ADAM10^{-/-}$ to generate $Rosa^{+/-}$ $dLck^{+/-}$ $ADAM10^{-/-}$ mice (Muzumdar et al., 2007). For single tdTomato fluorescent cre reporter mice $Ai9^{+/+}$ animals were bred to $ADAM10^{loxp/loxp}$ transgenic C57Bl/6 mice to generate $Ai9^{+/-}$ $ADAM10^{loxp/loxp}$ ($Ai9^{+/-}$ $ADAM10^{-/-}$) mice that were subsequently bred to controls or $dLck^{+/-}$ $ADAM10^{-/-}$ to generate $Ai9^{+/-}$ $dLck^{+/-}$ $ADAM10^{-/-}$ mice (Madisen et al., 2010).

$Ker14^{+/-}$ $ADAM10^{-/-}$ and $LysM^{+/-}$ $ADAM10^{-/-}$ harboring a conditional knockout of ADAM10 in epidermal keratinocytes or knockout of myeloid lineage cells have been previously established and investigated by our laboratory (Inoshima et al., 2012, Becker et al., 2014).

dLck$^{+/-}$ *ADAM10*$^{-/-}$ mice were crossed to with *Ker14*$^{+/+}$ *ADAM10*$^{-/-}$ to generate peripheral T cell and epidermal double knockout mice (*Ker 14*$^{+/-}$ *dLck* $^{+/-}$ *ADAM10*$^{-/-}$). In order to induce the epidermal knockout in Ker*14*$^{+/-}$ *ADAM10*$^{-/-}$ and *Ker 14*$^{+/-}$ *dLck* $^{+/-}$ *ADAM10*$^{-/-}$ mice topical application of with tamoxifen was applied (1mg per mouse per day for 5 days, applied to a 1 cm^2 area).

Generation of γδ T cell dLck^{+} *ADAM10 knockout mice.* In order to assess the contribution of γδ T cell during *S. aureus* SSTI pathogenesis, *dLck*$^{+/-}$ *ADAM10*$^{-/-}$ mice were bred to mice harboring a T- cell receptor delta chain rendering mice deficient in γδ T cell, TCRδ$^{-/-}$ (Jackson Laboratories; Prinz et al., 2006). Subsequently, *dLck*$^{+/-}$ *ADAM10*$^{-/-}$ were bred to TCRδ$^{-/-}$ and their progeny was crossed until *dLck*$^{+/-}$ *ADAM10*$^{-/-}$ TCRδ$^{-/-}$ mice were generated.

Animal models of infection and wounding. Prior to infections and procedures, animals were anesthetized by intraperitoneal injection of a mixture of ketamine (100 mg/kg) and xylazine (5 mg/kg). Wounded area was determined according to the formula A = (π/2) (length, mm) (width, mm).

Bacterial Strains and growth conditions. Bacterial strains and growth conditions. *S. aureus* strains YFP_{10B}, USA300-yfp, USA300/LAC, its isogenic Δ*hla* mutant, and Δ*hla* strains harboring plasmids encoding wild-type (WT) Hla (Δ*hla*::p*hla*) or the inactive Hla_{H35L} (Δ*hla*::phla_{H35L}) mutant were prepared for infection as described previously (Inoshima N et al., 2012, Inoshima I et al., 2011, Malone et al., 2009).

Primary and secondary backskin S. aureus SSTI. Prior to all back-skin infections, mice were shaved and depilatory cream was applied, removed with water on respective experimental flank. For primary backskin infections, right flanks of 4-6-week-old male mice were given a subcutaneous challenge with $3x10^7$ CFU *S. aureus* USA300 in 50 µL PBS (Inoshima et al.,

2012). Lesions were monitored or harvested at 24-hour intervals for 14 days or until lesions resolved. For recurrent SSTI modeling, the right flanks of 4- week-old male mice were given a subcutaneous challenge with $1x10^7$ CFU *S. aureus* USA300 or its isogenic variants in 50µL PBS. Lesional abscess area (mm^2) was monitored at 24-hour intervals for 14 days, after which mice were observed for a 7-day recovery period prior to reinfection via left flank subcutaneous injection of $3\text{-}4x10^7$ wild-type USA300. Secondary lesions were monitored for 14 days as previously described (Sampedro et al, 2014).

Secondary S. aureus pneumonia. Right flanks of 4- week-old female mice (12-16 grams) were weighed and infected with a subcutaneous challenge with $1x10^7$ CFU *S. aureus* USA300 or its isogenic variants in 50µL PBS. Lesional abscess area (mm^2) was monitored at 24-hour intervals for 14 days, after which mice were observed for a 7-day recovery period prior to reinfection via intranasal route of $3\text{-}5\ x10^8$ CFU *S. aureus* USA300 or its isogenic variants in 30µL PBS. Animals were monitored for morbidity and mortality at regular intervals for 5 days after infection as previously described (Bubeck Wardenburg et al., 2006). Mice that were over 20 grams at the time of secondary infection were removed from subsequent analysis.

Ear Epicutaneous S. aureus SSTI. Prior to infection the right ear of 4-6-week-old male mice was applied depilatory cream, removed with water, and then cleansed with 70% ethanol. The right ear pinnae was pricked 5-10 times with a 27G insulin syringe (BD) and 100 µL of $5x10^8$ was overlaid on pricked area for 10 minutes before being removed. The mean inoculating dose of *S. aureus* USA300 YFP_{10B} was determined to be $3\text{-}5x10^7$ CFU/lesion by plating serial dilutions of ear pinna homogenates 4 h after inoculation as described by Prabhakara and colleagues (Prahakara et al., 2013).

Backskin sterile wounding and infection after purified Hla challenge. Prior to sterile wounding *Ker 14$^{+/-}$ dLck $^{+/-}$ ADAM10$^{-/-}$* were treated with tamoxifen as previously described to induce conditional epidermal ADAM10 knockout (Inoshima et al., 2012). Subsequently, backskin of 4-6-week-old male mice was applied depilatory cream, removed with water before subcutaneous injection with purified recombinant Hla (5µg/ml) resuspended in 50 µL PBS at the site of epidermal *ADAM10* knockout. Animals were monitored for 2 days and subsequently anaesthetized, cleaned with 70% ethanol and punch biopsies excised the region containing Hla. 6 mm biopsy punches were used to make full-thickness wounds and animals were monitored every 24 hours until wounds resolved. After 3 weeks mice were challenged on the opposite flank with a subcutaneous challenge of 3x10^7 CFU *S. aureus* USA300 in 50 µL PBS and monitored every 24 hours until lesions healed.

Administration of therapies: rHla$_{H35L}$, ADAM10 inhibitor GI254023X, rIL-17. For therapy studies with B6 mice, mice received a single 30-µL intralesional injection of purified Hla$_{H35L}$ (7.5 µg) or the ADAM10 inhibitor GI254023X (1 µg). Recombinant Hla$_{H35L}$ for therapy studies was prepared as described elsewhere (Bubeck Wardenburg et al., 2008). Control treatment groups included a recombinant version of an irrelevant, genetically inactivated mutant protein toxin (*Bacteroides fragilis* fragilisyn) or dimethyl sulfoxide vehicle control, respectively. For exogenous addition of rIL-17 with control or *dLck$^+$ ADAM10$^{-/-}$* mice, a single dose of rIL-17 (1,000ng/100 µL; R&D Systems) in sterile PBS or vehicle alone (PBS). Similar doses of rIL-17 have been previously shown to be biologically active in mouse skin in vivo and do not have any direct bactericidal or bacteriostatic activity against *S. aureus in vitro* (Cho and Miller et al. 2010). All therapies were administered intralesionally 4-6 hours post primary backskin *S. aureus* SSTI with the inoculum of 1x10^7 CFU *S. aureus.*

Toxin protein purification. Histidine-tagged recombinant Hla and Hla_{H35L} were produced from *E. coli* and purified using nickel agarose beads (Qiagen) and dialyzed against PBS as previously described (Ragle and Bubeck Wardenburg 2009). Endotoxin treatment was performed by serial extraction in Triton-X followed by passage through a HiTrap desalting column (GE Healthcare).

Mouse sera sample analysis. We performed enzyme linked-immunosorbent assay (ELISA)–based determination of anti-Hla titers in naive serum on day 14 after primary sterile wounding, primary infection, and/or 14 days after secondary infection as previously described (Bubeck Wardenburg et al., 2008). ELISA absorbance readings were used to generate 4-parameter log dose-response curves using Prism 5.0b software. End point titers were calculated as the reciprocal of the highest dilution yielding a positive reaction, using a cutoff value of 3 times the mean assay background value obtained in the absence of serum addition. For rabbit red cell hemolysis assays, preincubation of 1.5 nmol/L recombinant Hla with a 1:100 dilution of serum harvested 14 days after reinfection was performed for 30 minutes before the addition of 5×10^7 rabbit red blood cells. Assays were performed in phosphate-buffered saline in a 96-well plate format in which unlysed cells were sedimented after 45 minutes of incubation and supernatants subjected to absorbance measurements at 450 nm. The percentage of lysis was scored relative to 100% detergent lysis. Passive immune serum samples were obtained from mice 24 hours after intraperitoneal delivery of 10 mg/kg anti-Hla monoclonal antibody 7B8 (Ragle and Wardenburg 2009).

Infected skin homogenate analysis. Skin lesion 8-mm punch biopsy specimens were obtained from anesthetized mice at the time points indicated after infection for determination of staphylococcal burden, cytokine analysis by ELISA for IL-1ß (R&D Systems) or using a

colorimetric myeloperoxidase activity kit (BioVision) according to the manufacturer's instructions, as described elsewhere (Inoshima et al., 2012; Becker et al., 2014).

Hematoxylin & eosin and immunohistochemistry on infected backskin. Bisected lesion punches were fixed in 10% formalin and embedded in paraffin. H&E, anti-CD3, anti-MPO stains were performed on paraffin sections (10 μm) by the Human Tissue Resource Center at the University of Chicago. All IHC slides were scanned into Cri Panoramic Scan Whole Slide Scanner using a 40x NA 0.95 LWD Zeiss objective. Average epidermal thickness measurements were evaluated using hematoxylin and eosin Panoramic Viewer, 3DHISTECH Ltd for 3 mice per group per time point. Average epidermal $CD3^+$ T cells from the left and right abscess edges were counted from 20x images for 3 mice per group per time point.

Whole mounted ear preparation and immunofluorescence. *S. aureus* USA300 YFP10B epicutaneously infected control and $Rosa^{+/-}$ $dLck^{+/-}$ $ADAM10^{-/-}$ ear pinna was harvested 24-hours post infection. Infected ear sheets were prepared by separating the dorsal and ventral sides of the ear with forceps and subsequently mounted onto slides with Prolong Gold mounting medium (Invitrogen). Confocal ear infection images were acquired at 4,096 x 4,096 pixels using a 40x (N.A.1.3; 0.75-1.0 digital zoom) oil-immersion objective on a Leica Microsystems SP8 laser scanning confocal microscope with 458nm, 488nm, and 514nm Argon excitation lasers. Z series maximum projections and statistical stitching of 10x2 tiles were performed using Leica Application Suite X software. Cell thresholding of maximum projections was preformed using Nikon Elements.

EdU cell labeling. Day 2 *S. aureus*-infected mice were pulsed with 100μg of 5-ethynyl-2'

-deoxyuridine (EdU) for 4 hrours before harvesting and analyzing their skins. EdU staining was performed using Click-iT EdU Alexa Fluor Imaging Kit (Life Technologies) per manufacturer's instructions.

Epidermal sheet staining and immunofluorescence. *S. aureus* USA300 YFP10B epicutaneously infected control and *Rosa*$^{+/-}$ *dLck*$^{+/-}$ *ADAM10*$^{-/-}$ ear pinna were harvested 24-hours post infection. For whole-mount ear-epidermal preparations, ears were split laterally, then incubated in 3.8% ammonium thiocyanate for 30 min at 37ºC before ear epidermis were separated from dermis. Epidermal sheets were then fixed in acetone for 10 minutes at room temperature, before proceeding to γδTCR immunostaining (BioLegend, Armenian Hamster, UV^{+} conjugated, 1:300). Tissue was mounted onto slides and mounted with Prolong Gold Diamond mountant (Invitrogen). Imaging was performed on a Zeiss Axioplan2 using a Plan-Apochromat 20X/0.8 air objective and probed using airyscanning between 400-488nm. Images presented are of maximum projections of a z series of 1024 x1024 pixel images. Two separate methods were performed to analyze the co-localization of GFP^{+} T cells with UV^{+} γδTCR antibody. First, using ImageJ maximum intensity projections and cell thresholding for both green and blue channels were performed. Subsequently, the green channel was assigned a fluorescent intensity value of sin (1.0) and multiplied by the fluorescent intensity of the blue channel to visualize cell overlap between GFP^{+} T cells and UV^{+} γδTCR antibody. For analysis of DETC dendrites and some cell counts, maximum intensity projection images were used to count cells and corresponding dendrites on DETCs in wounded and unwounded control skin. Second, 3D rendering of GFP^{+} T cells and UV^{+} γδTCR antibody stained cells in their respective channels were reconstructed using Imaris surface function and analyzed using surface to surface colocalization algorithm. Imaris

generated co-localization values and cell counts that were used to quantify DETC field counts and co-localization percentages.

Backskin staining and immunofluorescence. Backskin naïve and infected tissue was bisected and embedded in OCT compound (Tissue Tek) and frozen on dry ice, and cryo-sectioned (30 μm section thickness). Sections were fixed in 3.7% paraformaldehyde, rinsed with PBS, permeabilized 10 min with 0.1% Triton X-100 (Sigma) in PBS, then counterstained with 4'6'-diamidino-2-phenylindole (DAPI) and mounted with Prolong Gold Diamond. Using a 10x objective, 14- step Z series stack was made for tiled whole tissue section images using a Nikon Spinning Disk confocal microscope on laser lines 405 and 488. Offline stitching was performed with WUCCI split-point Image J plugin written by Mike Shih at Washington University Center for Cellular Imaging. Maximum intensity images produced in ImageJ are displayed. Cell counts and cell distance to abscess surface was analyzed using a surface distance transformation in the Imaris software.

Primary T cell Isolation. Spleens from control and *dLck*$^{+/-}$ *ADAM10*$^{-/-}$ mice were homogenized into single cell suspensions. Following AKC lysis treatment to remove red blood cells, suspensions were purified using a Pan T cell isolation kit according to manufacturer's instructions (negative selection, Miltenyi). For skin isolation of primary DECTS, epidermal cell suspensions using were prepared first prepared. Briefly, animals were sacrificed and abdominal and dorsal skin was excised and cut into strips and placed in 0.3% trypsin/GNK buffer. After 12 hours of incubation at 4°C, epidermis was separated from dermis and treated with fresh trypsin and DNase for 10 min at 37°C. Trypsin was inactivated and cell suspensions were subjected to Ficoll/Hypaque separation. Epidermal cell suspensions were then rested in T cell enrichment media (RPMI complete supplemented with IL-2 at 20 U/ml) overnight and then subjected to

FACs sorting. Both splenic and epidermal T cells were separated and isolated based on GFP^+ positivity for downstream *in vitro* analysis.

To verify Cre-mediated excision of the loxP-flanked ADAM10 locus in peripheral T cells, splenic T cells were purified as described above and FACs sorted into three groups: GFP^+ *dLck*$^{+/-}$ *ADAM10*$^{+/+}$, RFP^+ *dLck*$^{-/-}$ *ADAM10*$^{-/-}$, and GFP^+ *dLck*$^+$ *ADAM10*$^{-/-}$ T cells. Groups were subjected to a genomic prep using a Genomic DNA purification kit (Promega). DNA was then used in PCR analysis using *ADAM10* exon 3 primers that span part of the excised genomic fragment. ADAM10 exon 3 primers: 5'-ACCTCTTAGCGATACCACAAGCC and 5'-CCATGGAAGTGTCCCTCTTCATTCGTAGG. As a control, a second pair of primers amplified a segment of intact *ADAM10* genomic sequence, exon 11. *ADAM10* exon 11 primers: 5' -GGCCAGCCTATCTGTGGAAAC and 5'-GTTGGCATCGAAGCAGCAATC .

Flow cytometry. Conjugated antibodies for flow cytometry were purchased from Biolegend and included: APC-Cy7-CD3, PerCP-Cy5.5- CD4, and PE-CD8. Cell suspensions from the spleen were prepared as described above. Anti- mouse CD16/32 (Biolegend) was used for Fc receptor blocking 15 minutes prior to 30 min. antibody staining on ice. Flow cytometry was performed on FACS Aria sorter running FACS Diva software (BD Biosciences) and results were analyzed with FlowJo software.

Hla toxicity to primary T cells. Primary T cells were either isolated from the spleen or the skin as described above. To measure the role of ADAM10 in pore-forming toxin mediated injury, $2.5x10^5$ primary T cells were either cultured in a 96 well format in the presence of 100, 300, 600, and 800 µg/ml of active recombinant Hla for 3 hours or seeded at 5,000 cells per well in a 384 well format in the presence of 20, 50, 100, 200 µg/ml and then measured for lactate

dehydrogenase release using Pierce LDH Cytotoxicity Assay Kit or ATP release using a Promega Cell Titer-Glo kit, respectively.

Statistics. Statistical analysis for pairwise comparison was performed using the Student's t test performed on GraphPad Prism software with pair-wise comparisons performed using Bonferroni correction to adjust for multiplicity at a significance level of .05. All data are expressed as a mean ± SEM as indicated. P values less than 0.05 were considered statistically significant throughout all studies.

BIBLIOGRAPHY

Abtin A, Jain R, Mitchell AJ, Roediger B, Brzoska AJ, Tikoo S, Cheng Q, Ng LG, Cavanagh LL, von Andrian UH, Hickey MJ, Firth N, Weninger W. Perivascular macrophages mediate neutrophil recruitment during bacterial skin infection. Nat Immunol 2014; 15: 45-53.

Adhikari RP, Ajao AO, Aman MJ, Karauzum H, Sarwar J, Lydecker AD, Johnson JK, Nguyen C, Chen WH, Roghmann MC. Lower antibody levels to *Staphylococcus aureus* exotoxins are associated with sepsis in hospitalized adults with invasive *S. aureus* infections. J Infect Dis 2012; 206:915-23.

Alonzo F 3rd, Kozhaya L, Rawlings SA, Reyes-Robles T, DuMont AL, Myszka DG, Landau NR, Unutmaz D, Torres VJ. CCR5 is a receptor for *Staphylococcus aureus* leukotoxin ED. Nature 2013; 493:51-5.

Ani C, Farshidpanah S, Bellinhausen S, Nguyen HB. Variations in organism-specific severe sepsis mortality in the United States: 1999-2008. Crit Care Med 2015; 43: 65-77.

Antibiotic Resistance Threats in the United States, 2013.

Anderson AS1, Scully IL, Timofeyeva Y, Murphy E, McNeil LK, Mininni T, Nuñez L, Carriere M, Singer C, Dilts DA, Jansen KU. *Staphylococcus aureus* manganese transport protein C is a highly conserved cell surface protein that elicits protective immunity against *S. aureus* and Staphylococcus epidermidis. J Infect Dis 2012; 205:1688-96.

Archer NK, Harro JM, Shirtliff. Clearance of *Staphylococcus aureus* nasal carriage is T cell dependent and mediated through interleukin -17A expression and neutrophil influx. Infect Immun 2013; 81: 2070-2075.

Arvidson S, Janzon L, Lofdehl S, Novick RP. The role of the δ-lysin gene (hld) in the agr-dependent regulation of exoprotein synthesis in *Staphylococcus aureus*. Microbiology of the Staphylococci 1990: 419-31.

Barbee SD1, Woodward MJ, Turchinovich G, Mention JJ, Lewis JM, Boyden LM, Lifton RP, Tigelaar R, Hayday AC. Skint-1 is a highly specific, unique selecting component for epidermal T cells. Proc Natl Acad Sci USA 2011; 108: 3330-3335.

Becker REN, Berube BJ, Sampedro G, DeDent AC, Bubeck Wardenburg J. Tissue-specific patterning of the host immune response by *Staphylococcus aureus* α-toxin. J Innate Immun. 2014; 6: 619-631.

Berube BJ, Bubeck Wardenburg J. *Staphylococcus aureus* α-Toxin: Nearly a Century of Intrigue. Toxins 2013; 5:1140-66.

Berube BJ, Sampedro GR, Otto M, Bubeck Wardenburg JB. The psm α locus regulate production of *Staphylococcus aureus* α-toxin during infection. Infect Immun 2014; 82: 3350-3358.

Björkander S, Hell L, Johansson MA, Forsberg MM, Lasaviciute G, Roos S, Holmlund U, Sverremark-Ekström E. *Staphylococcus aureus*-derived factors induce IL-10, IFN-γ and IL-17A-expressing FOXP3+CD161+ T-helper cells in a partly monocyte-dependent manner. Sci Rep 2016; 6: 22083.

Blake KJ, Baral P, Voisin T, Lubkin A, Pinho-Ribeiro FA, Adams KL, Roberson DP, Ma YC, Otto M, Woolf CJ, Torres VJ, Chiu IM. *Staphylococcus aureus* produces pain through pore-forming toxins and neuronal TRPV1 that is silenced by QX-314. Nat Commun 9: 1-15.

Bocchini CE, Mason EO, Hulten KG, Hammerman WA, Kaplan SL. Recurrent community-associated *Staphylococcus aureus* infections in children presenting to Texas Children's Hospital in Houston, Texas. Pediatr Infect Dis J 2013; 32:1189-93.

Boucher HW, Corey GR. Epidemiology of methicillin-resistant *Staphylococcus aureus*. Clin Infect Dis 2008; 46 Suppl 5:S344-9.

Brown AF, Murphy AG, Lalor SJ, Leech JM, O'Keeffe KM, Mac Aogáin M, O'Halloran DP, Lacey KA, Tavakol M, Hearnden CH, Fitzgerald-Hughes D, Humphreys H, Fennell JP, van Wamel WJ, Foster TJ, Geoghegan JA, Lavelle EC, Rogers TR, McLoughlin RM. Memory Th1 Cells Are Protective in Invasive *Staphylococcus aureus* Infection. PLoS Pathog 2015; 11:e1005226.

Bubeck Wardenburg J, Patel RJ, Schneewind O. Surface proteins and exotoxins are required for pathogenesis of *Staphylococcus aureus* pneumonia. Infect Immun 2006; 75: 1040-1044.

Bubeck Wardenburg J, Schneewind O. Vaccine protection against *Staphylococcus aureus* pneumonia. J Exp Med 2008; 205: 287-294.

Cathcart J, Pulkoski-Gross A, Cao J. Targeting Matrix Metalloproteinases in Cancer: Bringing New Life to Old Ideas. Genes Dis 2015; 2: 26-34.

Cazander G1, Pritchard DI, Nigam Y, Jung W, Nibbering PH. Multiple actions of Lucilia sericata larvae in hard-to-heal wounds: larval secretions contain molecules that accelerate wound healing, reduce chronic inflammation and inhibit bacterial infection. Bioessays 2013; 35:1083-1092.

Chambers HF, Deleo FR. Waves of resistance: *Staphylococcus aureus* in the antibiotic era. Nat Rev Microbiol 2009; 7:629-41.

Challagundla L, Luo X, Tickler IA, Didelot X, Coleman D4, Shore AC, Coombs GW, Sordelli DO, Brown EL, Skov R, Larsen AR, Reyes J, Robledo IE, Vazquez GJ, Rivera R, Fey PD, Stevenson K, Wang SH, Kreiswirth BN, Mediavilla JR, Arias CA, Planet PJ, Nolan RL, Tenover FC, Goering RV, Robinson DA. Range expansion and the origin of USA300 North American epidemic methicillin-resistant *Staphylococcus aureus*. MBio 2018; 9: 1-15.

Chen AE, Cantey JB, Carroll KC, Ross T, Speser S, Siberry GK. Discordance between *Staphylococcus aureus* nasal colonization and skin infections in children. Pediatr Infect Dis J. 2009; 28:244–246.

Cheng AG, McAdow M, Kim HK, Bae T, Missiakas DM, Schneewind O. Contribution of coagulases towards *Staphylococcus aureus* disease and protective immunity. PLoS Pathog 2010; 6.

Cheng AG, DeDent AC, Schneewind O, Missiakas D. A play in four acts: *Staphylococcus aureus* abscess formation. Trends Microbiol 2011; 19: 225-232.

Cho JS, Pietras EM, Garcia NC, et al. Cho JS1, Pietras EM, Garcia NC, Ramos RI, Farzam DM, Monroe HR, Magorien JE, Blauvelt A, Kolls JK, Cheung AL, Cheng G, Modlin RL, Miller LS. IL-17 is essential for host defense against cutaneous *Staphylococcus aureus* infection in mice. J Clin Invest 2010; 120:1762-73.

Cho JS, Guo Y, Ramos RI, Hebroni F, Plaisier SB, Xuan C, Granick JL, Matsushima H, Takashima A, Iwakura Y, Cheung AL, Cheng G, Lee DJ, Simon SI, Miller LS. Neutrophil-derived IL-1β is sufficient for abscess formation in immunity against *Staphylococcus aureus* in mice. PloS Pathogen 2012; 8:1-20.

Chodaczek G, Papanna V, Zal MA, Zal T. Body-barrier surveillance by epidermal γδ TCRs. Nat Immunol 2012; 13: 272-282.

Cooper LZ, Madoff MA, Weinstein L. Hemolysis of rabbit erythrocytes by purified staphylococcal α-toxin. J Bacteriol 1964; 87: 127-135.

Cowin AJ, Adams D, Geary SM, Wright MD, Jones JC, Ashman LK. Wound healing is defective in mice lacking tetraspanin CD151. J Invest Dermatol 2006;126:680-689.

Creech BC, Al-Zubeidi DN, Fritz SA. Prevention of recurrent staphylococcal skin infections. Infect Dis Clin North Am 2016; 29: 429-464.

Cua DJ and Tato CM. Innate IL-17-producing cells: the sentinels of the immune system. Nat Rev Immunol 2010; 10: 749-489.

Cui L, Gao Y, Xie Y, Wang Y, Cai Y, Shao X, Ma X, Li Y, Ma G, Liu G, Cheng W, Liu Y, Liu T, Pan Q, Tao H, Liu Z, Zhao B, Shao Y, Li K. An ADAM10 promoter polymorphism is a functional variant in severe sepsis patients and confers susceptibility to the development of sepsis. Crit Care 2015; 19:73.

Dajcs JJ, Austin MS, Sloop GD, et al. Dajcs JJ, Austin MS, Sloop GD, Moreau JM, Hume EB, Thompson HW, McAleese FM, Foster TJ, O'Callaghan RJ. Corneal pathogenesis of *Staphylococcus aureus* strain Newman. Invest Ophthalmol Vis Sci 2002; 43:1109-151.

Dang CN, Prasad YD, Boulton AJ, Jude EB. Methicillin-resistant *Staphylococcus aureus* in the diabetic foot clinic: a worsening problem. Diabet Med 2003; 20:159-61.

Dantes R, Mu Y, Belflower R, Aragon D, Dumyati G, Harrison LH, Lessa FC, Lynfield R, Nadle J, Petit S, Ray SM, Schaffner W, Townes J, Fridkin S National burden of invasive methicillin-

resistant *Staphylococcus aureus* infections, United States, 2011. JAMA Intern Med 2013; 173:1970-8.

David MZ, Medvedev S, Hohmann SF, Ewigman B, Daum RS. Increasing burden of methicillin-resistant *Staphylococcus aureus* hospitalizations at US academic medical centers, 2003-2008. Infect Control Hosp Epidemiol 2012; 33:782-9.

David MZ, Daum RS. Community-assocuated methicillin-resistant *Staphylococcus aureus*: epidemiology and clinical consequences of an emerging epidemic. Clin Microbiol Rev 2010; 23: 616-687.

DeLeo FR, Kennedy AD, Chen L, Bubeck Wardenburg J, Kobayashi SD, Mathema B, Braughton KR, Whitney AR, Villaruz AE, Martens CA, Porcella SF, McGavin MJ, Otto M, Musser JM, Kreiswirth BN. Molecular differentiation of historic phage-type 80/81 and contemporary epidemic *Staphylococcus aureus*. Proc Natl Acad Sci U S A 2011; 108:18091-6.

DeLorenze GN, Nelson CL, Scott WK, Allen AS, Ray GT, Tsai AL, Quesenberry CP Jr, Fowler VG Jr. Polymorphisms in HLA Class II Genes Are Associated With Susceptibility to *Staphylococcus aureus* Infection in a White Population. J Infect Dis 2016; 213:816-23.

Demling RH and Waterhouse B. The infecreasing problem of wound bacterial burden and infection in acture and chronis soft-tissue wounds caused by Methicillin-Resistant *Staphylococcus aureus*. J Burn Wounds 2007; 7:e8.

Dillen CA, Pinsker BL, Marusina AI, Merleev AA, Farber ON, Liu H, Archer NK, Lee DB, Wang Y, Ortines RV, Lee SK, Marchitto MC, Cai SS, Ashbaugh AG, May LS, Holland SM, Freeman AF, Miller LG, Yeaman MR, Simon SI, Milner JD, Maverakis E, Miller LS. Clonnally expanded γδ T cells protect against *Staphylococcus aureus* skin reinfection. J Clin Invest 2018; 128: 1026-1042.

Donald RG, Flint M, Kalyan N, Johnson E, Witko SE, Kotash C, Zhao P, Megati S, Yurgelonis I, Lee PK, Matsuka YV, Severina E, Deatly A, Sidhu M, Jansen KU, Minton NP, Anderson AS. A novel approach to generate a recombinant toxoid vaccine against *Clostridium difficile*. Microbiology 2013; 159: 1254-1266.

Dornier E, Coumailleau F, Ottavi JF, Moretti J, Boucheix C, Mauduit P, Schweisguth F, Rubinstein E. TspanC8 tetraspanins regulate ADAM10/Kuzbanian trafficking and promote Notch activation in flies and mammals. J Cell Biol 2012; 199:481-96.

DuMont AL, Torres VJ. Cell targeting by the *Staphylococcus aureus* pore-forming toxins: it's not just about lipids. Trends Microbiol 2014; 22:21-7.

Duong M, Markwell S, Peter J, Barenkamp S. Randomized, controlled trial of antibiotics in the management of community-acquired skin abscesses in the pediatric patient. Ann Emerg Med. 2010; 55:401–7.

Dryla A1, Prustomersky S, Gelbmann D, Hanner M, Bettinger E, Kocsis B, Kustos T, Henics T, Meinke A, Nagy E. Comparison of antibody repertoires against *Staphylococcus aureus* in healthy individuals and in acutely infected patients. Clin Diagn Lab Immunol 2005; 12:387-98.

Drews SJ, Willey BM, Kreiswirth N, Wang M, Ianes T, Mitchell J, Latchford M, McGeer AJ, Katz KC. Verification of the IDI-MRSA assay for detecting methicillin-resistant *Staphylococcus aureus* in diverse specimen types in a core clinical laboratory setting. J Clin Microbiol 2006; 10: 3794-3796.

Dunyach-Remy C, Essebe Ngba C, Sotto A, Lavigne JP. *Staphylococcus aureus* toxins and diabetic foot ulcers: role in pathogenesis and interest in diagnosis. Toxins 2016; 7: 209.

Ebert T, Smith S, Pancari G, et al. Ebert T, Smith S, Pancari G, Clark D, Hampton R, Secore S, Towne V, Fan H, Wang XM, Wu X, Ernst R, Harvey BR, Finnefrock AC, Wang F, Tan C, Durr E, Cope L, Anderson A, An Z, McNeely T. A fully human monoclonal antibody to *Staphylococcus aureus* iron regulated surface determinant B (IsdB) with functional activity in vitro and in vivo. Hum Antibodies 2010; 19:113-28.

Foster TJ, Höök M. Surface protein adhesins of *Staphylococcus aureus*. Trends Microbiol 1998; 6:484-8.
Foster TJ. Immune evasion by staphylococci. Nat Rev Microbiol 2005; 3:948-58.

Fournier B. The function of TLR2 during staphylococcal disease. Front Cell Infect Microbiol 2017; 7: 166.

Friedman S, Levy R, Garrett W, Doval D, Bondarde S, Sahoo T, Lokanatha D, Julka P, Shenoy K, Nagarkar R, Bhattacharyya G, Kumar K, Nag S, Mohan P, Narang N, Raghunadharao D, Walia M, Yao W, Li J, Emm T, Yeleswaram S, Scherle P, Newton R. Clinical Benefit of INCB7839, a Potent and Selective Inhibitor of ADAM10 and ADAM17, in Combination with Trastuzumab in Metastatic HER2 Positive Breast Cancer Patients. Cancer Research 2009.

Fritz SA1, Tiemann KM, Hogan PG, Epplin EK, Rodriguez M, Al-Zubeidi DN, Bubeck Wardenburg J, Hunstad DA. A Serologic Correlate of Protective Immunity Against Community-Onset *Staphylococcus aureus* Infection. Clin Infect Dis 2013; 56:1554-61.

Gardner SE, Frantz RA. Wound Bioburden and infection-related complications in diabetic foot ulcers. Biol Res Nurs 2008; 10: 44-53.

Giacometti A1, Cirioni O, Schimizzi AM, Del Prete MS, Barchiesi F, D'Errico MM, Petrelli E, Scalise G. Epidemiology and microbiology of surgical wound infections. J Clin Microbiol 2000; 38: 918-922.

Gidengil CA, Gay C, Huang SS, Platt R, Yokoe D, Lee GM. Cost-effectiveness of strategies to prevent methicillin-resistant *Staphylococcus aureus* transmission and infection in an intensive care unit. Infect Control Hosp Epidemiol 2015; 36:17-27.

Giersing BK, Dastgheyb SS, Modjarrad K, Moorthy V. Status of vaccine research and development of vaccines for *Staphylococcus aureus*. Vaccine 2016; 34: 2962-2966.

Giraudo AT, Cheung AL, Nagel R. The sae locus of *Staphylococcus aureus* controls exoprotein synthesis at the transcriptional level. Arch Microbiology 1997; 168: 53-58.

Goerke C, Flucklger U, Steinhuber A, Zimmerli W, Wolz C. Impact of the regulatory loci agr, sarA, and sae of *Staphylococcus aureus* on the induction of α-toxin during device-related infection resolved by direct quantitative transcript analysis. Mol Microbiology 2001; 40: 1439-1447.

Gooljarsingh LT, Lakdawala A, Coppo F, Luo L, Fields GB, Tummino PJ, Gontarek RR. Characterization of an exosite binding inhibitor of matrix metalloproteinase 13. Protein Sci 2008; 17: 66-71.

Haddadin AS, Fappiano SA, Lipsett PA. Methicillin resistant *Staphylococcus aureus* (MRSA) in the intensive care unit. Postgrad Med J 2002; 78:385-92.

Haisma EM, Rietveld MH, de Breij A, van Dissel JT, El Ghalbzouri A, Nibbering PH. Inflammatory and antimicrobial responses to methicillin-resistant *Staphylococcus aureus* in an in vitro wound infection model. PLoS One 2013; 10: e82800.

Havran WL and Jameson JM. Epidermal T cells and wound healing. J Immunol 2010; 184: 5423-5428.

Hayday AC. Gammadelta T cells and the lymphoid stress-surveillance response. Immunity 2009; 31: 184-196.

Healthcare-Associated Infections - Healthy People. Available at: https://www.healthypeople.gov/2020/topics-objectives/topic/healthcare-associated-infections/objectives.

Helmer ME. Targeting of tetraspanin proteins--potential benefits and strategies. Nat Rev Drug Discov 2008; 7:747-58.

Hersh AL, Chambers HF, Maselli JH, Gonzales R. National trends in ambulatory visits and antibiotic prescribing for skin and soft-tissue infections. (2008) Arch Intern Medicine 168: 1585-1591.

Hidron AI, Edwards JR, Patel J, Hidron AI, Edwards JR, Patel J. NHSN annual update: antimicrobial-resistant pathogens associated with healthcare-associated infections: annual summary of data reported to the National Healthcare Safety Network at the Centers for Disease Control and Prevention, 2006-2007. Infect Control Hosp Epidemiol 2008; 29:996-1011.

Hinshaw LB1, Emerson TE Jr, Taylor FB Jr, Chang AC, Duerr M, Peer GT, Flournoy DJ, White GL, Kosanke SD, Murray CK, et al. Lethal *Staphylococcus aureus*-induced shock in primates: prevention of death with anti-TNF antibody. J Trauma 1992; 33:568-73.

Holland SM, DeLeo FR, Elloumi HZ, Hsu AP, Uzel G, Brodsky N, Freeman AF, Demidowich A, Davis J, Turner ML, Anderson VL, Darnell DN, Welch PA, Kuhns DB, Frucht DM, Malech HL, Gallin JI, Kobayashi SD, Whitney AR, Voyich JM, Musser JM, Woellner C, Schäffer AA, Puck JM, Grimbacher B. STAT3 mutations in the hyper-IgE syndrome. N Engl J Med 2007; 357:1608-19.

Holtfreter S, Kolata J, Bröker BM. Towards the immune proteome of *Staphylococcus aureus* – The anti-*S. aureus* antibody response. Int J Med Microbiol 2010; 300:176-92.

Hoven G, Rivas AJ, Neukrirch C, Klein S, Hamm C, Hoven G, Rivas AJ, Neukrirch C, Klein S, Hamm C, et al. Dissecting the role of ADAM10 as a mediator of *Staphylococcus aureus* α-toxin action. Biochem J 2016: 473;1929-1940.

Honda H, Krauss MJ, Coopersmith CM, Honda H, Krauss MJ, Coopersmith CM. *Staphylococcus aureus* nasal colonization and subsequent infection in intensive care unit patients: does methicillin resistance matter? Infect Control Hosp Epidemiol 2010; 31:584-91.

Hruz P, Zinkernagel AS, Jenikova G, Botwin GJ, Hugot JP, Karin M, Nizet V, Eckmann L. NOD2 contributes to cutaneous defense against *Staphylococcus aureus* through α-toxin-dependent innate immune activation. Proc Natl Acad Sci USA 2009: 106:12873-12878.

Hua L, Hilliard JJ, Shi Y, Tkaczyk C, Cheng LI, Yu X, Datta V, Ren S, Feng H, Zinsou R, Keller A, O'Day T, Du Q, Cheng L, Damschroder M, Robbie G, Suzich J, Stover CK, Sellman BR. Assessment of an anti-α-toxin monoclonal antibody for prevention and treatment of *Staphylococcus aureus*-induced pneumonia. Antimicrob Agents Chemother 2014; 58:1108-17.

Hua L, Cohen TS, Shi Y, Hua L, Hilliard JJ, Shi Y. MEDI4893* promotes survival and extends the antibiotic treatment window in a *S. aureus* immunocompromised pneumonia model. Antimicrob Agents Chemother 2015.

Hurley HJ, Knepper BC, Price CS, Mehler PS, Burman WJ, Jenkins TC. Avoidable antibiotic exposure for uncomplicated skin and soft tissue infections in the ambulatory care setting. Am J Med 2013; 12: 1099-1106

Huskins WC. Interventions to prevent transmission of antimicrobial-resistant bacteria in the intensive care unit. Curr Opin Crit Care 2007; 13:572-7.

Inoshima I, Inoshima N, Wilke GA, Inoshima I, Inoshima N, Wilke GA. A *Staphylococcus aureus* pore-forming toxin subverts the activity of ADAM10 to cause lethal infection in mice. Nat Med 2011; 17:1310-4.

Inoshima N, Wang Y, and Bubeck Wardenburg J. Genetic requirement for ADAM10 in severe *Staphylococcus aureus* skin infection. J Invest Dermatol 2011;132: 1513-6.

Ishigame H, Kakuta S, Nagai T, Nagai T, Kadoki M, Nambu A, Komiyama Y, Fujikado N, Tanahashi Y, Akitsu A, Kotaki H, Sudo K, Nakae S, Sasakawa C, Iwakura Y. Differential roles of interleukin-17A and -17F in host defense against mucoepithelial bacterial infection and allergic responses. Immunity 2009; 30:108-19.

Israel L, Wang Y, Bulek K, Della Mina E, Zhang Z, Pedergnana V, Chrabieh M, Lemmens NA4, Sancho-Shimizu V, Descatoire M, Lasseau T, Israelsson E, Lorenzo L, Yun L, Belkadi A, Moran A, Weisman LE, Vandenesch F, Batteux F, Weller S, Levin M, Herberg J, Abhyankar A, Prando C, Itan Y, van Wamel WJB, Picard C, Abel L, Chaussabel D, Li X, Beutler 2, Arkwright PD, Casanova JL, Puel A. Human adaptive immunity rescues an inborn error of innate immunity. Cell 2017; 168: 789-800.

Itohara S, Mombaerts P, Lafaille J, Iacomini J, Nelson A, Clarke AR, Hooper ML, Farr A, Tonegawa S. T cell receptor delta gene mutant mice: independent generation of αβ T cells and programmed rearrangements of gamma delta TCR genes. Cells 1993; 72: 337
Jameson J, Ugarte K, Chen N, et al. A Role for Skin T Cells in Wound Repair. Science 2002; 296: 747-749.

Jameson J and Havran WL. Skin γδ T cells functions in homeostasis and wound healing. Immunol Rev 2007; 215: 114-122.

Jansen KU, Girgenti DQ, Scully IL, Anderson AS. *Staphylococcus aureus* vaccine: problems and prospects. Vaccine 2013; 25: 2723-2730.

Järbrink K, Ni G, Sönnergren H, Schmidtchen A, Pang C, Bajpai R, Car J. Prevalence and incidence of chronic wounds and related complications: a protocol for a systematic review. Syst Rev 2016; 5: 152.

Jarvis W, Schlosser J, Chinn R, Tweeten S, Jackson M. National prevalence of methicillin-resistant *Staphylococcus aureus* in inpatients at US health care facilities, 2006. Am J Infect Control 2007; 35:631-7.

Jarvis WR, Jarvis AA, Chinn RY. National prevalence of methicillin-resistant *Staphylococcus aureus* in inpatients at United States health care facilities, 2010. Am J Infect Control 2012; 40:194-200.

Jayasinghe L, Miles G, Bayley H. Role of the amino latch of staphylococcal α-hemolysin in pore formation. J Biol Chem 2006; 4: 2195-2204.

Kaplan SL1, Forbes A, Hammerman WA, Lamberth L, Hulten KG, Minard CG, Mason EO. Randomized trial of "bleach baths" plus routine hygienic measures vs. routine hygienic measures alone for prevention of recurrent infections. Clin Infect Dis 2014; 58:679-682.

Kannan AK, Su Z, Gauvin DM, Lippert SE, Maire HP, McGaraughty SP, Kort ME, Scott VE, Gauld SB. IL-23 induces regulatory T cell plasticity with implications for inflammatory skin diseases. J Immunol 2017; 198: 220.

Kebaier C, Chamerland RR, Allen IC, Gao Xi, Broglie PM, Kebaier C, Chamerland RR, Allen IC, Gao Xi, Broglie PM. *Staphylococcus aureus* α- hemolysin mediates virulence in a murine model of severe pneumonia through activation of the NLRP3 inflammasome. J Infect Dis 2012; 205: 807-817.

Kennedy AD, Otto M, Braughton KR, Kennedy AD, Otto M, Braughton KR. Epidemic community-associated methicillin-resistant *Staphylococcus aureus*: recent clonal expansion and diversification. Proc Natl Acad Sci USA 2008; 105:1327-32.

Kennedy AD, Bubeck Wardenburg J, Gardner DJ, Kennedy AD, Bubeck Wardenburg J, Gardner DJ. Targeting of α-hemolysin by active or passive immunization decreases the severity of USA300 skin infection in a mouse model. J infect Dis 2010; 202: 1050-1058.

Kerschen E, Hernandez I, Zogg M, Maas M, Weiler H. Survival advantage of heterozygous factor V Leiden carriers in murine sepsis. J Thromb Haemost 2015; 13:1073-80.

Keyes BE, Asare A, Nikolva M, Pasolli HA, Fuchs E2. Impaired Epidermal to Dendritic T Cell Signaling Slows Wound Repair in Aged Skin. Cell 2016; 167(5):1323-133.

Kielian T, Cheung A, and Hickey WF. Diminished Virulence of an α-toxin mutant of *Staphylococcus aureus* in Experimental Brain Abscesses. Infect Immunity 2001; 60: 6902-6911.

Kisner RS. The wound healing society chronic wound ulcer healing guidelines update of the 2006 guidelines—blending old with new. Wound Repair Reg 2016; 24: 110-111.

Kim HK, DeDent A, Cheng AG, Kim HK, DeDent A, Cheng AG. IsdA and IsdB antibodies protect mice against *Staphylococcus aureus* abscess formation and lethal challenge. Vaccine 2010; 28:6382-92.

Kim HK, Emolo C, Dedent AC, Falugi F, Missiakas DM, Schneewind O. Protein A-specific monoclonal antibodies and the prevention of *Staphylococcus aureus* disease in mice. Infect Immun 2012.

Kim HK, Missiakas D, Schneewind O. Mouse models for infectious diseases caused by *Staphylococcus aureus*. J Immunol Methods 2014; 410:88-99.

Klein E, Smith DL, Laxminarayan R. Hospitalizations and deaths caused by methicillin-resistant *Staphylococcus aureus*, United States, 1999-2005. Emerg Infect Dis 2007; 13:1840-6.

Klevens RM, Edwards JR, Gaynes RP. The impact of antimicrobial-resistant, health care-associated infections on mortality in the United States. Clin Infect Dis 2008; 47:927-30.

Klevens RM, Edwards JR, Tenover FC, McDonald LC, Horan T, Gaynes R. Changes in the epidemiology of methicillin-resistant *Staphylococcus aureus* in intensive care units in US hospitals, 1992-2003. Clin Infect Dis 2006; 42:389-91.

Klevens RM, Morrison MA, Nadle J, Petit S, Gershman K, Ray S, Harrison LH, Lynfield R, Dumyati G, Townes JM, Craig AS, Zell ER, Fosheim GE, McDougal LK, Carey RB, Fridkin SK. Invasive methicillin-resistant *Staphylococcus aureus* infections in the United States. Jama 2007; 298:1763-71.

Knight A, Madrigal AJ, Grace S, Sivakumaran J, Kottaridis P, Knight A, Madrigal AJ, Grace S, Sivakumaran J, Kottaridis P. The role of Vdelta2-negative gamma delta T cells during cytomegalovirus reactivation in recipients of allogeneic stem cell transplants. Blood 2010; 116: 2164-2172.

Kolata J, Bode LG, Holtfreter S, Steil L, Kusch H, Holtfreter B, Albrecht D, Hecker M, Engelmann S, van Belkum A, Völker U, Bröker BM. Distinctive patterns in the human antibody response to *Staphylococcus aureus* bacteremia in carriers and non-carriers. Proteomics 2011; 11:3914-27.

Kothapalli KS, Ye K, Gadgil MS, Carlson SE, O'Brien KO, Zhang JY, Park HG, Ojukwu K, Zou J, Hyon SS, Joshi KS, Gu Z, Keinan A, Brenna JT. Positive Selection on a Regulatory Insertion-Deletion Polymorphism in FADS2 Influences Apparent Endogenous Synthesis of Arachidonic Acid. Mol Biol Evol 2016; 33:1726-39.

Kretsinger K, Broder KR, Cortese MM, Joyce MP, Ortega-Sanchez I, Lee GM, Kretsinger K, Broder KR, Cortese MM, Joyce MP, Ortega-Sanchez I, Lee GM. Preventing tetanus, diphtheria, and pertussis among adults: use of tetanus toxoid, reduced diphtheria toxoid and acellular pertussis vaccine recommendations of the advisory committee on immunization practices (ACIP) and recommendation of ACIP, supported by the healthcare infection control practices advisory committee (HICPAC), for use of Tdap among health-care personnel. MMWR Recomm Rep 2006; 15: 1-37.

Kuehnert MJ, Hill HA, Kupronis BA, Tokars JI, Solomon SL, Jernigan DB. Methicillin-resistant-*Staphylococcus aureus* hospitalizations, United States. Emerg Infect Dis 2005; 11:868-72.

Kuehnert MJ, Kruszon-Moran D, Hill HA, McQuillan G, McAllister SK, Fosheim G, McDougal LK, Chaitram J, Jensen B, Fridkin SK, Killgore G, Tenover FC. Prevalence of *Staphylococcus aureus* nasal colonization in the United States, 2001-2002. J Infect Dis 2006; 193:172-9.

Kyaw MH, Kern DM, Zhou S, Turnceli O, Jafri HS, Falloon J. (2015). Healthcare utilization and costs associated with *S. aureus* and *P. aeruginosa* in the intensive care unit: a retrospective observational cohort study in a US claims database. BMC Health Serv Res. 15: 241.

Laabei M, Recker M, Rudkin JK, Aldeljawi M, Gulay Z, Sloan TJ, Williams P, Endres JL, Bayles KW, Fey PD, Yajjala VK, Widhelm T, Hawkins E, Lewis K, Parfett S, Scowen L, Peacock SJ, Holden M, Wilson D, Read TD, van den Elsen J, Priest NK, Feil EJ, Hurst LD, Josefsson E, Massey RC. Predicting the virulence of MRSA from its genome sequence. Genome Res 2014; 24:839-49.

Lacey KA, Geoghegan JA, McLoughlin RM. The Role of *Staphylococcus aureus* Virulence Factors in Skin Infection and Their Potential as Vaccine Antigens. Pathogens 2016; 5:1.

Lau LM, Wee JL, Wright MD, Moseley GW, Hogarth PM, Ashman LK, Jackson DE. The tetraspanin superfamily member CD151 regulates outside-in integrin alphaIIbbeta3 signaling and platelet function. Blood 2004; 104:2368-75.

Lee BY, Singh A, David MZ, Bartsch SM, Slayton RB, Huang SS, Zimmer SM, Potter MA, Macal CM, Lauderdale DS, Miller LG, Daum RS. The economic burden of community-associated methicillin-resistant *Staphylococcus aureus*. Clin Microbiol Rev 2010; 23: 616-87.

Lee P, Gund R, Dutta A, Pincha N, Rana I, Ghosh S, Witherden D, Kandyba E, MacLeod A. Stimulation of hair follicle stem cell proliferation through an IL-1 dependent activation of gamma delta T cells. eLife 2017; 6: e28875.

Lewis JM1, Girardi M, Roberts SJ, Barbee SD, Hayday AC, Tigelaar RE. Selection of the cutaneous intraepithelial gammadelta T cells + T cell repertoire by a thymic stromal determinant. Nat Immunol 2006; 8: 843-850.

Lipsky BA1, Berendt AR, Deery HG, Embil JM, Joseph WS, Karchmer AW, LeFrock JL, Lew DP, Mader JT, Norden C, Tan JS. Diagnosis and treatment of diabetic foot infections. Clin Infect Dis. 2004 Oct 1;39(7):885-910. Epub 2004 Sep 10.

Lin L, Ibrahim AS, Xu X, Farber JM, Avanesian V, Baquir B, Fu Y, French SW, Edwards JE Jr, Spellberg B. Th1-Th17 cells mediate protective adaptive immunity against *Staphylococcus aureus* and Candida albicans infection in mice. PLoS Pathog 2009; 5:e1000703.
Liu C, Bayer A, Cosgrove SE, Daum RS, Fridkin SK, Gorwitz RJ, Kaplan SL, Karchmer AW, Levine DP, Murray BE, J Rybak M, Talan DA, Chambers HF. Clinical practice guidelines by the infectious diseases society of America for the treatment of methicillin-resistant *Staphylococcus aureus* infections in adults and children. Clin Infect Dis 2011; 52:e18-55.

Lizak M and Yarovinsky TO. Phospholipid scramblase 1 mediates type-1 interferon-induced protection against Staphylococcal α-toxin. Cell Host Microbe 2012; 1: 70-80.

Lopez de Armentia M, Gauron MC, and Colombo M. *Staphylococcus aureus* α-toxin induces the formation of dynamic tubules labeled with LC3 within host cells in a Rab7 and Rab1b-dependent manner. Front Cell and Infect Microbiol 2017: 431:1-15.

Lowy FD. *Staphylococcus aureus* infections. N Eng J Med 1998; 339: 520-532.

Ludwig A, Hundhausen C, Lambert MH, Broadway N, Andrews RC, Bickett DM, Leesnitzer MA, Becherer JD. Metalloproteinase inhibitors for the disintegrin-like metalloproteinases ADAM10 and ADAM17 that differentially block constitutive and phorbol ester-inducible shedding of cell surface molecules. Comb Chem High Throughput Screen 2005; 2:161-71.

Madisen L, Zwingman TA, Sunkin SM, Oh SW, Zariwala HA, Gu H, Ng LL, Palmiter RD, Hawrylycz MJ, Jones AR, Lein ES, Zeng H. A robust and high-throughput Cre reporting and characterization system for the whole mouse brain. Nat Neurosci 2010; 13: 133-140.

Malachowa N, Kobayashi SD, Braughton KR, Whitney AR, Parnell MJ, Gardner DJ, Deleo FR. *Staphylococcus aureus* leukotoxin GH promotes inflammation. J Infect Dis 2012; 206: 1185-1193.

Malone CL, Boles BR, Lauderdale KJ, Thoendel M, Kavanaugh JS, Horswill AR. Fluorescent reporters for *Staphylococcus aureus*. J Microbiol Methods 2009; 77: 251-260.

Maccario R, Revello MG, Comoli P, Montagna D, Locatelli F, Gerna G. HLA- unrestricted killing of HSV-1 infected mononuclear cells involvement of either $\gamma\delta^+$ or $\alpha\beta^+$ human cytotoxic T lymphocyte. J Immunology 1993; 150: 1437-1445.

Madoux F, Dreymuller D, Pettiloud JP, Santos R, Becker-Pauly C, Ludwig A, Fields GB, Bannister T, Spicer TP, Cudic M, Scampavia LD, Minond D. Discovery of an enzyme and substrate selective inhibitor of ADAM10 using an exosite-binding glycosylated substrate. Sci Rep 2016; 6:11.

Matthews AL, Szyroka J, Collier R, Noy PJ, Tomlinson MG. Scissor sisters: regulation of ADAM10 by the TspanC8 tetraspanins. Biochem Soc Trans 2017; 45:719-730.

Maurer K, Reyes-Robles T, Alonzo F, Durbin J, Torres VJ, Cadwell K. Autophagy mediates tolerance to *Staphylococcus aureus* α-toxin. Cell Host and Microbe 2015; 17: 429-440.

McAdow M, Kim HK, Dedent AC, Hendrickx AP, Schneewind O, Missiakas DM. Preventing *Staphylococcus aureus* sepsis through the inhibition of its agglutination in blood. PLoS Pathog 2011; 7: e1002307.

McCaig LF, McDonalad LC, Mandal S, Jernigan DB. *Staphylococcus aureus*-associated skin and soft tissue infections in ambulatory care. Emergency Infectious Disease 2006; 12: 1715-1723.

McLoughlin RM, Solinga RM, Rich J, Zaleski KJ, Cocchiaro JL, Risley A, Tzianabos, Lee JC. $CD4^+$ T cells and CXC chemokines modulate the pathogenesis of *Staphylococcus aureus* wound infections. PNAS 2006; 27: 10408-10413.

Mehraj J, Witte W, Akmatov MK, Layer F, Werner G, Krause G. Epidemiology of *Staphylococcus aureus* Nasal Carriage Patterns in the Community. Curr Top Microbiol Immunol 2016.

Mekkes JR, Loots MA, Van Der Wal AC, Bos JD. Causes, investigation and treatment of leg ulceration. J Am Acad Dermatol. 2004 Jan; 50:104-107.

Mikhailova M1, Xu X, Robichaud TK, Pal S, Fields GB, Steffensen B. Identification of collagen binding domain residues that govern catalytic activities of matrix metalloproteinase-2 (MMP-2). Matrix Biol 2012; 31:380-8.

Miles F, Voss L, Segedin E, Anderson BJ. Review of *Staphylococcus aureus* infections requiring admission to a pediatric intensive care unit. Arch Dis Child 2005; 90:1274-8.

Miller M, Cook HA, Furuya EY, Bhat M, Lee MH, Vavagiakis P, Visintainer P, Vasquez G, Larson E, Lowy FD. *Staphylococcus aureus* in the community: colonization versus infection. PLoS One 2009; 4:e6708.

Miller LG, Quan C, Shay A, Mostafaie K, Bharadwa K, Tan N, et al. A prospective investigation of outcomes after hospital discharge for endemic, community-acquired methicillin-resistant and -susceptible *Staphylococcus aureus* skin infection. Clin Infect Dis. 2007; 44:483–92.

Miller LG, Eisenberg DF, Liu H, Chang CL, Wang Y, Luthra R, Wallace A, Fang C, Singer J, Suaya JA. Incidence of skin and soft tissue infections in ambulatory and inpatient settings, 2005-2010. BMC Infect Dis 2015; 15: 362.

Miller LS, Cho JS. Immunity against *Staphylococcus aureus* cutaneous infections. Nat Rev Immunol 2011; 11:505-18.

Misstear K, McNeela EA, Murphy AG, Geoghegan JA, O'Keeffe KM, Fox J, Chan K, Heuking S, Collin N, Foster TJ, McLoughlin RM, Lavelle EC. Targeted nasal vaccination provides antibody-independent protection against *Staphylococcus aureus*. J Infect Dis 2014; 209:1479-1484.

Montgomery CP, Daniels M, Zhao F, Alegre ML, Chong AS, Daum RS. Protective immunity against recurrent *Staphylococcus aureus* skin infection requires antibody and interleukin-17A. Infect Immun 2014; 82:2125-34.

Montgomery CP, David MZ, Daum RS. Host factors that contribute to recurrent staphylococcal skin infection. Curr Opin Infect Dis 2015; 28:253-8.

Moran GJ, Krishnadasan A, Gorwitz RJ, Fosheim GE, McDougal LK, Carey RB, Talan DA, Emergency ID Net Study Group. Methicillin-resistant *S. aureus* infections among patients in the emergency department. N Engl J Med 2006; 17: 666-674.

Morelli JJ, Hogan PG, Sullivan ML, Muenks CE, Wang JW, Thompson RM, Burnham CA, Fritz SA. Antimicrobial Susceptibility Profiles of *Staphylococcus aureus* Isolates Recovered from Humans, Environmental Surfaces, and Companion Animals in Households of Children with Community-Onset Methicillin-Resistant *S. aureus* Infections. Antimicrob Agents Chemother 2015 59: 6634-6637.

Morfeldt E, Taylor D, von Gabain A, Arvidson S. Activation of α-toxin translation in *Staphylococcus aureus* by the trans-encoded antisense RNA, RNAIII. EMBO 1995; 14: 4569-4577.

Murphy AG, O'Keeffe KM, Lalor SJ, Maher BM, Mills KH, McLoughlin RM. *Staphylococcus aureus* infection of mice expands a population of memory γδ T cells that are protective against subsequent infection. J Immunol 2014; l92: 3697-3708.

Murumkar PR, Giridhar R, Yadav MR. Novel methods and strategies in the discovery of TACE inhibitors. Expert Opin Drug Discov 2013; 8:157-81.

Muschaweckh A, Petermann F, Korn T. IL-1β and IL-23 Promote Extrathymic Commitment of CD27+CD122- γδ T Cells to γδT17 Cells. J Immunol 2017; 199:2668-2679.

Muto CA, Jernigan JA, Ostrowsky BE, Richet HM, Jarvis WR, Boyce JM, Farr BM. SHEA guideline for preventing nosocomial transmission of multidrug-resistant strains of *Staphylococcus aureus* and enterococcus. Infect Control Hosp Epidemiol 2003; 24:362-86. Naber CK. *Staphylococcus aureus* bacteremia: epidemiology, pathophysiology, and management strategies. Clin Infect Dis 2009; 4: S231-7.

Naik S, Larsen SB, Gomez NC, Alaverdyan K, Sendoel A, Yuan S, Polak L, Kulukian A, Chai S, Fuchs E. Inflammatory memory sensitizes skin epithelial stem cells to tissue damage. Nature 2017; 550: 475-480.

National Nosocomial Infections Surveillance S. National Nosocomial Infections Surveillance (NNIS) System Report, data summary from January 1992 through June 2004, issued October 2004. Am J Infect Control 2004; 32:470-85.

Netea MG, Joosten LA, Latz E, Mills KH, Natoli G, Stunnenberg HG, O'Neill LA, Xavier RJ. Trained immunity: A program of innate immune memory in health and disease. Science 2016; 352: aaf1098.

Niebuhr M, Scharonow H, Gathamann M, Mameron D, Werfel T. *Staphylococcus* exotoxins are strong inducers of Il-22: a potential role in atopic dermatitis. J Allergy Clin Immunol 2010; 126: 1176-1183.

Nielsen MM, Lovato P, MacLeod AS, Witherden DA, Skov L, Dyring-Andersen B, Dabelsteen S, Woetmann A, Ødum N, Havran WL, Geisler C, Bonefeld CM. IL-1β-dependent activation of dendritic epidermal T cells in contact hypersensitivity. J Immunol 2014; 192: 2975-83.

Nielsen MM, Witherden DA, Havran WL. γδ T cells in homeostasis and host defense of epithelial barrier tissues. Nat Rev Immunol 2017; 17:733-745.

Nishihara R, VanderWeele TJ, Shibuya K, Mittleman MA, Wang M, Field AE, Giovannucci E, Lochhead P, Ogino S. Molecular pathological epidemiology gives clues to paradoxical findings. Eur J Epidemiol 2015; 30:1129-35.

Nishi A, Milner DA, Jr., Giovannucci EL, Nishihara R, Tan AS, Kawachi I, Ogino S. Integration of molecular pathology, epidemiology and social science for global precision medicine. Expert Rev Mol Diagn 2016; 16:11-23.

Noskin GA, Rubin RJ, Schentag JJ, Kluytmans J, Hedblom EC, Jacobson C, Smulders M, Gemmen E, Bharmal M. National trends in *Staphylococcus aureus* infection rates: impact on economic burden and mortality over a 6-year period (1998-2003). Clin Infect Dis 2007; 45:1132-40.

Nizet V. Understanding how leading bacterial pathogens subvert innate immunity to reveal novel therapeutic targets. J Allergy Clin Immunol 2007; 120:13-22.

Nygaard TK, Pallister KB, Zurek OW, Voyich JM. The impact of α-toxin on host cell plasma membrane permeability and cytokine expression during human blood infection by CA-MRSA USA300. J Leukoc Biol 2013; 94: 971-979.

Nygaard TK, Pallister KB, DuMont AL, DeWald M, Watkins RL, Pallister EQ, Malone C, Griffith S, Horswill AR, Torres VJ, Voyich JM. α-Toxin induces programmed cell death of human T cells, B cells, and monocytes during USA300 infection. Plos One 2012; 7: e36532

Oikonomopoulou K, Ricklin D, Ward PA, Lambris JD. Interactions between coagulation and complement-their role in inflammation. Semin Immunopathol 2012; 34:151-65.

Ogino S, Nishihara R, VanderWeele TJ, Wang M, Nishi A, Lochhead P, Qian ZR, Zhang X, Wu K, Nan H, Yoshida K, Milner DA Jr, Chan AT, Field AE, Camargo CA Jr, Williams MA, Giovannucci EL. Review Article: The Role of Molecular Pathological Epidemiology in the Study of Neoplastic and Non-neoplastic Diseases in the Era of Precision Medicine. Epidemiology 2016; 27:602-11.

Ogino S, Fuchs CS, Giovannucci E. How many molecular subtypes? Implications of the unique tumor principle in personalized medicine. Expert Rev Mol Diagn 2012; 12:621-8.

Ogino S, Campbell PT, Nishihara R, Beck AH, Begg CB, Bogdanov AA, Cao Y, Coleman HG, Freeman GJ, Heng YJ, Huttenhower C, Irizarry RA, Kip NS, Michor F, Nevo D, Peters U, Phipps AI, Poole EM, Qian ZR, Quackenbush J, Robins H, Rogan PK, Slattery ML, Smith-Warner SA, Song M, VanderWeele TJ, Xia D, Zabor EC, Zhang X, Wang M, Ogino S. Proceedings of the second international molecular pathological epidemiology (MPE) meeting. Cancer Causes Control 2015; 26:959-72.

Ortines RV, Liu H, Cheng LI, Cohen TS, Lawlor H, Gami A, Wang Y, Dillen CA, Archer NK, Miller RJ, Ashbaugh AG, Pinsker BL, Marchitto MC, Tkaczyk C, Stover CK, Sellman BR, Miller LS. Neutralizing Alpha-Toxin Accelerates Healing of *Staphylococcus aureus*-Infected Wounds in Nondiabetic and Diabetic Mice.Antimicrob Agents Chemother 2018; 62: e02288-17.

Pamer EG. Resurrecting the intestinal microbiota to combat antibiotic-resistant pathogens. Science 2016; 352:535-8.

Pantelyushin S, Haak S, Ingold B, Kulig P, Heppner FL, Navarini AA, Becher B. RORγt+ innate lymphoctyes and γδ T cells initiate psoriasiform plaque formation in mice. J Clin Invest 2012; 122: 2252-2256.

Parker D, Prince A. Immunopathogenesis of *Staphylococcus aureus* pulmonary infection. Semin Immunopathol 2011.

Poccia F, Gioia C, Martini F, Sacchi A, Piecentini P, Poccia F, Gioia C, Martini F, Sacchi A, Piecentini P. Zolendronic acid and interleukin-2 treatment improves immunocompetence in HIV-infected persons by activating Vgamma9Vdelta2 T cells. AIDS 2009; 23: 555-565.

Popovich KJ, Weinstein RA, Hota B. Are community-associated methicillin-resistant *Staphylococcus aureus* (MRSA) strains replacing traditional nosocomial MRSA strains? Clin Infect Dis 2008; 46:787-94.

Popov LM, Marceau CD, Starkl PM, Lumb JH, Shah J, Guerrera D, Cooper RL, Merakou C, Bouley DM, Meng W, Kiyonari H, Takeichi M, Galli S, Bagnoli F, Citi S, Carette JE, Amieva MR. The adherens junctions control susceptibility to *Staphylococcus aureus* α-toxin. Proc Ntl Acad Sci USA 2015; 112: 14337-42.

Powers ME, Kim HK, Wang Y, Bubeck Wardenburg J. ADAM10 mediates vascular injury induced by *Staphylococcus aureus* α-hemolysin. J Infect Dis 2012; 206:352-6.

Powers ME, Becker RE, Sailer A, Turner JR, Bubeck Wardenburg J. Synergistic action of *Staphylococcus aureus* α-toxin on platelets and myeloid lineage cells contribute to lethal sepsis. Cell Host Microbe 2015; 17(6): 775-87.

Prabhakara R, Foreman O, De Pascalis R, Lee GM, Plaut RD, Kim SY, Stibitz S, Elkins KL, Merkel TJ. Epicutaneous model of community-acquired *Staphylococcus aureus* skin infections. Infect Immun 2013; 81: 1306-1315.

Prinz I, Sansoni A, Kissenpfenning A, Ardouin L, Malissen M, Malissen B. Visualization of the earliest steps of gamma delta T cell development in the adult thymus. Nat Immunol 2006; 9: 995-1003.

Proctor RA. Challenges for a universal *Staphylococcus aureus* vaccine. Clin Infect Dis 2012; 54: 1179-1186.

Pruessmeyer J and Ludwig A. The good, the bad and the ugly substrates for ADAM10 and ADAM17 in brain pathology, inflammation, and cancer. Semin Cell Dev Biol 2009; 20: 164-167.

Ragle BE, Bubeck Wardenburg J. Anti-α- hemolysin monoclonal antibodies mediate protection against *Staphylococcus aureus* pneumonia. Infect Immunity 2009; 77:2712-8.

Rajendran PM, Young D, Maurer T, Chambers H, Perdreau-Remington F, Harris H. Randomized, double-blind, placebo-controlled trial of cephalexin for treatment of uncomplicated skin abscess in a population at risk for community-acquired methicillin-resistant *Staphylococcus aureus* infection. Antimicrob Agents Chemother 2007; 51: 4044-4048

Ricklin D, Ricklin-Lichtsteiner SK, Markiewski MM, Geisbrecht BV, Lambris JD. Cutting edge: members of the *Staphylococcus aureus* extracellular fibrinogen-binding protein family inhibit the interaction of C3d with complement receptor 2. J Immunol 2008; 181:7463-7.

Rigby KM, DeLeo FR. Neutrophils in innate host defense against *Staphylococcus aureus* infections. Semin Immunopathol 2012; 34:237-59.

Rooijakkers SH, Ruyken M, van Roon J, van Kessel KP, van Strijp JA, van Wamel WJ. Early expression of SCIN and CHIPS drives instant immune evasion by *Staphylococcus aureus*. Cell Microbiol 2006; 8:1282-93.

Rooijakkers SH, van Kessel KP, van Strijp JA. Staphylococcal innate immune evasion. Trends Microbiol 2005; 13:596-601.

Rouha H, Badarau A, Visram ZC, Battles MB, Prinz B, Magyarics Z, Nagy G, Mirkina I, Stulik L, Zerbs M, Jägerhofer M, Maierhofer B, Teubenbacher A, Dolezilkova I, Gross K, Banerjee S, Zauner G, Malafa S, Zmajkovic J, Maier S, Mabry R, Krauland E, Wittrup KD, Gerngross TU, Nagy E. Five birds, one stone: neutralization of α-hemolysin and 4 bi-component leukocidins of *Staphylococcus aureus* with a single human monoclonal antibody. MAbs 2015; 7:243-54.

Rose F, Dahlem G, Guthmann B, Grimminger F, Maus U, Rose F, Dahlem G, Guthmann B, Grimminger F, Maus U. Mediator generation and signaling events in alveolar epithelial cells attacked by *S. aureus* α-toxin. Am J Physiol Lung Cell Mol Physiol 2002; 282: 207-214.

Roghmann MC, Siddiqui A, Plaisance K, Standiford H. MRSA colonization and the risk of MRSA bacteraemia in hospitalized patients with chronic ulcers. J Hosp Infect 2001; 47: 98-103.

Rubinstein E, Cammarata S, Oliphant T, Wunderink R. Linezolid (PNU-100766) versus vancomycin in the treatment of hospitalized patients with nosocomial pneumonia: a randomized, double-blind, multicenter study. Clin Infect Dis 2001; 32:402-12.

Saadatian-Elahi M1, Teyssou R, Vanhems P. *Staphylococcus aureus*, the major pathogen in orthopaedic and cardiac surgical site infections: a literature review. Int J Surg. 2008; 6: 238-245.

Saint-Pol J, Eschenbrenner E, Dornier E, Boucheix C, Charrin S, Rubenstein E. Regulation of the trafficking and the function of the metalloprotease ADAM10 by tetraspanins. Biochem Soc Trans 2017; 45:937-944.

Sampedro GR, DeDent AC, Becker RE, Berube BJ, Gebhardt MJ, Cao H, Bubeck Wardenburg J. Targeting *Staphylococcus aureus* α-toxin as a novel approach to reduce severity of recurrent skin and soft-tissue infections. J Infect Dis 2014; 210:1012-8.

Sampedro GR and Buebeck Wardenburg J. *Staphylococcus aureus* in the intensive care unit: are these golden grapes ripe for a new approach? J Infect Dis 2017; 15: 64-70.

Schwiering M, Brack A, Stork R, Hellmann N. Lipid and phase specificty of α-toxin from *S. aureus*. Biochim Biophys Acta. 2013; 1828: 1962-1972.

Seegar TCM, Killingsworth LB, Saha N, Meyer PA, Patra D, Seegar TCM, Killingsworth LB, Saha N, Meyer PA, Patra D. Structural basis for regulated proteolysis by the α-secretase ADAM10. Cell 2017; 171: 1638-1648.

Serra R. Grande R, Butrico L, Rossi A, Settimio UF, Caroleo B, Amato B, Gallelli L, de Franciscis S. Chronic wound infections: the role of *Pseudomonas aeruginosa* and *Staphylococcus aureus*. Expert Rev Anti Infect Ther 2015; 13: 505-613.

Skevaki C, Pararas M, Kostelidou K, Tsakris A, Routsias JG. Single nucleotide polymorphisms of Toll-like receptors and susceptibility to infectious diseases. Clin Exp Immunol 2015; 180:165-77.

Skurnik D, Merighi M, Grout M, Gadjeva M, Maira-Litran T, Ericsson M, Goldmann DA, Huang SS, Datta R, Lee JC, Pier GB. Animal and human antibodies to distinct *Staphylococcus aureus* antigens mutually neutralize opsonic killing and protection in mice. J Clin Invest 2010; 120: 3220-33.

Simor AE. Staphylococcal decolonization: an effective strategy for prevention of infection? Lancet Infect Dis 2011; 11: 952-62.

Simor AE, Loeb M. Epidemiology of healthcare-associated *Staphylococcus aureus* infections. In: Crossley KB, Jefferson KK, Archer GL, Fowler Jr VG, eds. Staphylococci in human disease, 2nd edn. West Sussex: Blackwell Publishing, 2009: 290-309.

Spellberg B1, Ibrahim AS, Yeaman MR, Lin L, Fu Y, Avanesian V, Bayer AS, Filler SG, Lipke P, Otoo H, Edwards JE Jr. The antifungal vaccine derived from the recombinant N terminus of Als3p protects mice against the bacterium *Staphylococcus aureus*. Infect Immun 2008; 76:4574-4580.

Song L, Hobaugh MR, Shustak C, Cheley S, Bayley H, Gouaux JE. Structure of Staphylococcal α-hemolysin, a heptameric transmembrane pore. Science 1996; 274: 1859-1865.

Stevens DL, Ma Y, Salmi DB, McIndoo E, Wallace RJ, Bryant AE. Impact of antibiotics on expression of virulence-associated exotoxin genes in methicillin-sensitive and methicillin-resistant *Staphylococcus aureus*. J Infect Dis 2007; 195: 202-211.

Suaya JA, Mera RM, Cassidy A, O'Hara P, Amrine-Madsen H, Burstin S, Miller LG. (2014). Incidence and cost of hospitalizations associated with *Staphylococcus aureus* skin and soft tissue infections in the United States from 2001 through 2009. BMC Infectious Disease 2014; 14: 296.

Swierstra J, Debets S, de Vogel C, Lemmens-den Toom N, Verkaik N, Ramdani-Bouguessa N, Jonkman MF, van Dijl JM, Fahal A, van Belkum A, van Wamel W. IgG4 subclass-specific responses to *Staphylococcus aureus* antigens shed new light on host-pathogen interaction. Infect Immun 2015; 83:492-501.

Takeda Y1, Kazarov AR, Butterfield CE, Hopkins BD, Benjamin LE, Kaipainen A, Hemler ME. Deletion of tetraspanin Cd151 results in decreased pathologic angiogenesis in vivo and in vitro. Blood 2007; 109:1524-1532.

Thomsen IP, DuMont AL, James DB, Yoong P, Saville BR, Soper N, Torres VJ, CB Creech. Children with invasive *Staphylococcus aureus* disease exhibit a potently neutralizing antibody response to the cytotoxin LukAB. Infect Immun 2013; 82: 1234-1242.

Tkaczyk C, Hamilton MM, Sadowska A, Shi Y, Chang CS, Chowdhury P, Buonapane R, Xiao X, Warrener P, Mediavilla J, Kreiswirth B, Suzich J, Stover CK, Sellman BR. Targeting α-Toxin and ClfA with a Multimechanistic Monoclonal-Antibody-Based Approach for Prophylaxis of Serious *Staphylococcus aureus* Disease. MBio 2016; 7.

Tong SY, Davis JS, Eichenberger E, Halland TL, Fowler VG. (2015). *Staphylococcus aureus* infections: epidemiology, pathophysiology, clinical manifestations, and management. Clinical Microbiol Review 28: 603-61.

Torre A, Bacconi M, Sammicheli C, Galletti B, Laera D, Fontana MR, Grandi G, De Gregorio E, Bagnoli F, Nuti S, Bertholet S, Bensi G. Four-component *Staphylococcus aureus* vaccine 4C-staph enhances Fcγ receptor expression in neutrophils and monocytes and mitigates *S. aureus* infection in neutropenic mice. Infect Immunity 2015; 83: 3157-3163.

Vandenbroucke RE, Libert C. Is there new hope for therapeutic matrix metalloproteinase inhibition? Nat Rev Drug Discov 2014; 12:904-27.

Vandenesch F, Kornblum J, Novick RP. A temporal signal, independent of agr is required for hla but not spa transcription in *Staphylococcus aureus*. Journal of Bacteriology 1991; 173: 6313-20.

Vandenesch F, Lina G, Henry T. *Staphylococcus aureus* Hemolysins, bi-component Leukocidins, and Cytolytic Peptides: A Redundant Arsenal of Membrane-Damaging Virulence Factors? Front Cell Infect Microbio 2012; 2:12.

Varshney AK, Wang X, Aguilar JL, Scharff MD, Fries BC. Isotype switching increases efficacy of antibody protection against staphylococcal enterotoxin B-induced lethal shock and *Staphylococcus aureus* sepsis in mice. MBio 2014; 5:e01007-14.

Verdino P, Witherden DA, Ferguson MS, Corper AL, Schiefner A, Havran WL, Wilson IA. Molecular insights into γδ T cell costimulation by an anti-JAML antibody. Structure 2011; 19: 80-89.

Vincent JL. Nosocomial infections in adult intensive-care units. Lancet 2003; 361:2068-77.

Von Hoven G, Rivas AJ, Neukirch C, Klein S, Hamm C, Von Hoven G, Rivas AJ, Neukirch C, Klein S, Hamm C. Dissecting the role of ADAM10 as a mediator of *Staphylococcus aureus* α-toxin action. Biochem J 2016; 473: 1929-1940.

Wacker M, Wang L, Kowarik M, Dowd M, Lipowsky A, Faridmoayer A, Shields K, Park S, Alaimo C, Kelley KA, Braun M, Quebatte J, Gambillara V, Carranza P, Steffen M, Lee JC. Prevention of *Staphylococcus aureus* infections by glycoprotein vaccines synthesized in *Escherichia coli*. J Infect Dis 2014; 10: 1551-1561.

Walsh T, Moffa M, Bean H, Watson C, Bremmer D. Impact of antimicronial stewardship program guidance on the management of community-acquired pneumonia in hospitalized adults. Open Forum Infect Dis 2017; 4: S497.

Wang H, Sun X, Zhang Y, Li S, Chen K, Shi L, Nie W, Kumar R, Tzipori S, Wang J, Savidge T, Feng H. A chimeric toxin vaccine protects against primary and recurrent *Clostridium difficile* infection. Infect Immun 2012; 80: 2678-2688.

Wang R, Braughton KR, Kretschmer D, Bach THL, Quek SY, Li M, Kennedy AD, Dorward DW, Klebanoff SJ, Peschel A, DeLeo FR, Otto M. Identification of novel cytolytic peptides as key virulence determinants for community-associated MRSA. Nature 2007; 13: 1510-1514.

Weber S, Niessen MT, Prox J, Lüllmann-Rauch R, Schmitz A, Schwanbeck R, Blobel CP, Jorissen E, de Strooper B, Niessen CM, Saftig P. The disintegrin/metalloproteinase Adam10 is essential for epidermal integrity and Notch-mediated signaling. Development 2011;138: 495-505.

Werdin F, Tennehaus M, Schaller HE, Rennekampff HO. Evidence-based Management Strategies for Treatment of Chronic Wounds. Eplasty 2009; 9:e19.

WHO. Antimicrobial resistance: global report on surveillance. 2014: 1-232

Widmer AF, Lakatos B, Frei R. Strict infection control leads to low incidence of methicillin-resistant *Staphylococcus aureus* bloodstream infection over 20 years. Infect Control Hosp Epidemiol 2015; 36:702-9.

Williams DJ, Cooper WO, Kaltenbach LA, Dudley JA, Kirschke DL, Jones TF, Arbogast PG, Griffin MR, Creech CB. Comparative effectiveness of antibiotic treatment strategies for pediatric skin and soft-tissue infections. Pediatrics 2011; 128:e479-87.

Wilke GA, Bubeck Wardenburg J. Role of a disintegrin and metalloprotease 10 in *Staphylococcus aureus* α-hemolysin mediated cellular injury. Proc Natl Acad Sci USA 201; 107: 13473-13478.

Witherden DA and Havran WL. Molecular aspects of epithelial gamma delta regulation. Trends Immunol 2011; 32: 265-271.

Witherden DA, Verdino P, Rieder SE, Garijo O, Mills RE, Teyton L, Fischer WH, Wilson IA, Havran WL. The junctional adhesion molecule JAML is a costimulatory receptor for epithelial gamma delta T cell activation. Science 2010; 329: 1205-1210.

Wood JB, Jones LS, Soper NR, Xu M, Torres VJ, Buddy Creech C, Thomsen IP. Serologic detection of antibodies targeting the leucocidin LukAB strongly predicts *Staphylococcus aureus* in children with invasive infection. Journal of Pediatric Infection Disease 2018.

Wu Y, Liu X, Akhgar A, Jia J, Mok H, Sellman BR, Yu L, Roskos LK, Esser MT, Ruzin A. Prevalence of IgG and neutralizing antibodies against *Staphylococcus aureus* α-toxin in health human subjects and diverse patient populations. Infect Immun 2018; 86: e00671-17.

Xiong YQ, Willard J, Yeaman MR, Cheung AL, Bayer AS. Regulation of *Staphylococcus aureus* α-toxin gene (hla) expression by agr, sarA, and sae in vitro and in experimental infective endocarditis. J Infect Dis 2006; 194:1267-75.

Yu X, Robbie GJ, Wu Y, Esser MT, Jensen K, Schwartz H, Bellamy T, Hernandez-Illas M, Jafri HS. Safety, Tolerability, and Pharmacokinetics of MEDI4893, an investigational, extended-half-life, anti-*Staphylococcus aureus* α-toxin human monoclonal antibody, in healthy adults. Antimicrob Agents Chemother 2017; 61: e01020-16.

Zhang DJ Wang Q, Wei J, Baimukanova G, Buchholz, Stewart AF, Mao X, Killeen N. Selective Expression of the cre recombinase in late-stage thymocytes using the distal promoter of the lck gene. J Immunol 2005; 174: 6725-6731.

Zhou J, Fujiwara T, Ye S, Li X, Zhao H. Downregulation of Notch modulators, tetraspanin 5 and 10, inhibits osteoclastogenesis in vitro. Calcif Tissue Int 2014; 95:209-217.

Ziakas PD, Zacharioudakis IM, Zervou FN, Mylonakis E. Methicillin-resistant *Staphylococcus aureus* prevention strategies in the ICU: a clinical decision analysis*. Crit Care Med 2015; 43:382-93.

APPENDIX A

FIGURES

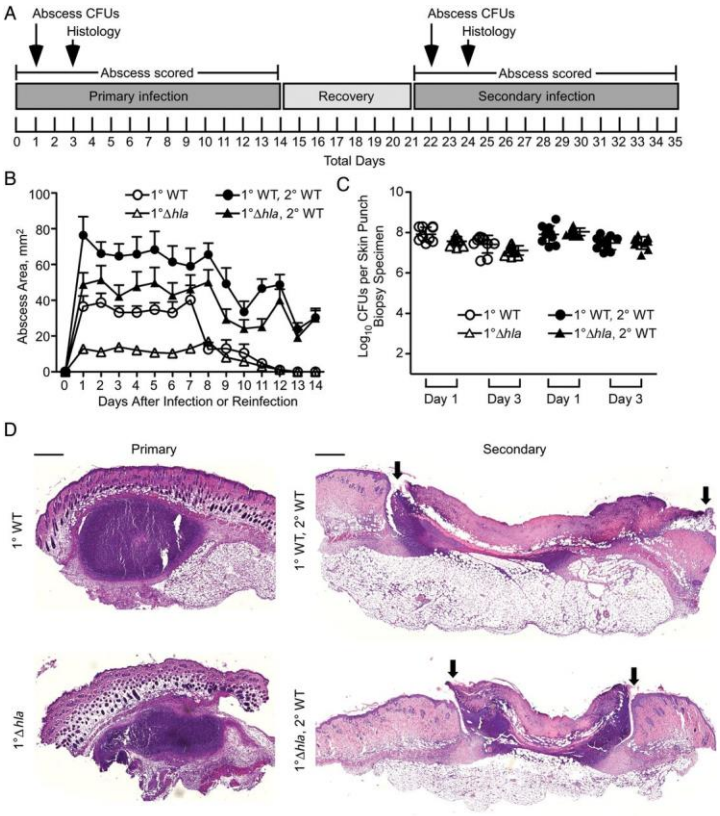

Figure 1: α-Toxin (Hla) modulates *S. aureus* abscess formation during recurrent skin and soft-tissue infection (SSTI). A. Timeline for recurrent SSTI mouse model demonstrating primary infection of mice at 4 weeks of age, with abscess scoring and infection recovery, and secondary infection, with abscess scoring. CFU, colony-forming units. B. Abscess mean area recordings in mice after primary infection with wild-type (WT; open circles) or Hla deficient (Δ*hla*; open triangles) *S. aureus* USA300 and in the same groups of mice then subjected to reinfection with WT *S. aureus* (filled symbols). Error bars represent standard error of the mean for each time point, calculated from recordings in groups of 20 mice. C. Recovery of WT *S. aureus* from the tissues of mice reinfected as in B, harvested 1 and 3 days after primary (open symbols) or reinfection (closed symbols); values are given as means with standard errors of the mean (error bars). D. Hematoxylin-eosin–stained sections of skin lesions harvested from mice after primary infection with WT or Δ*hla S. aureus* (left panels) or mice receiving primary infection with WT or Δ*hla S. aureus* followed by reinfection with WT *S. aureus* (right panels). Histopathologic samples were harvested 3 days after infection. Arrows demarcate extent of epidermal injury overlying the abscess lesion. Statistical analysis is displayed in Table 1. Error bars represent mean ± SD.

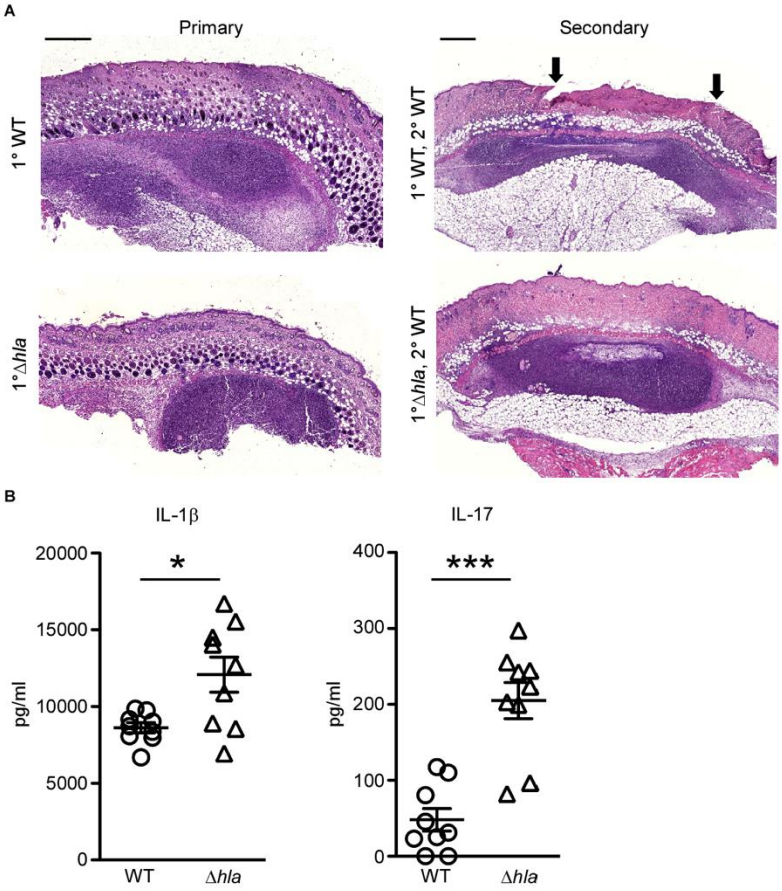

Figure 2: Exposure to α-toxin modifies the host response to primary and recurrent *S. aureus* SSTI. A. Hematoxylin and eosin-stained sections of skin lesions harvested from mice following primary infection with WT or Δ*hla S. aureus* (left panels) or mice receiving primary infection with WT or Δ*hla S. aureus* followed by reinfection with WT *S. aureus* (right panels). Histopathologic samples were harvested 1-day post-infection. Arrows demarcate extent of epidermal injury overlying the abscess lesion. B. Quantitative analysis of lesional IL-1β (left) and IL-17 (right) analyzed 1-day post-primary infection with WT or Δ*hla S. aureus.* *P≤0.05, ***P≤0.001 (Student t test). Error bars represent mean ± SD. N=5-10 animals analyzed per group.

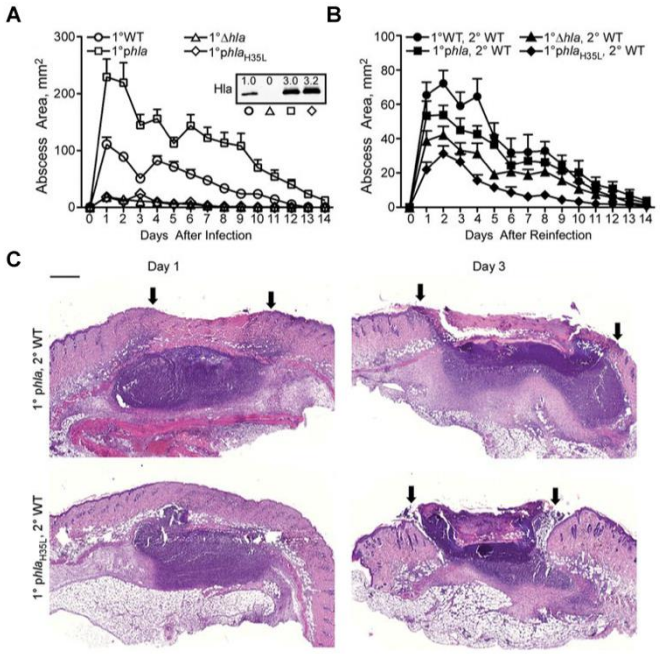

Figure 3: Contribution of active α-toxin in modulating the host response to recurrent *S.* aureus SSTI. A and B. Analysis of abscess formation in mice subjected to primary infection (1°) with wild-type (WT; circles), Δ*hla* (triangles), Δ*hla*::p*hla* (squares), or Δ*hla*::p*hla*$_{H35L}$ (diamonds) strains (A) or (B) after WT reinfection of mice infected as in A; 2°, secondary infection. Abscess mean area (n = 15) with plus standard error of the mean (SEM) over 14 days. For the inset in A, overnight culture supernatants of *S. aureus* WT, Δ*hla*, Δ*hla*::p*hla*, or Δ*hla*::p*hla*$_{H35L}$ were probed by α-Hla quantitative immunoblotting with relative expression level noted in comparison with the WT strain. C. Hematoxylin-eosin– stained sections of WT-reinfected skin lesions harvested from mice subjected to primary infection with Δ*hla*::p*hla* (upper panels) or Δ*hla*/p*hla*$_{H35L}$ (lower panels). Histopathologic samples were harvested 1 and 3 days after infection. Arrows demarcate extent of epidermal injury overlying the abscess lesion. Statistical anlysis is displayed in Table 2 and 3. Error bars represent mean ± SD. N=5-10 animals per group.

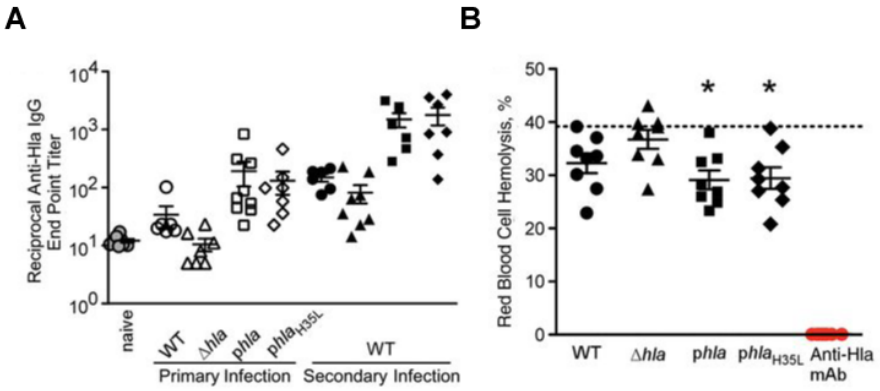

Figure 4: Quantitative and qualitative examination of anti-toxin serum during recurrent *S. aureus* SSTI. A. Reciprocal end point titer analysis of the anti-Hla response calculated from enzyme-linked immunosorbent assay (ELISA) measurements performed on serum samples collected from mice on day 14 after primary infections and secondary infection from animals in Figure 1B and 5B. A; 6–9 mice were analyzed in each group. Error bars represent mean ± SEM. IgG, immunoglobulin B. Percentage of red blood cell hemolysis observed in an in vitro assay assessing the ability of serum harvested from reinfected mice in Figure 1B and 5B to protect against Hla-mediated lysis of rabbit red blood cells. The percentage of hemolysis is calculated relative to 100% hemolysis obtained in detergent-lysed wells. Dotted line represent mean hemolysis in wells incubated with preinfection serum; mAb, monoclonal antibody. Red dots denote percent red blood cell hemolysis in the presence of serum derived from mice that received passive immunization with a neutralizing anti-Hla monoclonal antibody 24 hours prior to serum harvest. Table 4 displays statistical analysis for samples in A. *P≤0.05 **(**Student t test, sample vs preinfected serum control). Error bars represent mean ± SD. N=5-10 animals per group.

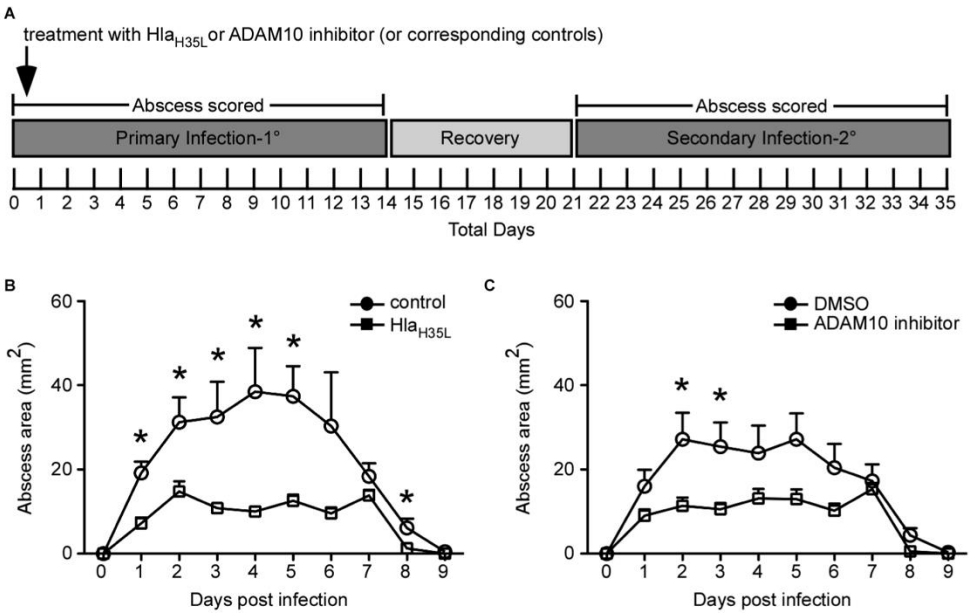

Figure 5: Treatment with Hla-inhibiting therapies blunts primary infection pathology. A. Timeline for recurrent *S. aureus* SSTI mouse model in which therapeutic interventions targeting Hla were delivered 6-8 hours following the onset of primary infection. B and C. Mean abscess lesion quantification in mice that received treatment with either purified, recombinant Hla$_{H35L}$ or a control protein 6-8 hours post-primary infection with WT *S. aureus* (B), or after having received treatment with either the ADAM10 inhibitor (GI254023X) or the DMSO vehicle 6-8 hours post-infection (C). *P≤0.05 **(**Student t test). Error bars represent mean ± SD. N=5-10 animals per group.

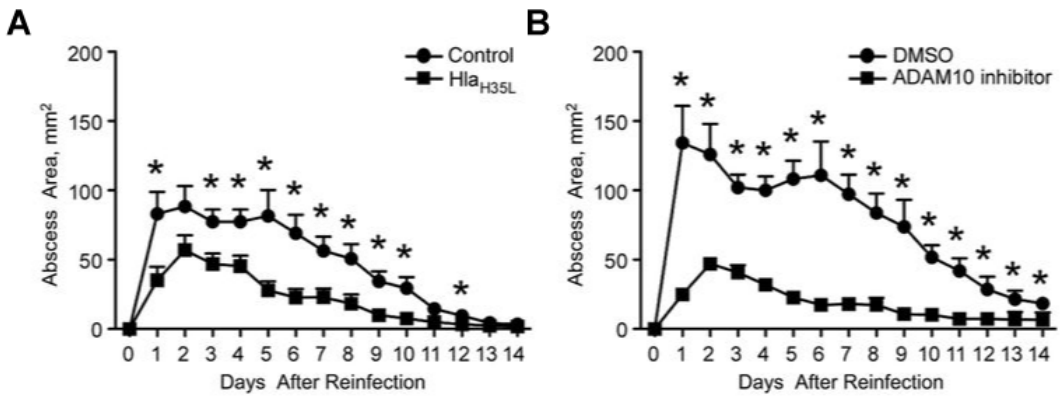

Figure 6: Early therapeutic delivery of toxin antagonist during primary *S. aureus* SSTI blunts secondary infection pathology. SSTI mean abscess areas in mice reinfected with WT *S. aureus* after being treated with either purified, recombinant Hla_{H35L} or a control protein 6–8 hours after primary infection (F) or being treated with either the ADAM10 inhibitor (GI254023X) or the dimethyl sulfoxide (DMSO) vehicle 6–8 hours after primary infection (G). *P≤0.05 (Student t test). Error bars represent mean ± SD. N=5-10 animals per group.

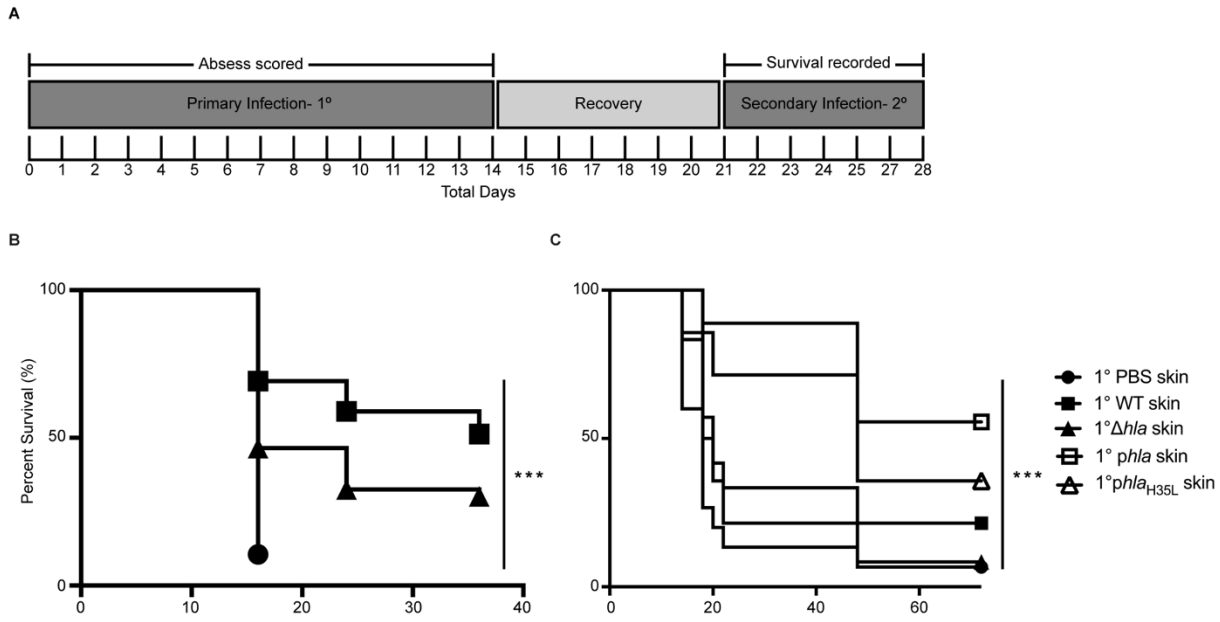

Figure 7: α-Toxin alters survival in *S. aureus* pneumonia after primary *S. aureus* SSTI. A. Timeline for a recurrent mouse model demonstrating primary *S. aureus* SSTI of mice at 4 weeks of age followed by a subsequent challenge of lethal *S. aureus* pneumonia. B. Survival recordings of C57BL/6 mice following intranasal infection with 4-5x10^8 CFU *S. aureus* USA300/LAC, monitored for five days with prior challenge to with vehicle (PBS; closed circles), wild-type (WT; closed squares) or Hla deficient (Δ*hla*; closed triangles) *S. aureus* USA300 SSTI. Statistical pairwise comparisons are displayed in Table 5. C. *S. aureus* pneumonia survival recordings in mice as in (B) after primary *S. aureus* SSTI infection with vehicle (PBS; closed circles), wild-type (WT; closed squares), Hla deficient (Δ*hla*; closed triangles), or Δ*hla*::p*hla* (open squares), or Δ*hla*::p*hla*$_{H35L}$ (open triangles) *S. aureus* USA300. ***p=0.0001, Gehan-Breslow-Wilcoxon test. N=5-10 animals per group.

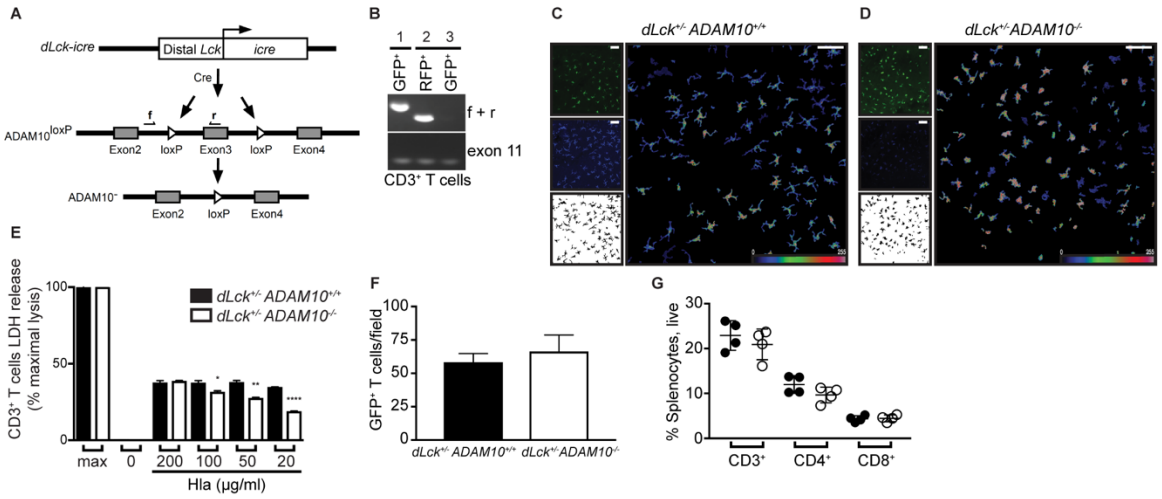

Figure 8: Generation and validation of peripheral T cell-specific *ADAM10* knockout mice. A. Schematic demonstrating the breeding strategy to derive mice harboring deletion of *ADAM10* in peripheral T cells under the control of the *Lck distal* (*dLck*) promoter. Labels "f" and "r" indicate sites of forward and reverse PCR primers utilized to document Cre-recombinase- dependent excision of exon 3 in (B). B. PCR-based analysis performed on the genomic DNA from purified splenic $CD3^+$ T cells sorted for cre expression by GFP^+ positivity to demonstrate excision of exon 3 in mice harboring the *Rosa mT/mG*$^+$ *dLck*^{cre} *ADAM10*$^{loxP/loxP}$ genotype (*Rosa*$^{+/-}$ *dLck*$^{+/-}$ *ADAM10*$^{-/-}$, B. Lane 3) genotype. C and D. Maximum projections of z series images of epidermal sheets prepared from naïve *Rosa*$^{+/-}$ *dLck*$^{+/-}$ *ADAM10*$^{+/+}$ and *Rosa*$^{+/-}$ *dLck*$^{+/-}$ *ADAM10*$^{-/-}$ mouse ear skin (inset 1) with immunostaining for γδ TCR to detect DETCs (inset 2) and subsequent binary map of cells made from their GFP^+ intensity (inset 3, given value =1) multiplied by the total anti-γδ TCR fluorescence intensity per pixel (large display). Scale bars, 50µm. E. Purified splenic $CD3^+$ T cells were obtained from control or *dLck*$^{+/-}$ *ADAM10*$^{-/-}$ mice and subjected *in vitro* to varying concentrations of purified recombinant Hla for 4 hours and cell death was measured by LDH release, *P≤0.05,**P≤0.01, ****P≤ 0.0001 (Student t test). F Microscopic quantification of GFP^+ T cell numbers per field in (C). G. Flow cytometric percentages of total splenic $CD3^+$ T cells and frequencies of T cell subclasses based on $CD4^+$ or $CD8^+$ T cell markers. Error bars represent mean ± SD. Analysis was performed using independent samples, N=4-10 animals, with the excpetion of E. where samples from groups of animals were pooled.

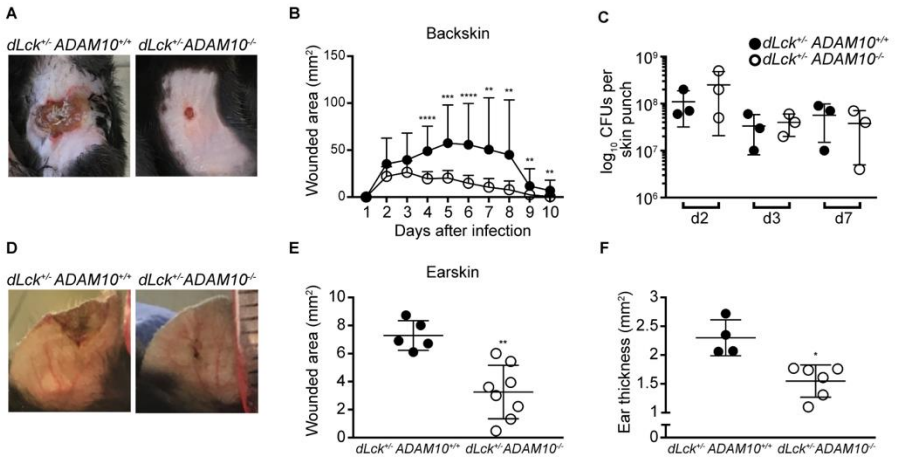

Figure 9: α-Toxin dependent injury to T cells exacerbates epithelial injury during *S. aureus* skin infection. A. Representative examples of backskin wounds from control and *dLck*$^{+/-}$ *ADAM10*$^{-/-}$ mice taken day 5 post subcutaneous *S. aureus* SSTI. B. Wounded area recordings from control and *dLck*$^{+/-}$ *ADAM10*$^{-/-}$ mice infected with $3x10^7$ staphylococci were monitored until wounds were healed. C. Mice were infected as in (B) and skin lesion homogenates were enumerated for CFU at days 2, 3, and 7 postinfection by serial dilution analysis. D. Representative example earskin wounds of 4-6 week old mice day 2 post epicutaneous *S. aureus* challenge. E. Wounded area recording from day 2 wounded control and *dLck*$^{+/-}$ *ADAM10*$^{-/-}$ were calculated as in (B) from epicutaneous *S. aureus* challenge of the ear pinna. F. Ear swelling from mice in (E) was measured by ear thickness recordings using a tissue caliper. *P≤0.05, **P≤0.01, ***P≤0.001, ****P≤ 0.0001 (Student t test). Error bars represent mean ± SD. N=4-10 animals were analyzed per group.

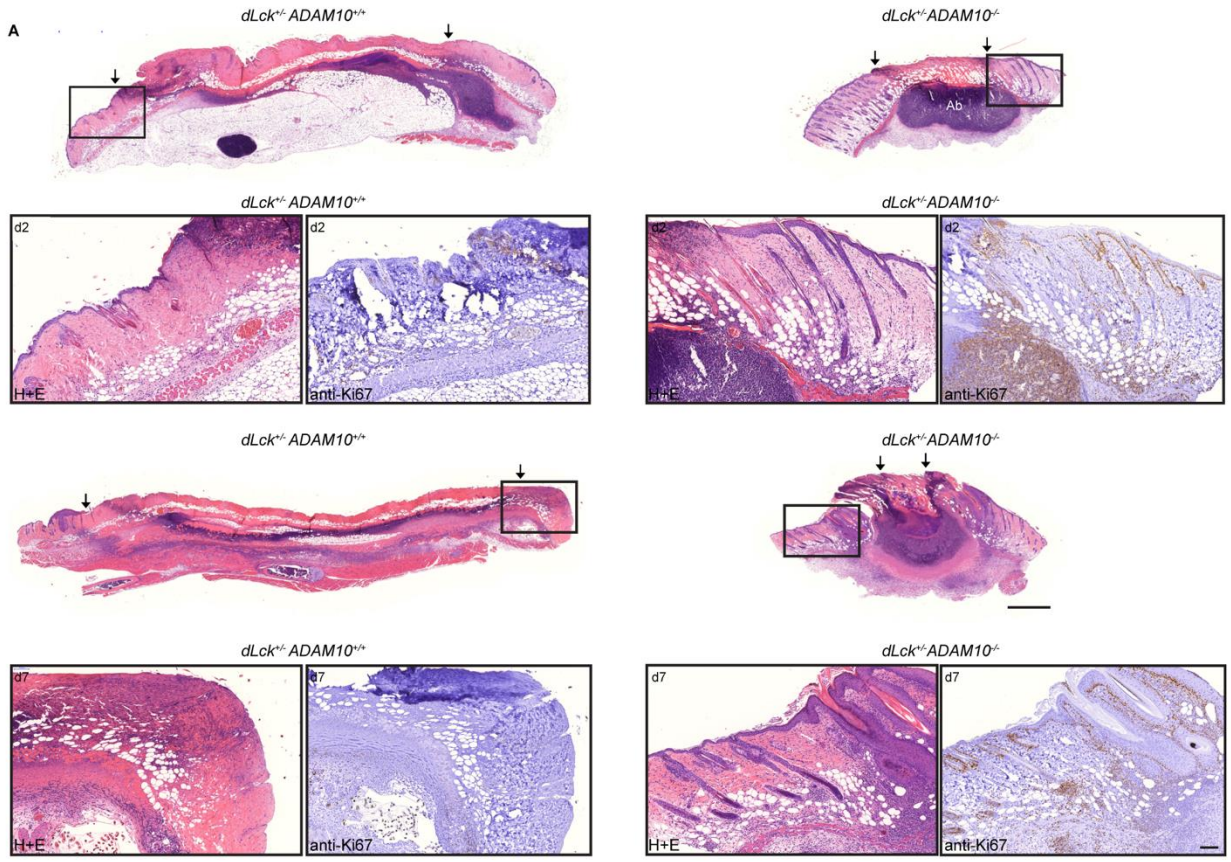

Figure 10: Contribution and dynamics of toxin-injured cutaneous T cells during *S. aureus* SSTI. A. Representative backskin images of hematoxylin/eosin-stained (H&E) semi-thin sections of control and *dLck*$^{+/-}$ *ADAM10*$^{-/-}$ mice subcutaneously challenged with *S. aureus* on day 2 and day 7. Arrows demarcate wounded edges overlying the abscess. Main image scale bar, 1000μm. Inset images are of a higher magnification view of skin tissue distant from the wounded edge in control and *dLck*$^{+/-}$ *ADAM10*$^{-/-}$ mice. Inset samples were serially stained with H&E and proliferation marker Ki67. Control mice display loss of epidermal architecture and epidermal proliferation on non-wounded tissue edges when compared to *dLck*$^{+/-}$ *ADAM10*$^{-/-}$ animals at both time points. Inset scale bar, 100μm. Analysis was performed using independent animals, N=3-5.

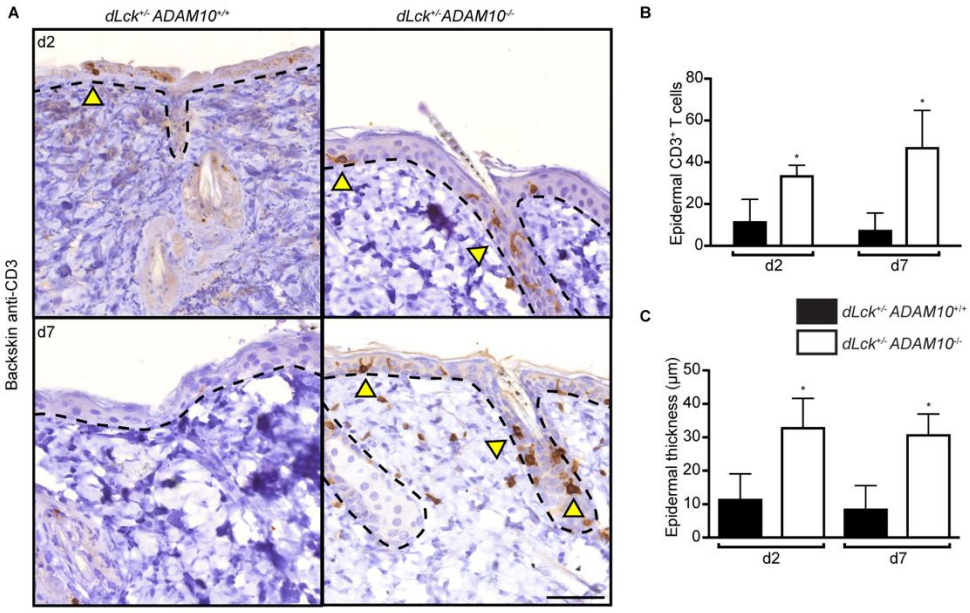

Figure 11: α-Toxin dependent injury to T cells dampens epidermal barrier function adjacent to the wound bed. A. Representative images of epidermis adjacent to wound bed in *S. aureus* SSTI infected control and *dLck*$^{+/-}$ *ADAM10*$^{-/-}$ mice stained with anti-CD3 on day 2 and day 7 post infection. Dashed lines denote epidermal/dermal boundaries and epidermal T cells are highlighted with yellow arrow heads. Scale bar, 50 μm. B. Quantification of CD3^{+}T cells in epidermis adjacent to wound bed from (A). C. Quantification of epidermal thickness adjacent to wound bed analyzed from groups of mice in Figure 10. Quantifications are of independent samples, N=3-5 per group. *P≤0.05 (Student t test). Error bars represent mean ± SD.

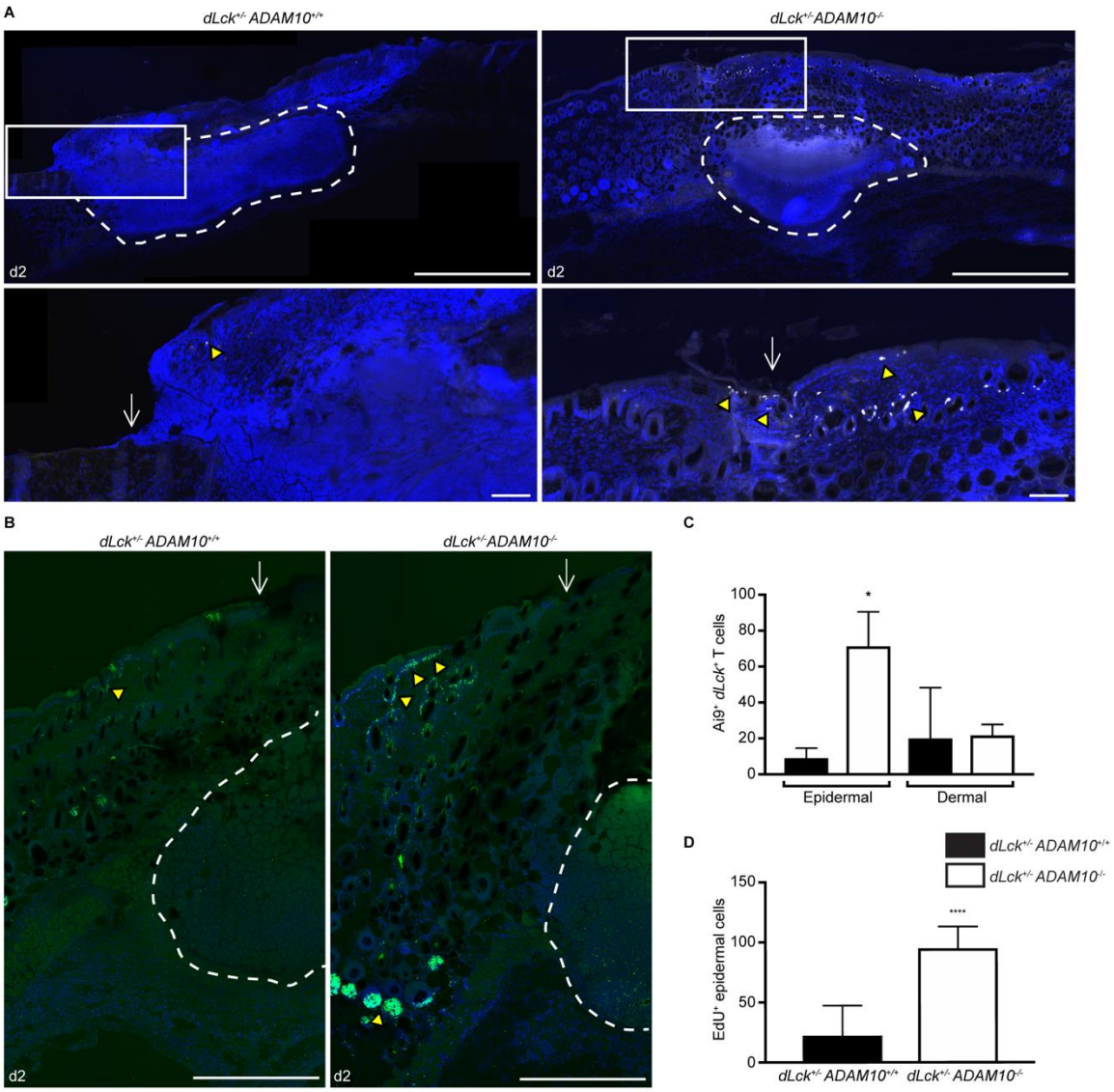

Figure 12: Epidermal T cells protected from α-toxin-mediated injury upregulate keratinocyte proliferation at the wound edge. Day 2 harvested backskins of 6 week-old male control or *Ai9*$^{+/-}$ *dLck*$^{+/-}$ *ADAM10*$^{-/-}$ mice subcutaneously infected with 3 x10^{7} WT *S. aureus* were harvested, thinly sectioned, and counter-stained with Dapi. A. Top panels depict representative max-projected fluorescent tile scan images from both of these groups. Dashed lines enclose the *S. aureus* abscess and viewing windows mark the position of bottom panel images. White arrows demarcate the wound edge. Bottom panel images are a zoomed-in view of the wound bed edge. Scale bar of large tile scans and smaller inset are 1000μm and 100μm, respectively. B. Immunofluorescence images of representative *S. aureus*- infected control and *Ai9*$^{+/-}$ *dLck*$^{+/-}$ *ADAM10*$^{-/-}$ in (A) were pulsed with EdU 4 hrs before harvesting and subsequently immunostained for EdU. Yellow arrowheads denote proliferating cells that have incorporated EdU. Scale bar, 500μm. C and D. Quantification of *Ai9*$^{+}$ *dLck*$^{+}$ T cells and EdU incorporation from animals in A. *P≤0.05, ****P≤ 0.0001 (Student t test). Quantifications are from independent samples, N=2-4 animals per group.

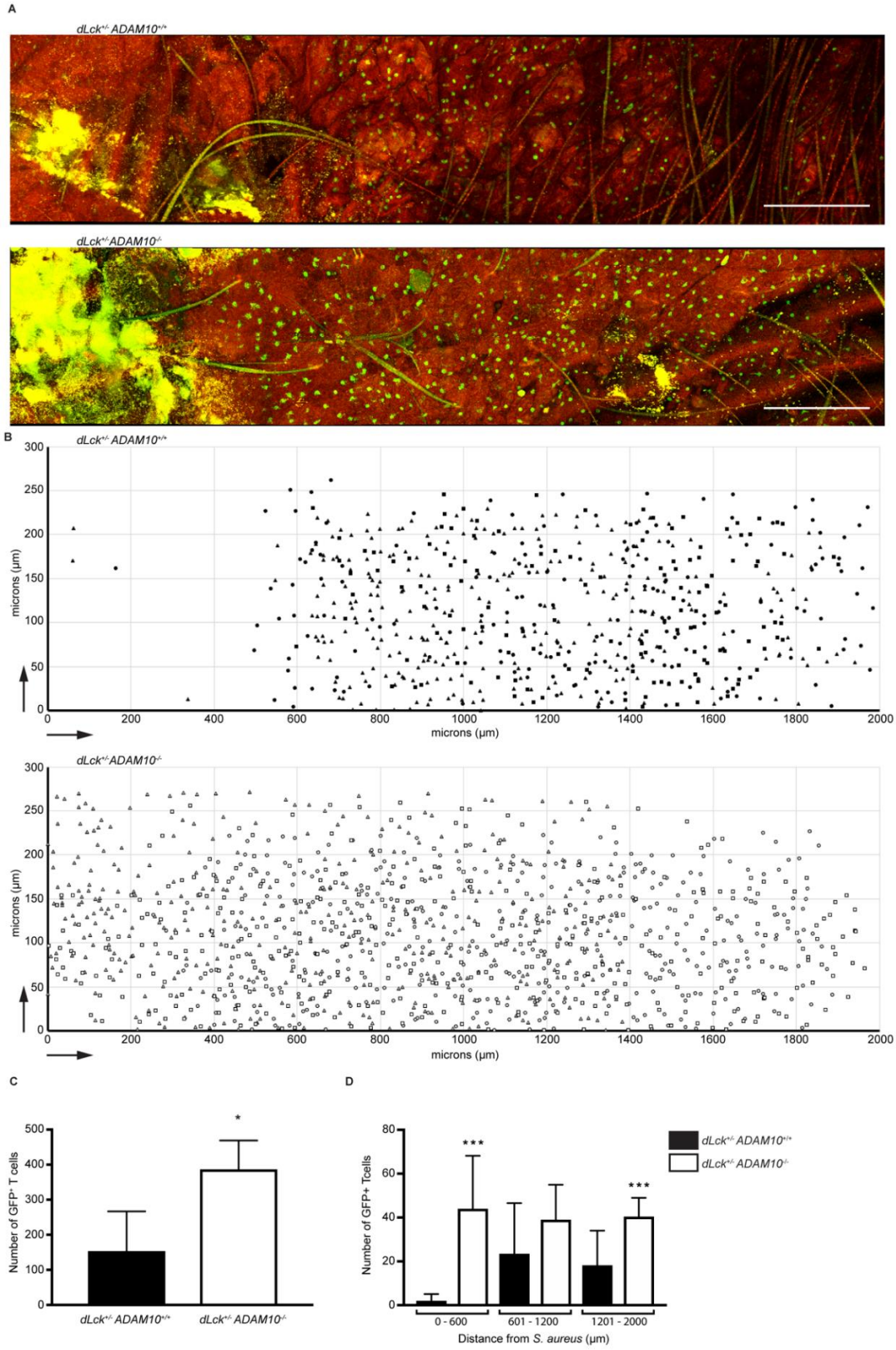

Figure 13: α-Toxin radially kills epidermal T cells. A. Representative confocal max projection fluorescent tile scans of *S. aureus* USA300 YFP10B epicutaneously infected control and *Rosa*$^{+/-}$

Figure 13, continued: *dLck*$^{+/-}$ *ADAM10*$^{-/-}$ whole mounted ear pinna at a 24-hours post infection. B. Spatial distribution map of 3 male mice replicates per group assigns the spatial location of GFP^{+} T cells in X,Y coordinate position relative to the USA300 YFP10B clump origin site (0,0μm) to 2000μm distance away. Scale bar, 250 μm. C. Total T cell number quantifications in (B). C. Quantity of T cells in distance bins relative to *S. aureus* origin site. *P≤0.05, **P≤0.01 (Student t test). Error bars represent mean ± SD. Quantifications are from independent samples, N=3.

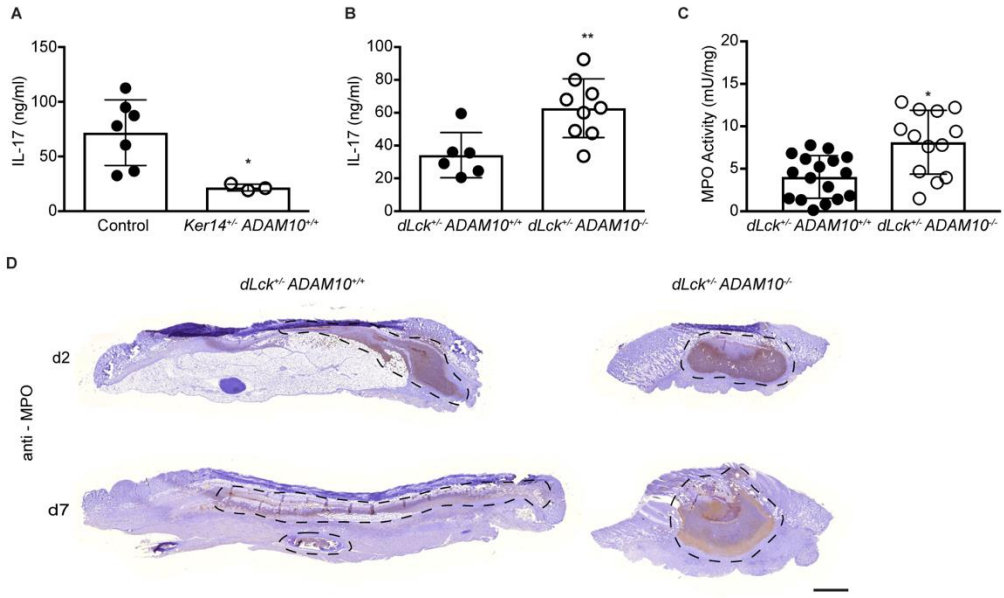

Figure 14: α-Toxin injury to cutaneous T cells alters the level of IL-17 and neutrophil activity in the tissue microenvironment. A and B. Level of IL-17 in *S. aureus*-infected backskin homogenates 2 days post infection in (A) *Ker14*$^{+/-}$ *ADAM10*$^{+/+}$ and *Ker14*$^{+/-}$ *ADAM10*$^{-/-}$ mice and in (B) *dLck*$^{+/-}$ *ADAM10*$^{+/+}$ and *dLck*$^{+/-}$ *ADAM10*$^{-/-}$ mice assessed by ELISA. C. Myeloperoxidase activity in skin homogenates as treated in (B) for control and *dLck*$^{+/-}$ *ADAM10*$^{-/-}$ mice measured by a MPO activity assay. *P≤0.05, **P≤0.01(Student t test). Error bars represent mean ± SD. D. Representative backskin images of anti-MPO stained semi-thin sections of control and *dLck*$^{+/-}$ *ADAM10*$^{-/-}$ mice subcutaneously challenged with *S. aureus* and sacrificed day 2 and day 7 post-infection. Dashed lines enclose the largest regions of anti-MPO stained tissue. Scale bar, 1000μm. Analysis was performed on independent samples, N=5-17.

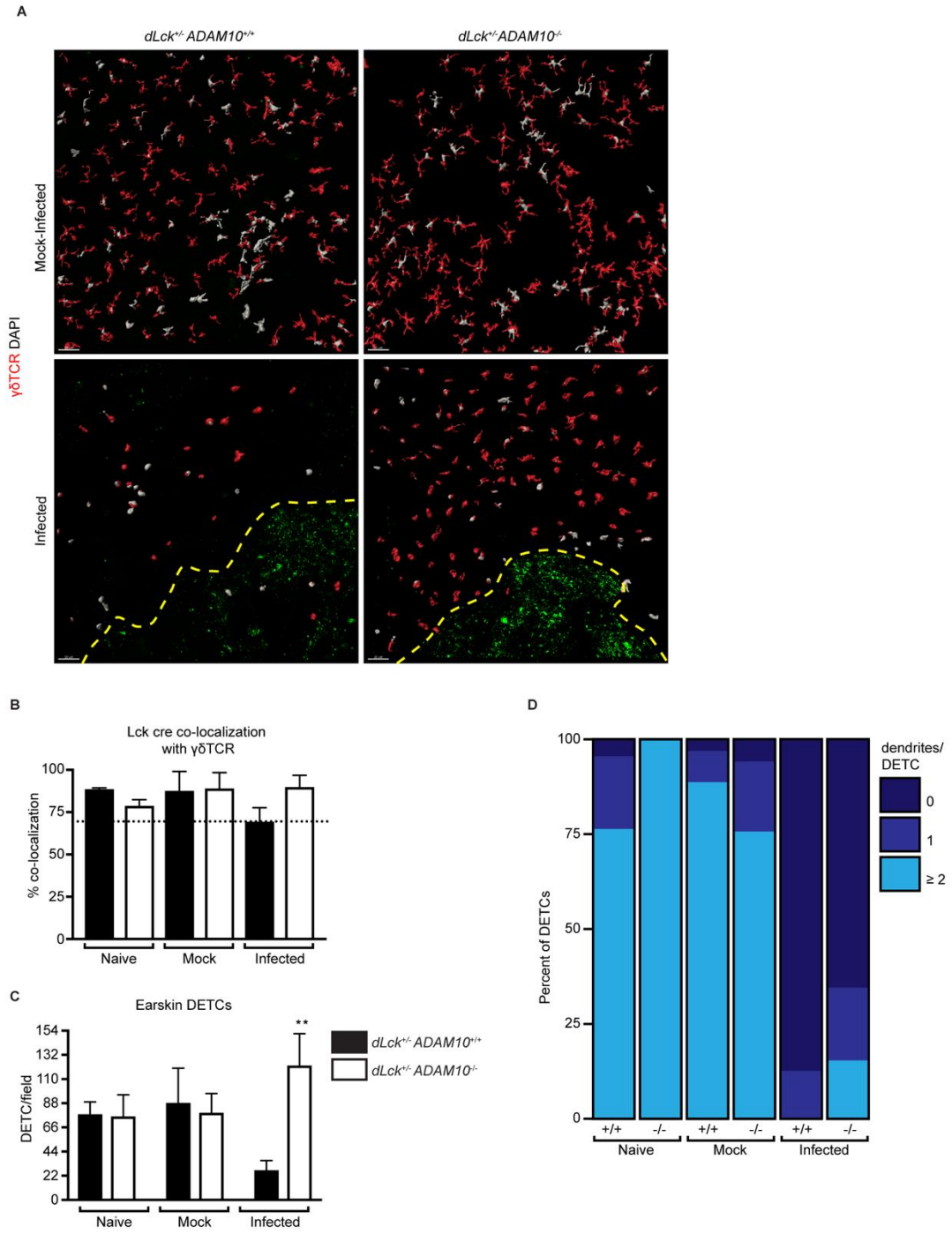

Figure 15: DETCs are the main intoxicated T cell subset in the epidermis during *S. aureus* SSTI. A. Representative sagittal z-series image of 3D reconstructed cells (white) from epidermal sheets prepared from control and *Rosa*$^{+/-}$ *dLck*$^{+/-}$ *ADAM10*$^{-/-}$ mice immunostained with γδTCR (red) 24 hours post challenge with epicutaneously mock-infected vehicle or *S. aureus*. Dashed yellow line

Figure 15, continued:
demarcates *S. aureus* border. Scale bar, 50 μm. B. Co-localization of GFP^+ $dLck^+$ T cells with γδTCR UV^+ stain in (A) using Imaris surface-surface co-localization algorithm. Dashed line represents lowest co-localization value of 70%. C. Quantification of DETCs per field in (A). D. Dendrite morphology analysis of DETCs per field in (C). **P≤0.01(Student t test). Error bars represent mean ± SD. Quantifications were performed using samples from independent animals, N=3-5.

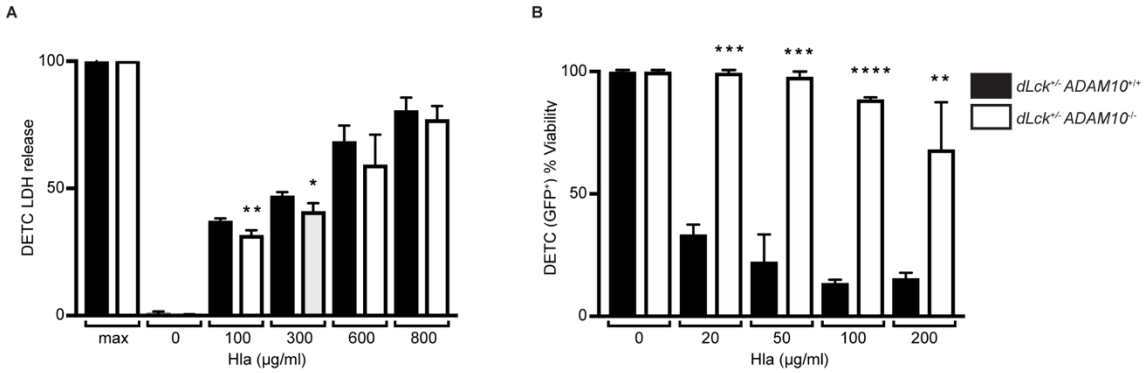

Figure 16: *ADAM10* knockout γδ T cells are resistant to lysis by *S. aureus* α-toxin. A. Isolation of semi-purified naïve DETCs from control and $dLck^{+/-}$ $ADAM10^{-/-}$ mice subjected *in vitro* to varying concentrations of purified recombinant Hla for 4 hours and cell death measured by LDH release. B. Purified and sorted naïve GFP^{+} $dLck^{+}$ DETCs from control and $Rosa^{+/-}$ $dLck^{+/-}$ $ADAM10^{-/-}$ mice subjected *in vitro* to varying concentrations of purified recombinant Hla for 4 hours and cell viability was determined by ATP release from cells. *P≤0.05, **P≤0.01, ***P≤0.001, ****P≤ 0.0001 (Student t test). Error bars represent mean ± SD. Analysis was performed on pooled sample from N=4-6 animals per group.

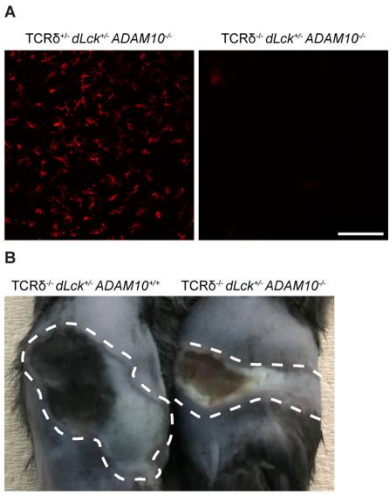

Figure 17: Generation of TCRδ$^{-/-}$ *dLck*$^{+/-}$ *ADAM10*$^{-/-}$ mice. A. Sagittal z-series from epidermal sheets prepared from 6-week old male TCRδ$^{+/-}$ *dLck*$^{+/-}$ *ADAM10*$^{-/-}$ (left) or TCRδ$^{-/-}$ *dLck*$^{+/-}$ *ADAM10*$^{-/-}$ mice immunostained with γδTCR (blue). B. Images of day 3 *S. aureus*-infected backskins from TCRδ$^{-/-}$ *dLck*$^{+/-}$ *ADAM10*$^{+/+}$ and TCRδ$^{-/-}$ *dLck*$^{+/-}$ *ADAM10*$^{-/-}$ animals. N=1

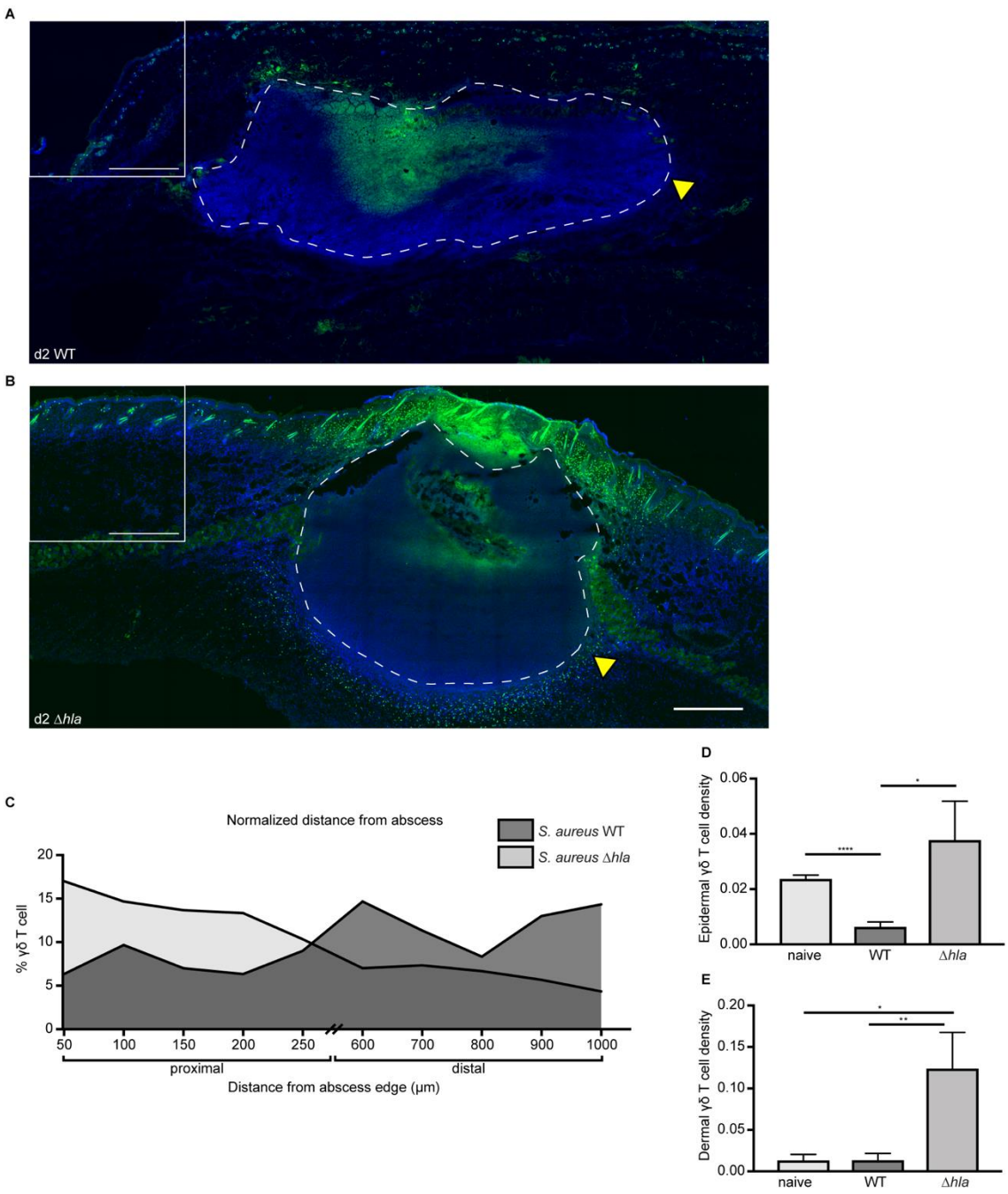

Figure 18: α-Toxin alters γδ T cells spatial distribution around the *S. aureus* abscess. Day 2 harvested backskins of 6 week-old male *Tcrd-H2BEGFP*$^{+/+}$ mice naïve or infected with 3 x10^7 WT (A) or Δ*hla* (B) *S. aureus* were harvested, thinly sectioned, and counter-stained with Dapi. Representative max-projected fluorescent tile scan images from infected mice are represented in primary images in A and B. Dashed lines enclose the *S. aureus* abscess, yellow arrowheads mark the position of inset images of the abscess border. Scale bar of large tile scans and smaller inset are 1000μm and 100μm, respectively. C. Normalized distance distributions of γδ T cells with respect to the *S. aureus* abscess. Data obtained from an Imaris

Figure 18, continued: distance transformation algorithm. D and E. Quantification of the density of GFP^+ γδ T cells in tile scanned tissue samples from *Tcrd-H2BEGFP*$^{+/+}$ naïve, *S.aureus* WT-infected, and *S.aureus* Δ*hla*-infected mice. *P≤0.05, **P≤0.01, , ****P≤ 0.0001 (Student t test). Quantifications are of independent samples, N=3 animals per group.

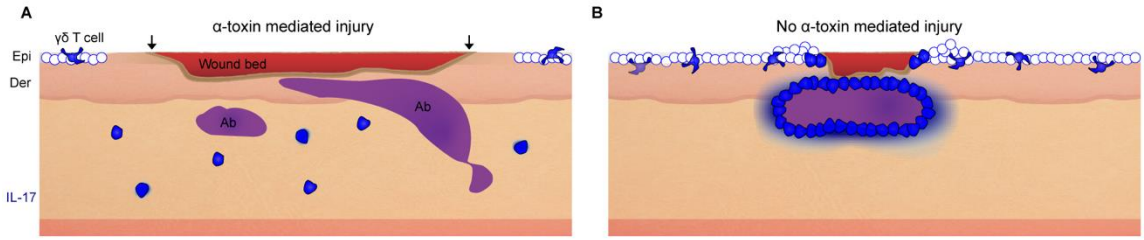

Figure 19: A model of α-toxin mediated injury to the skin microenvironment in the context of *S. aureus* SSTI. A. α-Toxin-mediated injury at early time points during *S. aureus* skin infection injures both keratinocytes (white circles) and adjacent resident T cells (blue cells). Dead or severly injured γδ T cells cannot cluster near the wound bed nor the abscess to provide a spatial signal that in conjunction with their chemical activatory signal such as, secretion of IL-17 (blue gradient) can form a spatial-chemical gradient that correctly orients keratinocyte proliferation at the wound bed (red) and neutrophils infiltrate to the nidus of infection (Ab, purple abscess). B. If α-toxin-mediated injury to the skin microenvironment does not occur during *S. aureus* infection, resident γδ T cells cluster both at the wounded edge and around the abscess concomitantly accelerating wound bed closure and confining the staphylococci. (Epi: epidermis; Der: dermis)

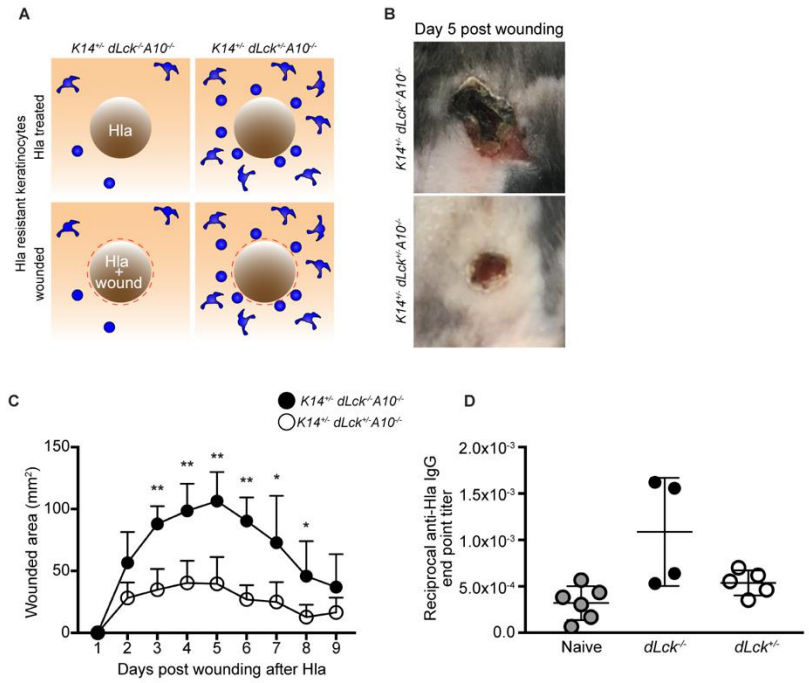

Figure 20: α-Toxin injury to T cells impedes sterile wound repair. A. Schematic of the skin from a bird's eye view of control and *Ker14*$^{-/-}$*14 dLck*$^{+/-}$ *ADAM10*$^{-/-}$ mice after subcutaneous challenge with purified Hla (Hla treated area represented as brown circle, top two panels) and subsequent sterile wounding of Hla treated area (sterile punch represented as red dashed line, lower bottom panels). Blue cartoon T cells depict their quantity and spatial relationship to the Hla-treated wound site. T cell specific *ADAM10* knockout mice are protected from toxin injury to T cells (top panels) whereas, *Ker14*$^{-/-}$ *dLck*$^{-/-}$ *ADAM10*$^{-/-}$ T cells are intoxicated by Hla (bottom panels). B. Representative images of day 5 post sterile wounding of *Ker14*$^{-/-}$ *dLck*$^{-/-}$ *ADAM10*$^{-/-}$ and *Ker14*$^{-/-}$ *dLck*$^{+/-}$ *ADAM10*$^{-/-}$ mice. C. Measured mean area of wound over a 10 day time course. D. Reciprocal end point titer analysis of the anti-Hla response calculated from enzyme-linked immunosorbent assay (ELISA) measurements performed on serum samples collected from naïve mice (gray enclosed circles) or Hla-treated, sterile wounded *Ker14*$^{-/-}$ *dLck*$^{-/-}$ *ADAM10*$^{-/-}$ mice (black enclosed circles), and *Ker14*$^{-/-}$ *dLck*$^{+/-}$ *ADAM10*$^{-/-}$ mice (open circles). IgG, immunoglobulin. *P≤0.05, **P≤0.01 (Student t test). Error bars represent mean ± SD. Analysis was performed on independent samples, N=4-6 animals per group.

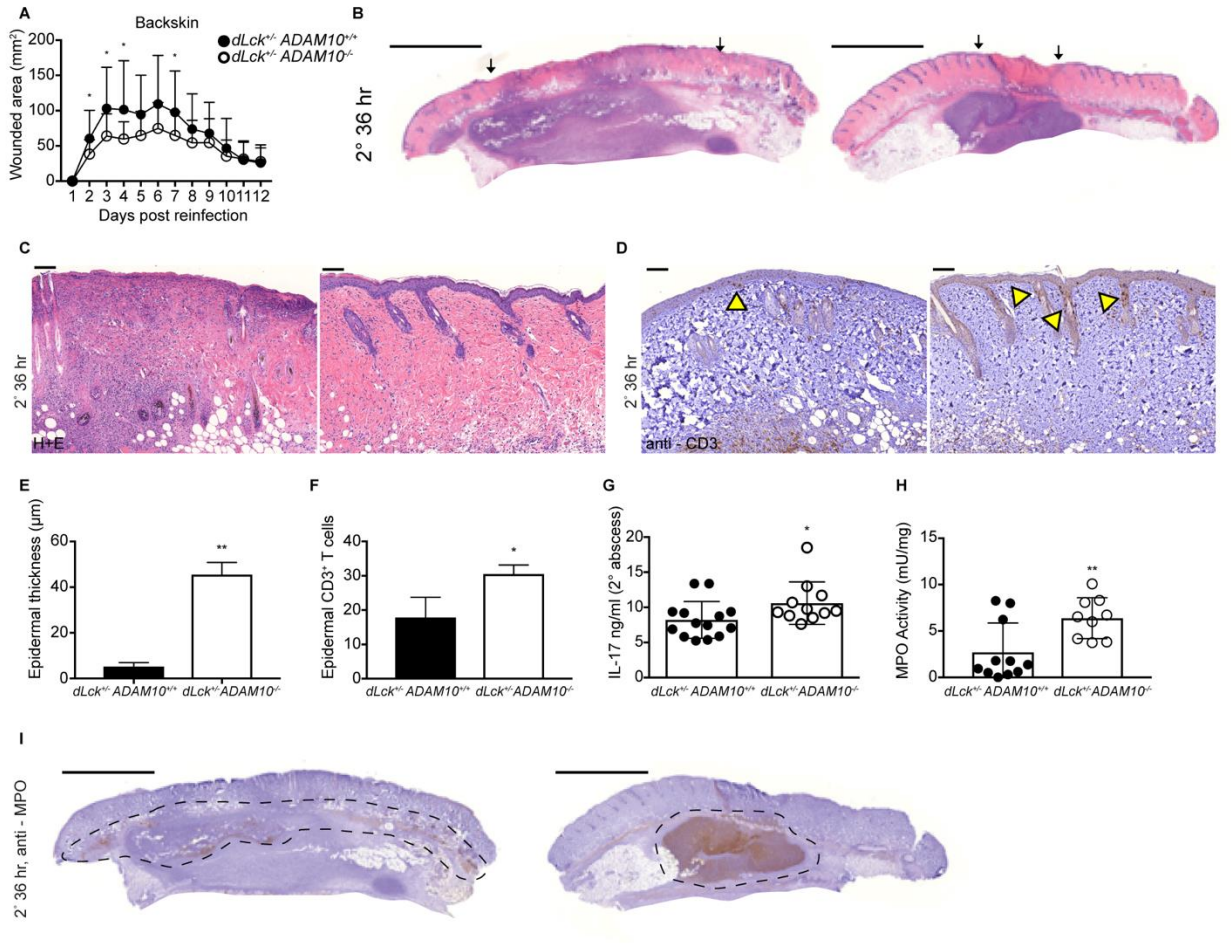

Figure 21: *dLck*$^{+/-}$ *ADAM10*$^{-/-}$ animals mitigate recurrent *S. aureus* SSTI. A. *S. aureus* reinfection wounded mean area recordings in control and *dLck*$^{+/-}$ *ADAM10*$^{-/-}$ mice that were previously subjected to primary *S. aureus* infection as described in Figure 1A. B. Representative day 2 backskin images of hematoxylin/eosin-stained (H&E) semi-thin sections of control and *dLck*$^{+/-}$ *ADAM10*$^{-/-}$ mice subcutaneously challenged with recurrent *S. aureus* on day 2. Black arrows demarcate wounded edges overlying the abscess. Scale bar, 1000µm. C. Higher magnification view of epidermis distal from the *S. aureus* wounded edge stained with H&E as in (B). D. Zoomed in view of representative images from thinly serially sectioned anti-CD3 stained samples from control and *dLck*$^{+/-}$ *ADAM10*$^{-/-}$ mice in (B). Epidermal T cells are highlighted with yellow arrowheads. Scale bar, 50 µm. E. Quantification of epidermal thickness adjacent to wound bed in (C). F. Quantification of CD3^{+} T cells in epidermis adjacent to wound bed from (D). G. Expression level of IL-17 as measured by ELISA in *S. aureus*-infected backskin homogenates 2 days post *S. aureus* SSTI seconday challenge in control and *dLck*$^{+/-}$ *ADAM10*$^{-/-}$ mice. H. Myeloperoxidase activity in day 2 secondary *S. aureus*-infected skin homogenate samples for control and *dLck*$^{+/-}$ *ADAM10*$^{-/-}$ mice. I. Representative backskin images of anti-MPO stained semi-thin sections of control and *dLck*$^{+/-}$ *ADAM10*$^{-/-}$ mice subcutaneously challenged with recurrent *S. aureus* SSTI on day 2. Dashed lines enclose the largest regions of anti-MPO stained tissue. Scale bar, 1000µm. *P≤0.05, **P≤0.01 (Student t test). Error bars represent mean ± SD. Analysis was performed on independent samples, N=4-6 animals per group.

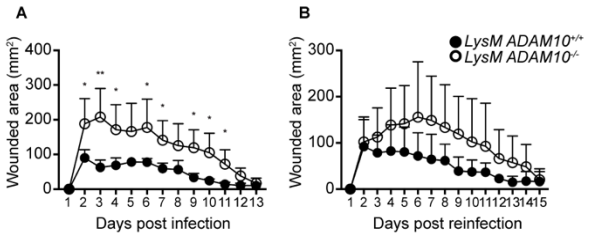

Figure 22: Myeloid lineage knockout of *ADAM10* does not confer protection during recurrent *S. aureus* SSTI. A. Abscess mean area recordings after primary *S. aureus* infection in $LysM^{+/-}$ $ADAM10^{+/+}$ (open circles) or $LysM^{+/-}$ $ADAM10^{-/-}$ (filled circles) 4-week of age male mice collected over a 2-week period. B. After a one week recovery period the same groups of mice were then subjected to reinfection with WT *S. aureus* on their opposite flank. Abscess mean area recordings were collected over a 2-week period. *P≤0.05, **P≤0.01 (Student t test).Error bars represent mean ± SD. Analysis was performed on independent samples, N=4-6 animals per group.

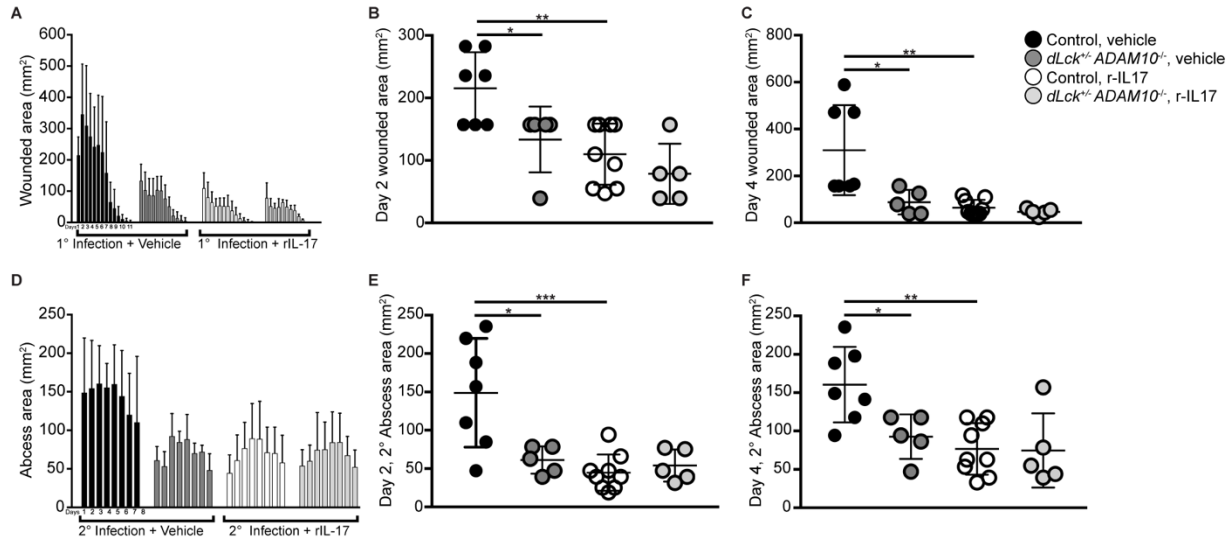

Figure 23: Administration of exogenous IL-17 after primary *S. aureus* SSTI restores the immune response against recurrent *S. aureus* infection in *dLck*$^{+/-}$ *ADAM10*$^{+/+}$ animals. A. Control and *dLck*$^{+/-}$ *ADAM10*$^{-/-}$ mice were intralesionally administered a single dose of vehicle (PBS) or rIL-17 (1,000ng/100µl) into the abscess 6 hours after primary *S. aureus* infection. Primary mean total *S. aureus* backskin lesions were recorded and monitored until wounds resolved. D. The same groups of mice were reinfected with WT *S. aureus* on the opposite flank 3-weeks after primary infection as described in (Figure 2A). Black bars: PBS- treated *dLck*$^{+/-}$ *ADAM10*$^{+/+}$ mice; open bars: PBS-treated *dLck*$^{+/-}$ *ADAM10*$^{-/-}$; dark gray bars: rIL-17 treated *dLck*$^{+/-}$ *ADAM10*$^{+/+}$; light gray bars: *dLck*$^{+/-}$ *ADAM10*$^{-/-}$. B, C, E, and F. Selected day 2 and day 4 time points from primary (A) and secondary (D) *S. aureus* challenge were tested for statistical difference between groups (PBS treated *dLck*$^{+/-}$ *ADAM10*$^{+/+}$: filled circles; PBS treated *dLck*$^{+/-}$ *ADAM10*$^{-/-}$: open circles; r-IL-17 treated *dLck*$^{+/-}$ *ADAM10*$^{+/+}$: dark gray circles; *dLck*$^{+/-}$ *ADAM10*$^{-/-}$: light gray circles). *P≤0.05, **P≤0.01, ***P≤0.001 (Student t test). Error bars represent mean ± SD. Analysis was performed on independent samples, N=5 animals per group.

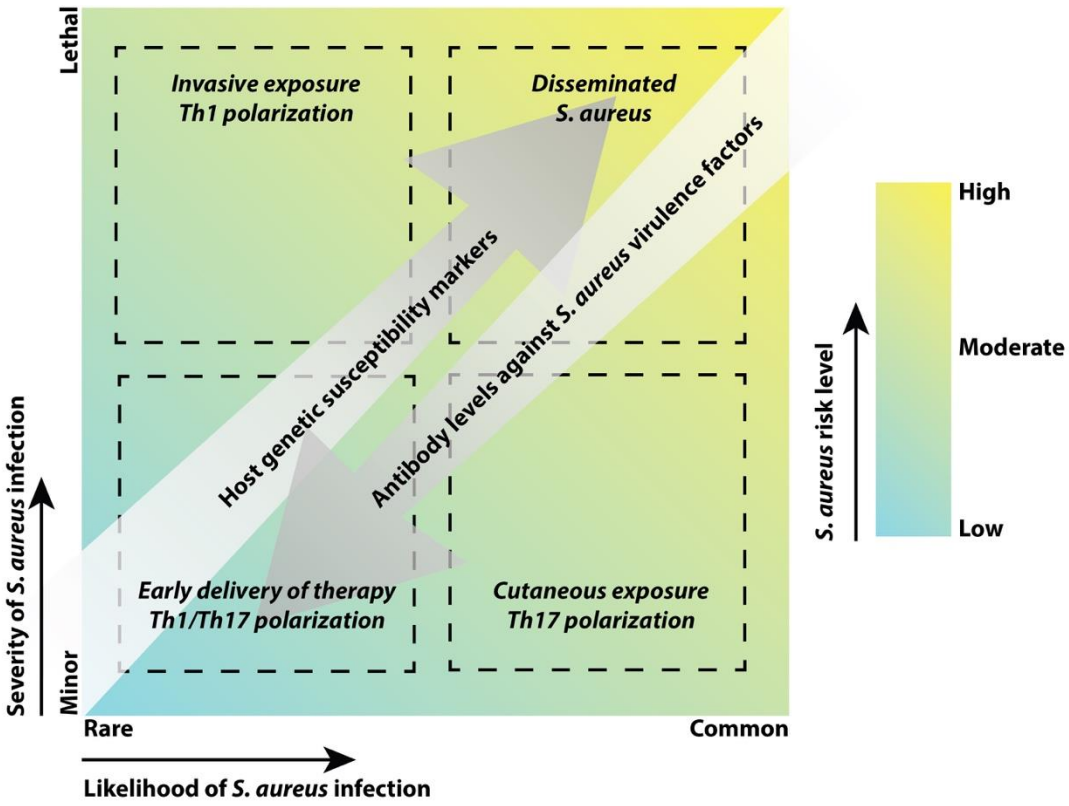

Figure 24: MPE-based risk model of *S. aureus* clinical disease in the hospital setting. This depiction captures patient health scenarios as a function of the severity of *S. aureus* infection, the patient's previous exposure history, and host markers of the immunologic response. The tissue context and severity of infection define whether exposure will elicit resistance to infection or will predispose the patient to recurrent infections. Novel treatment options such as monoclonal antibodies and host-targeted therapies may be capable of modulating the course of disease in *S. aureus*-infected patients that typically suffer from the most severe manifestations of *S. aureus* infection.

APPENDIX B

TABLES

Table 1: Statistical analysis of data presented in Figure 1B

Day[b]	*P* value [a]	
	Primary infection[c] WT vs Δ*hla*	Secondary infection[c] 1° WT, 2° WT vs 1° Δ*hla*, 2° WT
1	NA	NA
2	0.0003	0.0298
3	< 0.0001	0.1641
4	< 0.0001	0.0201
5	< 0.0001	0.1618
6	< 0.0001	0.1752
7	0.0006	0.1044
8	0.002	0.3171
9	0.3026	0.1115
10	0.3055	0.0649
11	0.3454	0.2326
12	0.3426	0.0033
13	0.8416	0.312
14	NA	0.4073

[a] *P* values were determined using the unpaired student's t-test at significance level P< 0.05.
[b] Abscess area of resulting lesions following primary or secondary infections were scored over a 2 week period.
[c]WT or Δ*hla* primary *S. aureus* skin infections were followed by WT secondary skin infection. NA, not applicable, abscess lesion 0.

Table 2: Statistical analysis of data presented in Figure 3A

Day[b]	*P* value, Primary Infections[a]					
	WT vs Δ*hla*	WT vs Δ*hla*::p*hla*	WT vs Δ*hla*::p*hla*$_{H35L}$	Δ*hla* vs Δ*hla*::p*hla*	Δ*hla* vs Δ*hla*::p*hla*$_{H35L}$	Δ*hla*::p*hla* vs Δ*hla*::p*hla*$_{H35L}$
1	2×10^{-6}	0.0028	2×10^{-6}	1×10^{-5}	0.9232	1×10^{-5}
2	4×10^{-8}	0.0026	2×10^{-8}	5×10^{-5}	0.1881	5×10^{-5}
3	1×10^{-5}	0.0002	0.0017	7×10^{-6}	0.0150	2×10^{-5}
4	3×10^{-7}	0.0009	3×10^{-7}	8×10^{-7}	0.7066	8×10^{-7}
5	7×10^{-6}	0.0084	5×10^{-6}	2×10^{-7}	0.2729	2×10^{-7}
6	9×10^{-6}	0.0008	2×10^{-5}	8×10^{-6}	0.5075	8×10^{-6}
7	2×10^{-5}	0.0015	1×10^{-5}	2×10^{-5}	0.6617	2×10^{-5}
8	5×10^{-6}	0.0007	5×10^{-6}	3×10^{-5}	0.9001	3×10^{-5}
9	2×10^{-6}	0.0023	2×10^{-6}	0.0003	0.3852	0.0003
10	4×10^{-6}	0.0072	3×10^{-6}	0.0003	0.1622	0.0003
11	4×10^{-5}	0.0033	2×10^{-5}	0.0003	0.1648	0.0003
12	0.0011	0.0013	0.0005	0.0004	0.3356	0.0004
13	0.7918	7×10^{-5}	0.1887	7×10^{-5}	0.3356	6×10^{-5}
14	0.5203	0.0002	0.3343	0.0002	0.3356	0.0002

[a]Primary skin infections with different *S. aureus* strains. Mice were infected a single time subcutaneously with the indicated strain. *P* values were determined using pair-wise comparison with Bonferroni correction to adjust for multiplicity at significance level 0.05.
[b] Abscess area of resulting lesions were scored over a 2 week period.

Table 3: Statistical analysis of data presented in Figure 3B

Day[b]	*P* value, Secondary infections[a]					
	WT vs Δ*hla*	WT vs Δ*hla*::p*hla*	WT vs Δ*hla*::p*hla*$_{H35L}$	Δ*hla* vs Δ*hla*::p*hla*	Δ*hla* vs Δ*hla*::p*hla*$_{H35L}$	Δ*hla*::p*hla* vs Δ*hla*::p*hla*$_{H35L}$
1	0.0101	0.2397	0.000006	0.2138	0.0156	0.0038
2	0.0033	0.0574	0.0002	0.1320	0.0902	0.0040
3	0.0140	0.1701	0.0024	0.2078	0.2169	0.0359
4	0.0084	0.0539	0.0003	0.1443	0.0200	0.0001
5	0.0192	0.5219	0.0027	0.0177	0.0316	0.0010
6	0.2657	0.3668	0.0148	0.7647	0.0219	0.0130
7	0.1993	0.5771	0.0242	0.2073	0.0018	0.0027
8	0.1046	0.3859	0.0007	0.4278	0.0270	0.0047
9	0.1422	0.5226	0.0014	0.4489	0.0201	0.0104
10	0.2988	0.5781	0.0069	0.2173	0.0767	0.0318
11	0.5653	0.5988	0.0455	0.2920	0.0928	0.0280
12	0.7626	0.4384	0.1812	0.2872	0.2513	0.0582
13	0.6543	0.3034	0.4632	0.5576	0.3040	0.1296
14	0.0101	0.2397	0.000006	0.2138	0.0156	0.0038

[a]Mice received primary subcutaneous infections with the indicated *S. aureus* strain, followed by secondary infection on the opposite flank with WT *S. aureus*. *P* values were determined using pair-wise comparison with Bonferroni correction to adjust for multiplicity at significance level 0.05.
[b] Abscess area of resulting lesions were scored over a 2 week period.

Table 4: Statistical analysis of data presented in Figure 4A

Primary infection sera[a]		Secondary infection sera[b]		Primary vs. Secondary[c]	
Comparison	*P* value[e]	Comparison	*P* value[e]	Comparison	*P* value[e]
WT vs Δ*hla*	ns	WT vs Δ*hla*	ns	WT 1° vs 2°	*
WT vs Δ*hla*::p*hla*	ns	WT vs Δ*hla*::p*hla*	**	Δ*hla* 1° vs 2°	**
WT vs Δ*hla*::p*hla*$_{H35L}$	ns	WT vs Δ*hla*::p*hla*$_{H35L}$	**	Δ*hla*::p*hla*$_{WT}$ 1° vs 2°	***
Δ*hla* vs Δ*hla*::p*hla*	***	Δ*hla* vs Δ*hla*::p*hla*	***	Δ*hla*::p*hla*$_{H35L}$ 1° vs 2°	***
Δ*hla* vs Δ*hla*::p*hla*$_{H35L}$	**	Δ*hla* vs Δ*hla*::p*hla*$_{H35L}$	***		
Δ*hla*::p*hla* vs Δ*hla*::p*hla*$_{H35L}$	ns	Δ*hla*::p*hla* vs Δ*hla*::p*hla*$_{H35L}$	ns		

[a,b,c]Mice received primary subcutaneous infections with the indicated strain, followed by secondary infection on the opposite flank with WT *S. aureus*. Sera were collected following primary and secondary infection and endpoint titers to Hla calculated from nonlinear regression of ELISA data using Graphpad Prism software.[d]*P* values were determined using ANOVA with Bonferroni post testing. **P*<0.05, ***P*<0.01, ****P*<0.001, ns-not significant

Table 5: Statistical analysis of data presented in Figure 7B

Pairwise comparison[a] using Long-rank test or Gehan-Breslow-Wilcoxon test

	Log-rank test	Gehan-Breslow-Wilcoxon test
PBS vs. WT	****	****
PBS vs. Δ*hla*	**	**
WT vs. Δ*hla*	*	*

[a]Mice received primary subcutaneous infections with the indicated strain, followed by a secondary lethal dose of WT *S. aureus* pneumonia. Statistical survival curve pairwise comparisons were made using Graphpad Prism software. P≤0.05, **P≤0.01, ***P≤0.001, ****P≤ 0.0001